VELOCITY AND TEMPERATURE PROFILES FOR TURBULENT FLOW OF LIQUID-LIQUID DISPERSIONS IN PIPES

by

AZIMUDDIN AHMAD FARUQUI

A THESIS

submitted to

OREGON STATE UNIVERSITY

in partial fulfillment of
the requirements for the
degree of

DOCTOR OF PHILOSOPHY

June 1962

APPROVED:

[redacted]

Professor of Chemical Engineering

In Charge of Major

[redacted]

Head of Department of Chemical Engineering

[redacted]

Chairman of School Graduate Committee

[redacted]

Dean of Graduate School

Date thesis is presented July 14, 1961

Typed by Mary Adams

TABLE OF CONTENTS

TABLE OF CONTENTS (Continued)

LIST OF FIGURES

LIST OF FIGURES (Continued)

LIST OF TABLES

ACKNOWLEDGMENT

The author is privileged to make the following acknowledgments:

To Dr. J. G. Knudsen for suggesting the problem and his assistance and suggestions during the course of the investigation.

To the National Science Foundation for financial assistance in the form of a research assistantship.

To the Chemical Engineering Department for the use of its facilities.

To the Mathematics Department for the use of the ALWAC-III computer.

To Mr. R. C. Mang for performing the more intricate machining work.

To Messrs. A. Petersen, R. Pan and R. Adolf for their help, at various periods, in setting up the equipment and taking the data.

VELOCITY AND TEMPERATURE PROFILES FOR TURBULENT FLOW OF LIQUID-- LIQUID DISPERSIONS IN PIPES

CHAPTER I

INTRODUCTION

Problems associated with two phase flow systems have been encountered for quite some time but it has been only recently that thorough studies on the processes of momentum transfer and heat transfer to these systems have been undertaken. Most of the work, however, has been restricted to gas-solid, gas-liquid and solid-liquid dispersions. Little work has been devoted to liquid-liquid systems.

Moreover the research on two phase systems has been restricted to measuring friction factors, heat transfer coefficients, effective viscosities and effective conductivities. One of the interesting aspects of this field observed by recent workers has been that some solid-liquid and liquid-liquid dispersions behave as non-Newtonian fluids. No work has been published on the measurement of temperature and velocity profiles for the flow of liquid-liquid dispersions.

The object of this study was to measure the velocity profiles, temperature profiles, friction factors and heat transfer coefficients for the turbulent flow of liquid-liquid dispersions in smooth circular tubes to determine the momentum and heat transfer characteristics of the two phase fluid. The fluid system studied

was a dispersion of a commercial petroleum solvent in water.

The velocity profile was used to determine the viscosity of the dispersion. This viscosity was then used to correlate the pressure loss data on a conventional friction factor plot. The temperature profile data allowed determination of the correct Prandtl number to use in the heat transfer j factor.

CHAPTER II

THEORY AND PREVIOUS WORK

Momentum equation for two phase flow.

When a fluid flows in a potential field a force balance on an element of volume δV of the fluid gives rise to the momentum equation. The force balance is actually an application of Newton's second law of motion and is made by equating the inertial force to the external forces. For a viscous fluid the external forces are the various normal and shear stresses and the potential forces. In the x-direction the inertial force is

$$\frac{\rho}{g_c}\frac{du}{dt}\delta V$$

where ρ = density of the fluid

du/dt = acceleration of the fluid in the x-direction

g_c = gravitational constant.

The stresses are

$$\left(\frac{\partial \tau_{xx}}{\partial x}+\frac{\partial \tau_{yx}}{\partial y}+\frac{\partial \tau_{zx}}{\partial z}\right)\delta V$$

where τ_{xx} = normal stress (pressure) in x-direction

$\tau_{\alpha\beta}$ = shear stress acting on a plane perpendicular to α and in the direction of β .

The field force is

$$-\rho\frac{\partial \Omega}{\partial x}\delta V$$

where Ω is the potential of the field per unit mass of the fluid.

Equating these three forces, the momentum equation for the x-direction

becomes

$$\frac{\rho}{g_c}\frac{du}{dt}\delta V = \left(\frac{\partial \tau_{xx}}{\partial x} + \frac{\partial \tau_{yx}}{\partial y} + \frac{\partial \tau_{zx}}{\partial z}\right)\delta V - \rho\frac{\delta \Omega}{\partial x}\delta V \quad (1)$$

Similar equations for the y and z directions can be written.

For a single phase fluid the size of the element δV can be taken sufficiently small so that equation (1) applies. However if it is desired to express the behavior of a two-phase dispersed fluid by a single momentum equation there are certain restrictions to the size of the element δV. The element must be taken such that

$$\delta V \geqslant \delta V_{min} \quad (2a)$$

where δV_{min} must be large enough to contain a statistical sample of the dispersed phase droplets.

The derivation of the stress terms in equation (1) is based on the assumption that the stress is linear with distance. Baron, Sterling and Schueler (2) have shown that if the stress is not linear equation (1) will still hold, provided

$$\delta x \ll 2\frac{\partial \tau_{xx}}{\partial x} \Big/ \frac{\partial^2 \tau_{xx}}{\partial x^2} \quad (2)$$

with similar inequalities for δy and δz. This restriction puts an upper limit on δV. So the condition that equation (1) may be used for two-phase dispersions can be written as

$$\delta V_{max} \geqslant \delta V \geqslant \delta V_{min} \quad (3)$$

Baron, Sterling and Schueler have further shown that for turbulent flow the region δV_{max} may be taken as the region of viscous flow in the turbulent field. The authors have used the Kolmogoroff

characteristic dimension to evaluate this region. The Kolmogoroff dimension, as reported by Batchelor (3), is given by

$$\delta x_{max} = \left(\frac{\mu}{\rho}\right)^{3/4} \left(\varepsilon\right)^{-1/4}$$

where μ = the viscosity of the fluid

and ε = the rate of energy dissipated per unit mass.

Baron, Sterling and Schueler have shown that for dispersions of carbon tetrachloride in water the Kolmogoroff dimension is of the order of 0.5 mm. For liquid-liquid dispersions the dispersed phase droplets are definitely smaller than this. So the authors concluded that a cube of side 0.5 mm. will contain a statistical number of dispersed phase droplets. This showed that liquid-liquid dispersions can be treated as single phase liquids.

Baron, Sterling and Schueler have further noted that the dispersion they studied behaved as a Newtonian liquid. However Finnigan (10) and Cengel (4) who have worked with the dispersion studied in this work have noted that it behaved as a non-Newtonian fluid. Other workers (e.g., Dodge and Metzner 9 and Shaver and Merrill 24) have treated suspensions of solid particles in liquids as non-Newtonian fluids. Russell, Hodgson and Govier (23) and Charles, Govier and Hodgson (5) have done some work on the flow of mixtures of oil and water. They have studied bubble, stratified and mixed flow of the two liquids but have not considered the problem of completely dispersed flow.

The shear-stress-rate of shear behavior of most liquids can be

characterized by an equation of the type

$$g_c \tau = K \left(\frac{du}{dy} \right)^n \qquad (6)$$

where τ = shear stress

du/dy = rate of shear (velocity gradient)

y = distance measured normal to the flow and away from the wall.

and n and K are constants for the liquid.

If $n = 1$, $K = \mu$ where μ is called the viscosity of the liquid. In this case the liquid is Newtonian. For $n \neq 1$ the liquid is non-Newtonian. If $n < 1$ the fluid is termed pseudoplastic and if $n > 1$ the liquid is termed dilatant.

Turbulent flow of Newtonian fluids.

For the steady laminar flow of incompressible Newtonian fluids in circular ducts the momentum equation can be simplified to

$$\frac{\partial P_f}{\partial x} = \frac{\mu}{g_c} \frac{1}{r} \frac{\partial}{\partial r} \left(r \frac{\partial u}{\partial r} \right) \qquad (7)$$

where x = length along the tube

$\frac{\partial P_f}{\partial x}$ = pressure gradient due to friction

r = distance measured radically from center of tube.

and u = point velocity of the fluid.

This equation can be solved to give the velocity as a function of the radius (e.g. see Knudsen and Katz [12, p. 84-86]).

When the fluid is in turbulent motion, eddies are formed and dissipated in the fluid and the shear stress can no longer be

characterized by relationships of the type given by equation (6). For Newtonian fluids in turbulent motion Prandtl proposed that

$$\tau = \frac{\mu}{g_c}\frac{du}{dy} + \frac{\rho}{g_c}\left(\underline{l}\frac{du}{dy}\right)^2 \qquad (8)$$

where $\underline{l}$, the Prandtl mixing length, is defined as the distance a particle moves in the y-direction before loosing its identity. The term $\frac{\rho}{g_c}\left(\underline{l}\frac{du}{dy}\right)^2$ is referred to as the turbulent shear stress and is much greater than the viscous shear in the turbulent region.

The term $\frac{\mu}{\rho}$ is called the molecular diffusivity of momentum and the analogous term for turbulent motion, $\underline{l}^2\frac{du}{dy}$, is the eddy diffusivity of momentum, $\mathcal{E}_M$. It can be shown that for steady laminar or turbulent flow in a tube the shear stress in the fluid is a linear function of the radius (12, p.79), i.e.

$$\tau = \tau_w\left(1 - \frac{y}{r_w}\right) \qquad (9)$$

where τ_w is the shear stress of the wall and r_w the radius of the pipe. Hence for the turbulent region equation (8) can be written as

$$\tau_w\left(1 - \frac{y}{r_w}\right) = \frac{\rho}{g_c}\left(\underline{l}\frac{du}{dy}\right)^2 \qquad (10)$$

By further assuming that $\underline{l}$ is a linear function only of y, this equation can be solved for u to give

$$u^+ = u/u^* = 5.75 \log y^+ + c_1 \qquad (11)$$

where u^* = the friction velocity, $\sqrt{\tau_w g_c/\rho}$

$y^+ = (y\, u^* \rho)/\mu$, a dimensionless distance.

The constant c_1 has been experimentally determined to be 5.5. So the

velocity profile equation for the turbulent region can be written as

$$u^+ = 5.75 \log y^+ + 5.5 \qquad (12)$$

When a fluid is in turbulent motion in a tube it is assumed, based upon experimental evidence (29), that there is a layer of the fluid near the wall in laminar motion. In this region there are no eddies and no turbulent shear, hence $\epsilon_M = 0$. The thickness of this sublayer extends to $y^+ = 5$. The velocity profile in this layer can be shown to be

$$u^+ = y^+ \qquad y^+ < 5 \qquad (13)$$

Between the laminar sublayer and the turbulent core there is a region where the eddy diffusivity increases rapidly from zero to a value many times greater than the molecular diffusivity. The extent of this region is taken to be from $y^+ = 5$ to $y^+ = 30$. The velocity distribution in this region has been determined to be

$$u^+ = 11.5 \log y^+ - 3.05 \qquad 5 < y^+ < 30 \qquad (14)$$

For $y^+ > 30$ there is assumed to be complete turbulence and the velocity profile is given by equation (12). The turbulent core extends over most of the tube cross-section. In terms of velocity defects equation (12) can be written as

$$\frac{u_m - u}{u^*} = 5.75 \log \frac{r_w}{y} \qquad (15)$$

where u_m is the maximum point velocity at the center of the tube.

For flow past a solid boundary the shear stress at the wall is proportional to the average kinetic energy of the fluid

$$\tau_w = f \rho U^2 / 2 g_c \qquad (16)$$

where the constant of proportionality, f, is called the friction factor and U is the average velocity of the fluid. For flow in tubes the expression for the friction factor becomes

$$f = \frac{g_c D}{2\rho U^2} \left[- \frac{d P_f}{dx} \right] \tag{17}$$

where D = diameter of the tube

$\frac{d P_f}{dx}$ = pressure gradient due to friction losses.

By dimensional analysis it can be shown that both for turbulent and laminar flow of Newtonian fluids in smooth tubes the friction factor is a function only of the Reynolds number, Re. This flow parameter is defined by

$$Re = (DU\rho)/\mu = (D\ G)/\mu \tag{18}$$

where G is the mass flow rate per unit cross-section area. The relationship between the friction factor and Reynolds number has been determined by various workers. Among the equations proposed for turbulent flow are

$$f = 0.079\ (Re)^{-0.25} \tag{19}$$

$$f = 0.046\ (Re)^{-0.20} \tag{20}$$

and

$$1/\sqrt{f} = 4.0 \log \left[Re \sqrt{f} \right] - 0.40 \tag{21}$$

For Reynolds numbers up to 100,000 there is no appreciable difference between these equations. Equation (21), referred to as the Nikuradse equation, is usually recommended for evaluating friction factors since it applies over a wide range of Reynolds numbers.

It should be noted that with the use of equation (16) the

expressions for u^+ and y^+ become

$$u^+ = \frac{u}{U\sqrt{f/2}} \text{ and } y^+ = Re\,\frac{Y}{D}\sqrt{\frac{f}{2}} \qquad (22)$$

These expressions are used to evaluate u^+ and y^+ for velocity profile calculations.

Turbulent flow of non-Newtonian fluids.

Studies on the flow of non-Newtonian fluids have been initiated only recently and little has been published in this field. Dodge and Metzner (9) have used dimensional analysis to obtain the various groups involved in the turbulent motion of non-Newtonian fluids in pipes. Starting with the assumption that

$$u = f(r_w, \rho, \tau_w, K, n, y) \qquad (23)$$

they obtained the relationship

$$u^+ = f\left(Z, \frac{Y}{r_w}, n\right) \qquad (24)$$

where $$Z = \rho\frac{r_w^{\,2}\,(u^*)^{2-n}}{K}$$

They further showed that the exact form of the velocity distribution equation for the turbulent core should be

$$u^+ = A_n \log y^+ + B_n \qquad (25)$$

where $$y^+ = Z\left(\frac{Y}{r_w}\right)^n = \left[y^n \rho\,(u^*)^{2-n}\right] \Big/ K$$

and A_n and B_n are functions of n. They also showed that in terms of velocity defects the equation is of the form

$$\frac{u - u_m}{u^*} = n\,A_n \log \frac{Y}{r_w} \qquad (26)$$

For the evaluation of friction factors for turbulent non-Newtonian flow they obtained the equation

$$\sqrt{\frac{1}{f}} = A_{1n} \log \left[Re\ (f)^{1 - n/2} \right] + C_n \qquad (27)$$

for non-Newtonian flow the Reynolds number is defined by

$$Re = \frac{D^n U^{2-n} \rho}{K} \left(\frac{n}{6n+2} \right)^n 8 \qquad (28)$$

For $n = 1$, this reduces to $Re = \frac{D U \rho}{\mu}$.

A_{1n} and C_n are functions of n.

By analyzing the experimental friction factor data for non-Newtonian liquids these authors proposed that

$$A_n = \frac{5.66}{(n)^{0.75}}\ ,\ A_{1n} = \frac{4.0}{(n)^{0.75}}\ ,\ C_n = \frac{-0.40}{(n)^{1.2}}$$

and $$B_n = -\frac{0.40}{(n)^{1.2}} + \frac{2.458}{(n)^{0.75}} \left[1.960 + 1.255n - 1.628n \log (3\ \tfrac{1}{n}) \right] \qquad (29)$$

For Newtonian flow these constants become

$$A_1 = 5.66\ ,\ A_{11} = 4.0\ ,\ C_1 = -0.4\ ,\ B_1 = 5.1 \qquad (30)$$

With these values equations (25), (26) and (27) become

$$u^+ = 5.66 \log y^+ + 5.1 \qquad (31)$$

$$\frac{u - u_m}{u^*} = 5.66 \log \left(\frac{y}{r_w} \right) \qquad (32)$$

and

$$\sqrt{\frac{1}{f}} = 4.0 \log (Re \sqrt{f}) - 0.4 \qquad (33)$$

Equation (33) is identical to equation (20), while equations (31) and (32) differ slightly respectively from equations (12) and (15). It should be kept in mind that the constants in equation (12) have been determined experimentally. Hence these small differences can be expected.

Shaver and Merrill (24) have done some experimental work on pseudoplastic liquids. They have measured both friction factors and velocity profiles. They have correlated their friction factor data by

$$f = (0.079)/n^5 \, Re^{\gamma} \qquad (34)$$

where $\gamma = (2.63)/(10.5)^n$

For n = 1 this reduces to equation (18). Both Dodge and Metzner's (9) and Shaver and Merrill's results show the same trend in friction factors: for a particular Reynolds number the friction factor decreases with n. Maude and Whitmore (16) have studied the turbulent flow of suspensions of fine emery powder in water. They treated the suspensions as Newtonian fluids and found that the friction factors obtained were less than those predicted by equation (21). This could be due to pseudo-plastic behavior of the suspensions.

Shaver and Merrill (24) have presented their velocity profile data as $(u_m - u)/u^*$ vs. $\log \frac{y}{r_w}$ for various values of n. Except for a small portion near the center of the tube, their data can be correlated by an equation like

$$\frac{u_m - u}{u^*} = F_n \log\left(\frac{r_w}{y}\right) \qquad (35)$$

where F_n is a function of n. From their data it is seen that F_n increases as n decreases. This trend is opposite of that predicted by Dodge and Metzner (9). According to equations (26) and (29) derived by Dodge and Metzner, the slope of $(u_m - u)/u^*$ vs. $\log (r_w/y)$ should vary with n as $(n)^{0.25}$. It is evident that

for n = 0, the ultimate pseudo-plastic liquid, the shear stress will be constant throughout the tube. This means the velocity profile will be flat. This is predicted by Dodge and Metzner's equation. Clearly more experimental work is required in this field.

No published work has been found on the velocity profiles in liquid-liquid dispersions.

Heat transfer to Newtonian fluids.

Considerable work has been done on the evaluation of the temperature profiles for the turbulent flow of Newtonian fluids. The energy equation for this type of flow of an incompressible fluid is (assuming no heat generation and neglecting viscous dissipation)

$$u \frac{\partial T}{\partial x} = \frac{1}{r} \frac{\partial}{\partial r} \left[r (\alpha + \varepsilon_H) \frac{\partial T}{\partial r} \right] \qquad (36)$$

where T = temperature of the fluid

α = molecular thermal diffusivity, $\frac{k}{C_p \rho}$, where k is the thermal conductivity of the fluid and C_p the heat capacity.

and ε_H = eddy diffusivity of heat.

Equation (36) is analogous to the momentum equation for turbulent flow which may be written as

$$\frac{g_c}{} \frac{\partial P_f}{\partial x} = \frac{1}{r} \frac{\partial}{\partial r} \left[r \left(\frac{\mu}{\rho} + \varepsilon_M \right) \frac{\partial u}{\partial r} \right] \qquad (37)$$

using the concept of the eddy diffusivity of momentum, ε_M, introduced previously. Since u is a function of r equation (36) has to be solved in conjunction with equation (37). The term ε_H is also a

function of r, but there is no generally accepted analytical or empirical expression for it.

One of the first solutions of the energy equation obtained was by assuming that heat was transferred by a mechanism analogous to the transfer of momentum. It is assumed that, analogous to equation (8), the equation for heat transfer in a fluid can be written as

$$\frac{q_r}{C_p \rho A_r} = - (\alpha + \varepsilon_H) \frac{dT}{dy} \qquad (38)$$

where q_r is the amount of heat being conducted and A_r is the surface area across which it is being conducted. Martinelli (15) solved this equation for the following conditions:

(a) Velocity and temperature profiles are fully developed i.e. there are no entrance effects

(b) The fluid properties are constant

(c) There is uniform heat flux along the tube wall

(d) The ratio of ε_H to ε_M is constant.

As in obtaining equations for the velocity profiles, Martinelli assumed the existence of three heat transfer regimes: laminar sub-layer, transition zone and the turbulent core. The results obtained by Martinelli were:

(a) Laminar sub-layer, $y^+ < 5$

$$\frac{T - T_w}{T_c - T_w} = \frac{\frac{\varepsilon_H}{\varepsilon_M} Pr \frac{y}{r}}{\frac{\varepsilon_H}{\varepsilon_M} Pr + \ln (1 + 5 \frac{\varepsilon_H}{\varepsilon_M} Pr) + 0.5 F_1 \ln \frac{Re}{60} \sqrt{\frac{f}{2}}} \qquad (39)$$

(b) Transition zone, $5 < y^+ < 30$

$$\frac{T - T_w}{T_c - T_w} = \frac{\frac{\varepsilon_H}{\varepsilon_M} Pr + \ln\left[1 + \frac{\varepsilon_H}{\varepsilon_M} Pr\left(\frac{y}{y'} - 1\right)\right]}{\frac{\varepsilon_H}{\varepsilon_M} Pr + \ln\left(1 + 5\frac{\varepsilon_H}{\varepsilon_M} Pr\right) + 0.5\, F_1 \ln \frac{Re}{60}\sqrt{\frac{f}{2}}} \quad (40)$$

(c) Turbulent core, $y^+ > 30$

$$\frac{T - T_w}{T_c - T_w} = \frac{\frac{\varepsilon_H}{\varepsilon_M} Pr + \ln\left(1 + 5\frac{\varepsilon_H}{\varepsilon_M} Pr\right) + 0.5\, F_1 \ln \frac{Re}{60}\sqrt{\frac{f}{2}}\,\frac{y}{r_w}}{\frac{\varepsilon_H}{\varepsilon_M} Pr + \ln\left(1 + 5\frac{H}{M} Pr\right) + 0.5\, F_1 \ln \frac{Re}{60}\sqrt{\frac{f}{2}}} \quad (41)$$

where y' = value of y at $y^+ = 5$

Pr = Prandtl number, $C_p \frac{\mu}{k}$

T_c = Temperature at tube center

T_w = Wall temperature

and F_1 is a function of $\frac{\varepsilon_H}{\varepsilon_M}$, Reynolds number and Prandtl number.

These equations and subsequent ones by other workers show the marked effect of the Prandtl number on the temperature profile. It is seen that if the temperature profiles given by equations (39), (40) and (41) are plotted the profiles become flatter the higher the Prandtl number. For a Prandtl number of unity the temperature profile coincides with the velocity profile plotted as $\frac{u}{u_m}$ for the same Reynolds number. For High Prandtl number fluids (ordinary liquids, $Pr > 3$) nearly 80% of the temperature drop occurs in the laminar sub-layer. For these liquids the Reynolds number has little effect on the temperature profile in the turbulent core.

Deissler (8) has solved the energy equation assuming that

$\varepsilon_H = \varepsilon_M$. He has considered the variation of viscosity with temperature and has covered a wide range of Prandtl numbers.

Sleicher (25) has also solved the energy equation for various values of Prandtl numbers. He used the method of separation of variables to solve the equation. For the case of constant wall temperature he obtained the solution

$$\frac{T - T_w}{T_{bl} - T_w} = \sum_s C_s \; R_s \exp\left(-\lambda_s^2 x^*\right) \qquad (42)$$

where R_s is a function of $\frac{r}{r_w}$ and satisfies the equation

$$\frac{d}{d\left(\frac{r}{r_w}\right)}\left[\frac{r}{r_w}\left(\frac{\alpha + \varepsilon_H}{\alpha}\right)\frac{d\,R_s}{d\left(\frac{r}{r_w}\right)}\right] + \lambda_s^2 \frac{u}{U}\frac{r}{r_w} R_s = 0 \qquad (43)$$

λ_s are eigenvalues of this equation, x^* is $\frac{x}{RePr\; r_w}$, C_s's are constants and T_{bl} is the initial bulk temperature of the fluid. Sleicher has given values of λ_s and C_s as functions of Reynolds numbers and Prandtl numbers. The functions R_s have also been tabulated for various values of Reynolds and Prandtl numbers. Sleicher has noted that the ratio $\frac{\varepsilon_H}{\varepsilon_M}$, in addition to being dependent on Reynolds and Prandtl numbers, is also a function of the radius. He has given experimentally calculated values of this ratio for air.

When heat is transferred between a solid boundary and a flowing fluid the rate of heat transfer is given by

$$dq = h_i \, dA_w \, (T_w - T_m) \qquad (44)$$

where dq = differential rate of heat transfer

dA_w = differential wall area across which heat is transferred

T_m = bulk fluid temperature

and h_i is defined as the local heat transfer coefficient. As stated above a laminar film exists at the fluid-solid boundary. Heat transfer across this layer is by molecular conduction alone. Thus the rate of heat transfer can also be expressed as follows:

$$dq = - k A_w \left(\frac{\partial T}{\partial y} \right)_{y = 0} \tag{45}$$

where $\left(\frac{\partial T}{\partial y} \right)_{y = 0}$ is the temperature gradient at the boundary.

Equating the left hand sides of equations (44) and (45) and rearranging the following result is obtained

$$h_i = - \frac{k}{T_w - T_m} \left(\frac{\partial T}{\partial y} \right)_{y = 0} \tag{46}$$

This shows that if an expression for T as a function of y (or r) is available one can evaluate the heat transfer coefficient. Likewise the heat transfer coefficient can be evaluated from the temperature profiles of Martinelli (15) and Sleicher (24).

The average heat transfer coefficient, h, over a length L of the pipe is given by

$$h = \frac{1}{L} \int_0^L h_i \, dx \tag{47}$$

For step changes in the wall temperature at the beginning of the heating section h_i will be very large for small values of L. It will decrease as L increases becoming constant for $L \gg 12 D$ for

high Prandtl number fluids. Similarly the average heat transfer coefficient becomes constant and equal to h_i for $L \geqslant 60\ D$. Considered in the light of equation (46) this means that for L/D $\geqslant 12$ the temperature profile is fully developed and is independent of the distance from the beginning of heating.

From equation (42) Sleicher and Tribus (26) have shown that the fully developed heat transfer coefficient is given by

$$\frac{hD}{k} = \frac{\lambda_0^2}{2} \tag{48}$$

The term $\frac{hD}{k}$ is a dimensionless heat transfer coefficient parameter called the Nusselt number, Nu. The results obtained from equation (48) agree very well with experimental results. Sleicher and Tribus have also shown that for high Prandtl number fluids, the fully developed Nusselt numbers calculated for either constant wall temperature conditions or constant heat flux conditions are the same. This means that the temperature profiles for these cases will also be similar.

A semi-empirical approach to obtain a relation between the heat transfer coefficient and the flow variables of the fluid is based on dimensional analysis. For $L/D \geqslant 60$ it is assumed that

$$h = f\ (D,\ U,\ \rho\ ,\ \mu,\ C_p,\ k) \tag{49}$$

From this the dimensionless groups obtained are the Stanton number, h/C_pG, St, the Reynolds number and the Prandtl number. Experimentally it is found that the exact form of the relationship is

$$St = 0.023\ (Re)^{-0.2}\ (Pr)^{-2/3} \tag{50}$$

Since it is seen that St = Nu/Re Pr, equation (50) can also be written as

$$Nu = 0.023\ (Re)^{0.8}\ (Pr)^{1/3} \qquad (51)$$

These two equations are most frequently used for predicting heat transfer coefficients. Equation (50) is called the Colburn equation and equation (51) the Dittus-Boelter equation. The conditions on these equations are

(a) $L/D > 60$

(b) $Re > 10{,}000$

(c) $0.7 \leqslant Pr \leqslant 100$

When there is a wide difference between the fluid and the wall temperatures, it is found that the best correlation is obtained if the physical properties in the Reynolds and the Prandtl numbers are evaluated at the film temperature, $T_{0.5}$. This temperature is defined as the average of the wall and the bulk fluid temperatures.

Colburn (7) has correlated the heat transfer coefficient to the friction factor by combining equations (50) and (19). The resulting equation is

$$St\ (Pr)^{2/3} = f/2 = j_H \qquad (52)$$

where j_H is called the Colburn j factor for heat transfer.

Reichardt (22) has used a completely theoretical approach to show that

$$St = \frac{(f/2)\ (\phi/\theta)}{1 + (Pr - 1)\ \beta \sqrt{f/2}} \qquad (53)$$

where $$\theta = \frac{U}{u_m}, \quad \phi = \frac{T_w - T_m}{T_w - T_c}$$

and $$\beta = \int_0^{\frac{u_m}{u^*}} \frac{q_{mo}}{q}\, du^+ \qquad (53)$$

q_{mo} being the heat transferred by molecular conduction only. For liquids with high Prandtl and Reynolds numbers the function ϕ may be taken to be ≈ 1. Also for high Reynolds numbers Θ may be taken to be ≈ 0.83. Friend and Metzner (11) have found empirically that

$$= 11.8\ (Pr)^{-1/3} \qquad (54)$$

Substituting this value of β and using $\Theta = 0.83$ and $\phi = 1.0$ Friend and Metzner obtained the equation

$$St = \frac{f/2}{1.2 + 11.8\sqrt{f/2}\ (Pr_w - 1)\ (Pr_w)^{-1/3}} \qquad (54)$$

In this equation the Prandtl number is evaluated at the wall film temperature. This is evident from the nature of the integral which rapidly approaches zero as you move away from the tube wall.

Heat transfer to two phase systems and non-Newtonian liquids.

Most of the research on heat transfer to dispersions is concerned with mixtures of water and steam. Some work has been done on heat transfer to slurries but little has been published on heat transfer to liquid-liquid dispersions.

Orr and Dallavalle (20) studied heat transfer to solid-liquid suspensions and correlated their data by equation (51), all the groups being evaluated with the suspension properties at the bulk

temperatures. Since all properties were evaluated at the bulk temperatures they multiplied the right hand side of the equation by a viscosity correction term, $\left[\frac{\mu_c}{\mu_w}\right]^{0.14}$. Finnigan (10) and Wright (30) have previously done work on heat transfer to the liquid-liquid dispersions studied in this work. Finnigan used equation (51) with the Prandtl number exponent of 0.4 to correlate his results. Wright used equation (50) to correlate his result. Both workers used the dispersion properties to evaluate the Reynolds number, but they used the thermal conductivity of the continuous phase in the Prandtl and Nusselt numbers. There was considerable scatter in their data.

Metzner and Friend (18) studied the problem of heat transfer to non-Newtonian liquids in turbulent flow and used equation (54) to correlate their results. They related the Prandtl number for non-Newtonian fluids to the Prandtl number at the wall by

$$\frac{Pr}{Pr_w} = \left[\frac{16}{Re\ f}\right]^{\frac{n-1}{n}} \left[\frac{3n+1}{4n}\right] \qquad (55)$$

The Reynolds number for non-Newtonian fluids is defined by equation (28) and the Prandtl number is defined by

$$Pr = \left[\frac{C_p}{k}\right] \left[\frac{U}{D}\right]^{n-1} \frac{K}{8} \left[\frac{6n+2}{n}\right]^n \qquad (56)$$

Equation (54) is restricted to

$$\frac{Pr\ Re}{(n)^{0.25}} \sqrt{\frac{f}{2}} > 5000$$

Among the substances they studied were some slurries that behaved as pseudo-plastic liquids.

No published work has been found on the temperature profiles of dispersions or pseudo-plastic materials. Substances behaving in a pseudo-plastic manner are mostly liquids with high non-Newtonian Prandtl numbers. So it can be expected that the turbulent temperature profiles for them will be quite flat.

CHAPTER III

EXPERIMENTAL APPARATUS

A schematic flow diagram of the apparatus used is shown in Figure (1). The dispersion used was contained in the supply tank equipped with a variable speed stirrer. The turbine pump circulated the liquid through the system. From the pump the dispersion flowed through an orifice, the test section, a baffle mixer, a cooler and was then returned to the tank. The liquid used was a dispersion of a commercial solvent (Shell Solv 360) in water. This same system had been used by Finnigan (10), Cengel (4) and Wright (30). The physical properties of the solvent have been studied by Finnigan. A table showing these properties is given in the Appendix. The two liquids are immiscible and on thorough mixing form an unstable milk-white emulsion water being the continuous phase. The solvent was kept uniformly dispersed in water by the combined action of the pump and the stirrer.

The major portions of the apparatus are described below.

Supply Tank, Pump and Cooler

The supply tank and turbine pump were used by Finnigan (10) and are described in detail by him (10, p. 29-32). The cooler was a Ross two-pass shell and tube heat exchanger with cooling water supplied to the tube side.

Piping System

All the piping system, except for the test section, was constructed of standard 2-in. and 1 1/4-in. brass pipe. The test section was a 1-in. OD, 0.830-in. ID copper tube 9 1/2 feet long. It will be described in detail subsequently. A flexible rubber hose was located at the efflux point of the system to facilitate in diverting the flow to a weighing tank. The valve on the by-pass line (no. 2, Figure 1) and the one before the hose were used to adjust the flow rate through the system. A tee with a plug was provided at the lower end of the test section so that the system could be drained independently of the tank.

The orifice used was the same one previously used by Finnigan (10). In some trial runs it was found that the flow rates obtained by weighing the samples did not check with those obtained from Finnigan's calibration. For this reason the orifice was recalibrated and the new calibration curve obtained is given in the Appendix.

Test Section

A view of the test section is shown in Figure (2). To emphasize the part where the probes are introduced it has been shown on an expanded scale. The test section was a straight copper tube 9 1/2 feet long, 1-in. OD and 0.830-in. ID. Holes 1/16-in. in diameter were made at points 2 1/2 feet and 8 1/2 feet from the entrance to the test section. These served as pressure taps to measure the friction loss across 6 feet of the test section. This

positioning gave a calming section of about 36 diameters before the first static pressure tap. This length is far in excess of that required for attaining the fully developed friction factor (12, p. 236).

As shown in Figure (2), a 6 foot length of the test section was heated by steam. The steam jacket was a 3-in. standard iron pipe except at the point where the velocity and temperature probes were introduced into the test section. At this point the jacket was square in cross-section for a length of 4 1/2-in. The heated section of the tube extended from 3 feet to 9 feet from the entrance to the test section. This provided a calming length of about 43 diameters before the beginning of heating. It is usually considered that an entrance length of at least 50 diameters is required before a fully developed velocity profile is obtained (12, p. 236). However it was assumed that for purposes of heat transfer coefficient measurements the velocity profile was fully developed after 43 diameters.

The point velocity was measured by a probe similar to that used by Knudsen and Katz (13). The probe is shown in Figure (3). It was made from stainless steel hypodermic tubing 0.049-in. OD and 0.033-in. ID. The impact measuring hole was circular and about 0.040-in. in diameter. One end of the probe was sealed by an epoxy resin while the other end was sealed into a piece of lucite by the same resin. The probe was calibrated by comparing the average velocity calculated by integrating the measured point velocities over the tube cross-section with the measured average velocity. A 1/4-in.

copper tube led from the lucite to the differential manometers. Marks were made on both ends of the probe so that after insertion it could be turned to point the opening directly upstream. The impact tube was located on the same diameter as a pressure tap and the velocity head of the flowing fluid was measured by a differential manometer connected between the impact tube and the pressure tap.

The temperature probe used is shown in Figure (3). The thermocouple was made of 36 gage iron and constantin wires. The hypodermic tubing used was the same as that for the velocity probe described above. After the tubing was bent, the thermocouple wires were threaded through it with the cloth covering on so that they were insulated from the tubing. The bead was then made on the thermocouple wires and the lower part of the bead and the exposed part of the wires were covered with Glyptol. The wires were then pulled back into the hypodermic tubing so that only the top of the bead was slightly above the tubing. The thermocouple was checked to make certain it was insulated from the tubing. The calibration was also checked at a few points and was found to agree with the published standard values (14). A mark was also made on the thermocouple probe so that once inserted into the test section it could be turned facing upstream.

The velocity and the temperature probes were inserted into the tube at a point 8 1/2 feet from the entrance to the test section. This part of the test section is shown in detail in Figure (4). Two diametrically opposed holes 1/16-in. in diameter were provided

for the insertion of the velocity probe. Packing glands, as shown in Figure (4) were silver soldered on these holes. Neoprene rubber gaskets were used as packing material. The threaded 1/4-in. diameter, 2 3/4-in. long rods were used to press the packing firmly in place and to protect the probe from the steam. The packing gland for the temperature probe was similar to those made for the velocity probe and is also shown in Figure (4). The threaded rod was 3/8-in. in diameter. The hole for the temperature probe was 7/32-in. in diameter and was located so that the temperature probe was about 1/8 inch above the velocity probe. It was opposite the static pressure tap and at right angles to the velocity probe. In this way the two probes would not interfere with each other. For clarity in Figure (4), both probes are shown to be at the same level.

The steam jacket was a rectangular box where the probes were introduced. Square plates of 1/4-in. sheet iron, with 5 1/2-in. sides and with a 3 1/2-in. diameter hole in the center were welded on the steam jacket at points shown in Figure (2). Plates of 1/4-in. sheet iron each 4 1/2-in. by 6-in. were bolted to the welded base plates. The probe sleeves, the static pressure line and the thermocouple wire were brought out of the steam jacket through holes in these plates. Each of these plates could be removed individually so that adjustments on the probe sleeves and packings could be made.

Traversing Mechanism

The probes were moved by a traversing mechanism shown in Figure (5). Each mechanism was screwed to the appropriate plate of the jacket. The probe passed through a hole in the moving block which was moved by the turning screw. The probe was held in place in the moving block by two screws in the block. A Tumico dial gage was used to give the position of the block and hence that of the probe. The gage had a travelling distance of one inch and a smallest division of 0.0005 inch.

The Pressure Measuring System

All pressure differences were measured with differential manometers. To cover the wide range of differences, manometers with various liquids were used. The manometer system is shown schematically in Figure (6). Copper tubing, 1/4 inch in diameter, was used as the pressure transmitting line and water was used as the pressure transmitting liquid. About three feet of horizontal tubing was provided at each pressure tap to eliminate the possibility of the dispersion getting into the vertical portion of the tubing. As shown in Figure (6) provision was made for flushing the tubing with water. Needle valves were provided at appropriate places so that the manometers could be isolated from the system and flushed individually or simultaneously. This permitted the removal of any dispersion that may have entered the lines.

For measuring the pressure drop across the orifice two manometers, one with mercury and the other with an oil of a specific

gravity of 2.94, were used. The velocity head and the friction loss across the test section were measured by a set of three manometers, one with mercury another with the 2.94 specific gravity oil and an inclined one with an oil of a specific gravity of 1.75. Appropriate valves were provided to obtain the required differential pressure readings. Since all these liquids were under water in the manometers, the density used in calculating the pressure differentials was the density of the appropriate liquid minus the density of water. The equivalent density of the manometer liquids is given in the Appendix.

The Temperature Measuring System

The bulk temperature rise due to heating of the dispersion was measured by two thermometers calibrated to 0.2° F. These were placed in the thermometer wells shown in Figure (1). The wall temperature of the heated test section was measured by thermocouples made of 30 gage iron and constantan wire. The wall thermocouples were placed in grooves 1 1/2-in. long and 1/16-in. deep and 1/8-in. wide machined on the outside of the test section wall at distances of 5, 24, 42 and 63 ins. from the beginning of the heated section. The last of these grooves was just above the point where the temperature probe was introduced. Two thermocouples were placed in each groove and then soldered in place. As mentioned above the temperature probe also contained a thermocouple.

A schematic diagram of the thermocouple system is shown in

Figure (7). The numbering of the thermocouples used in presenting the data is also given in this Figure. The distances beside the thermocouples give the distance the thermocouple is from the start of the test section. A Leeds and Northrup (No. 737621) potentiometer with a rated accuracy of 0.05% and a smallest division of 0.001 millivolt was used to measure the E.M.F.s generated.

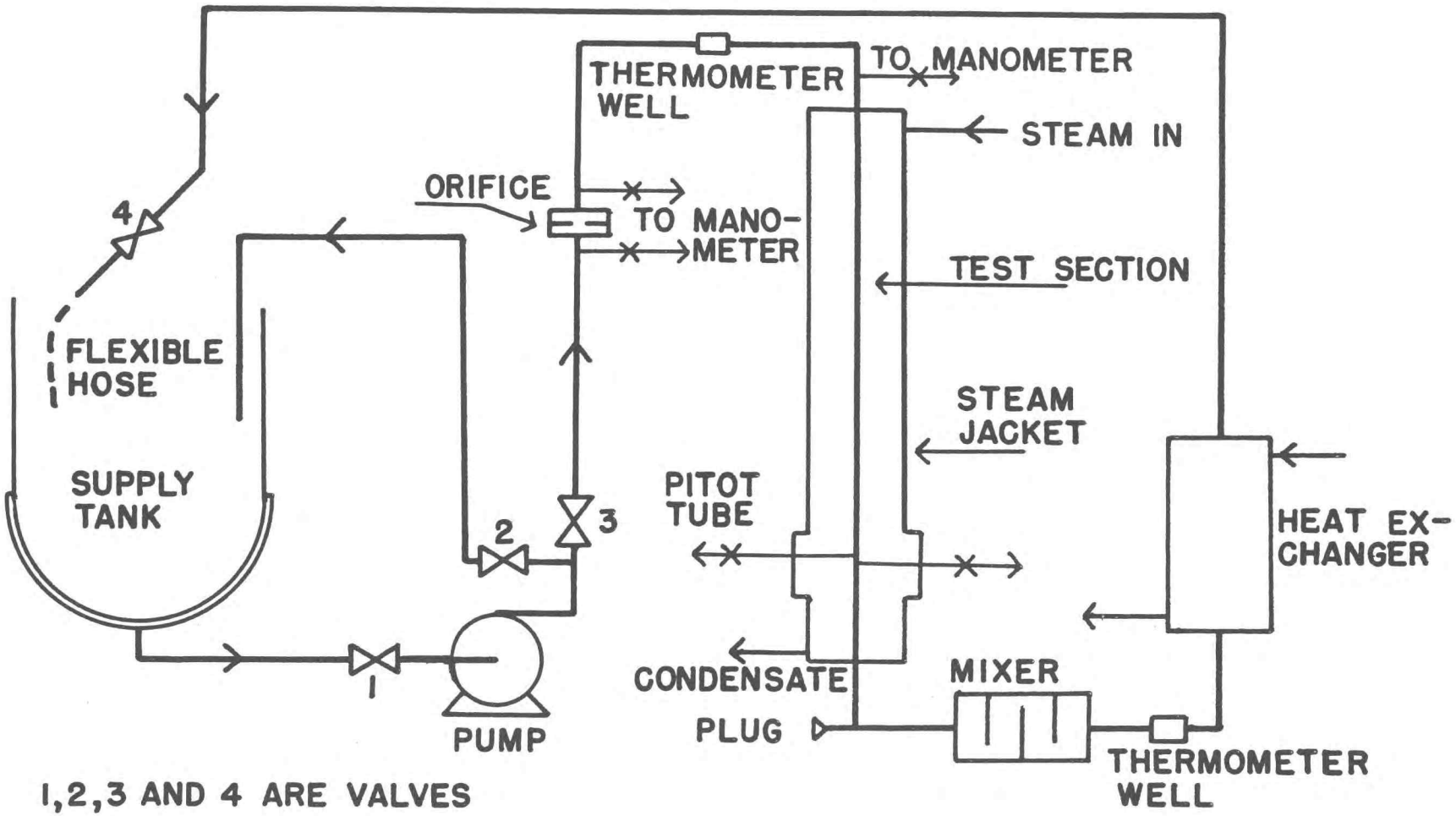

FIGURE 1 SCHEMATIC FLOW DIAGRAM

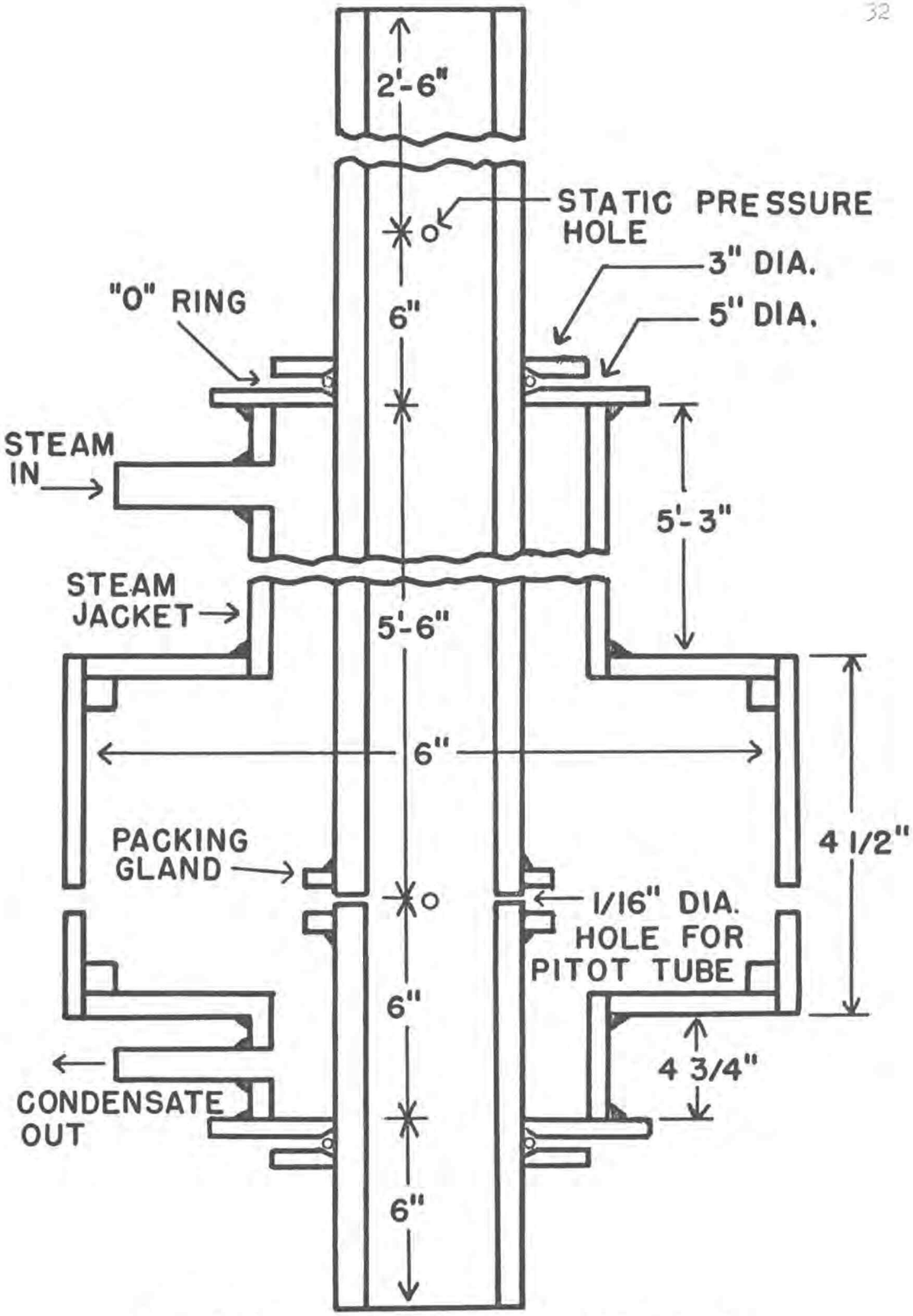

DETAIL OF TEST SECTION
FIGURE 2

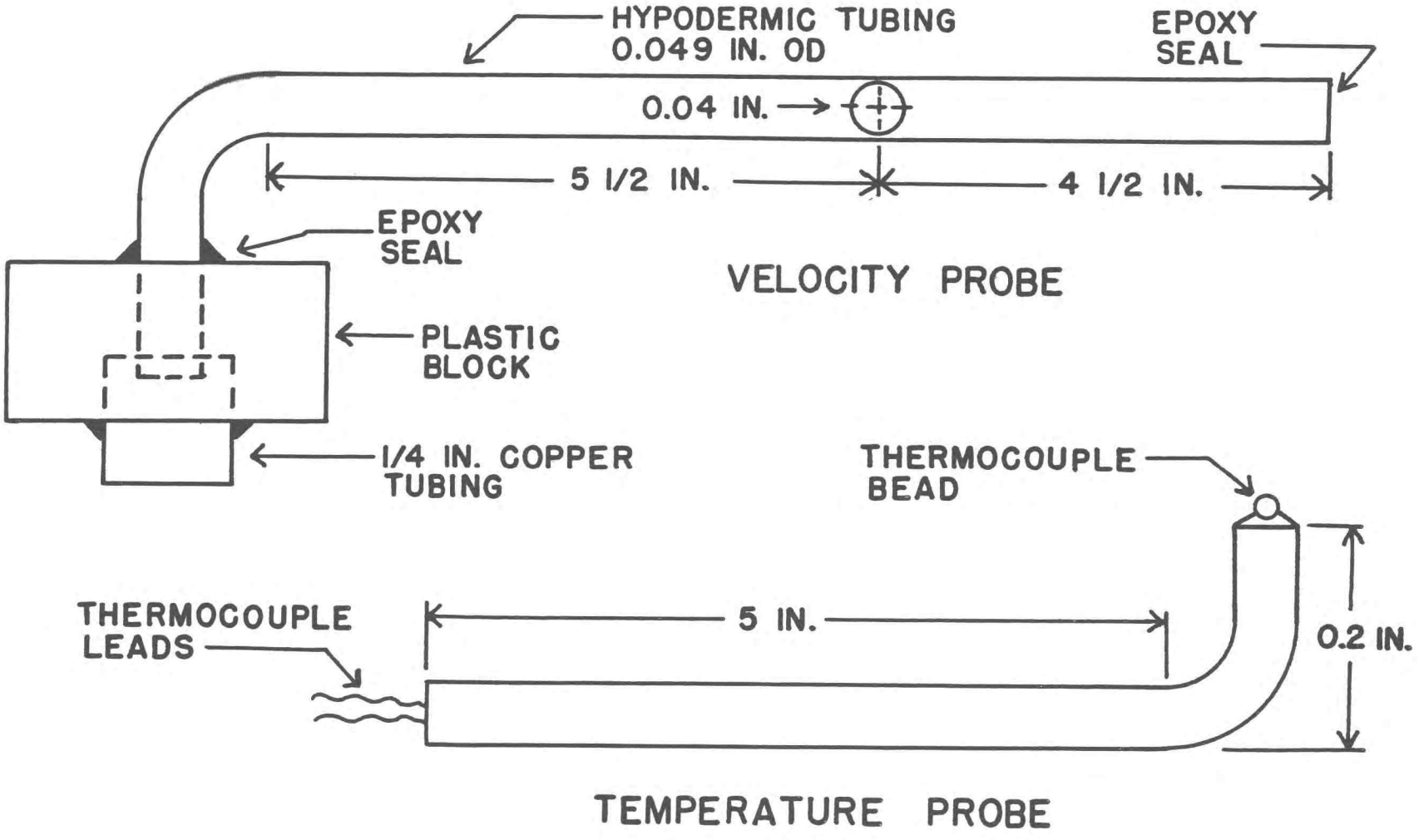

FIGURE 3 VELOCITY AND TEMPERATURE PROBES

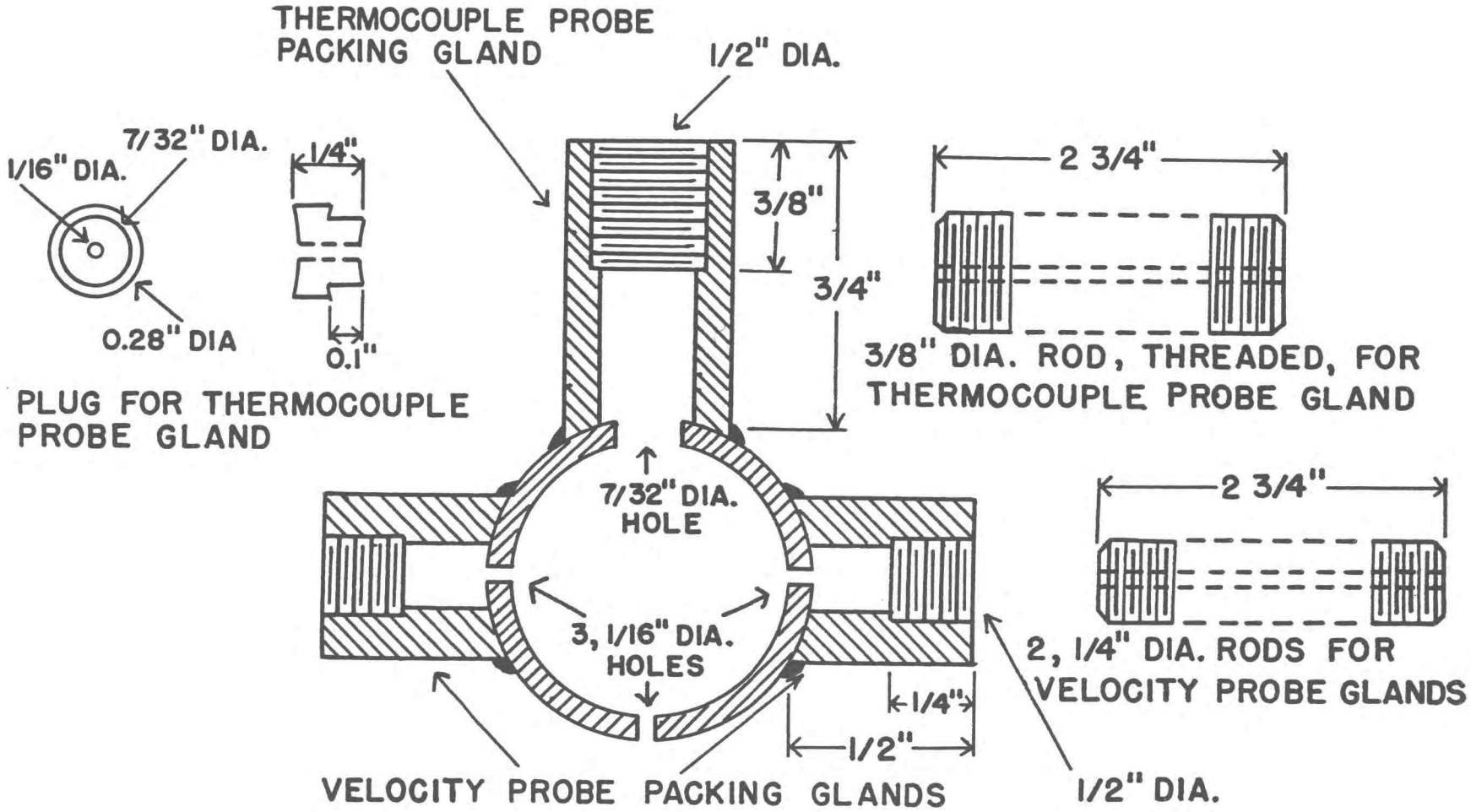

FIGURE 4 DETAIL OF PACKING GLANDS

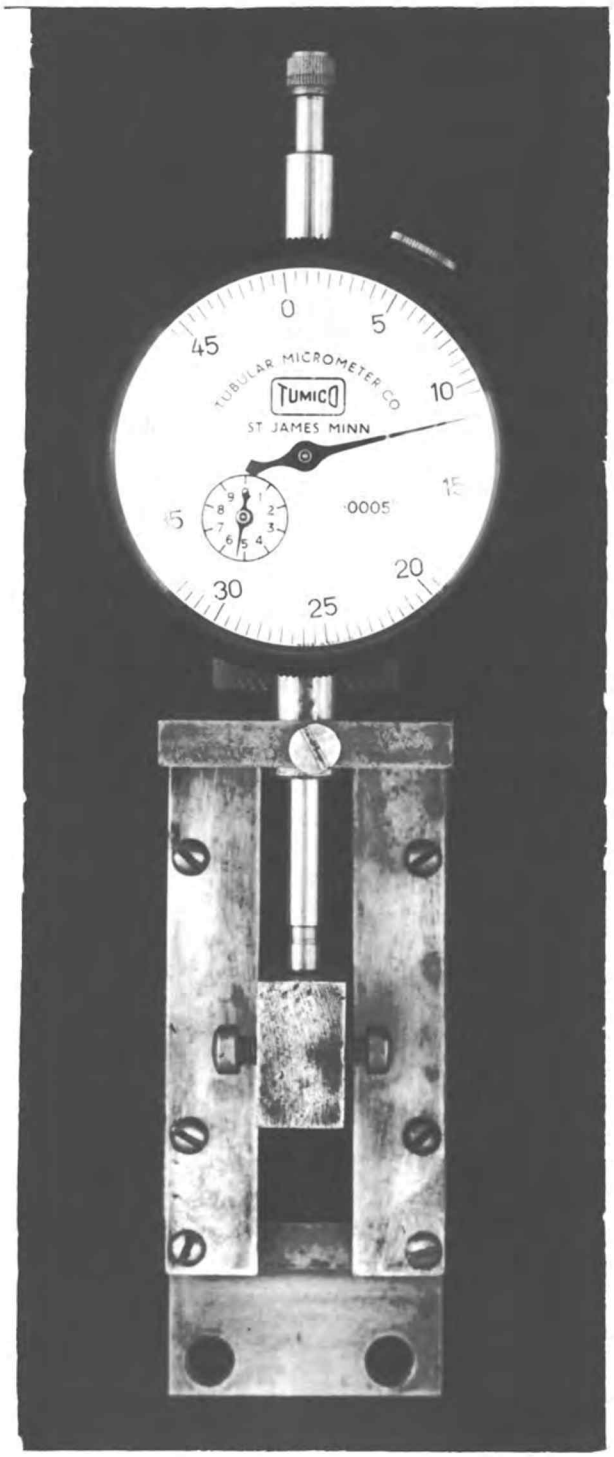

FIGURE 5 TRAVERSING MECHANISM

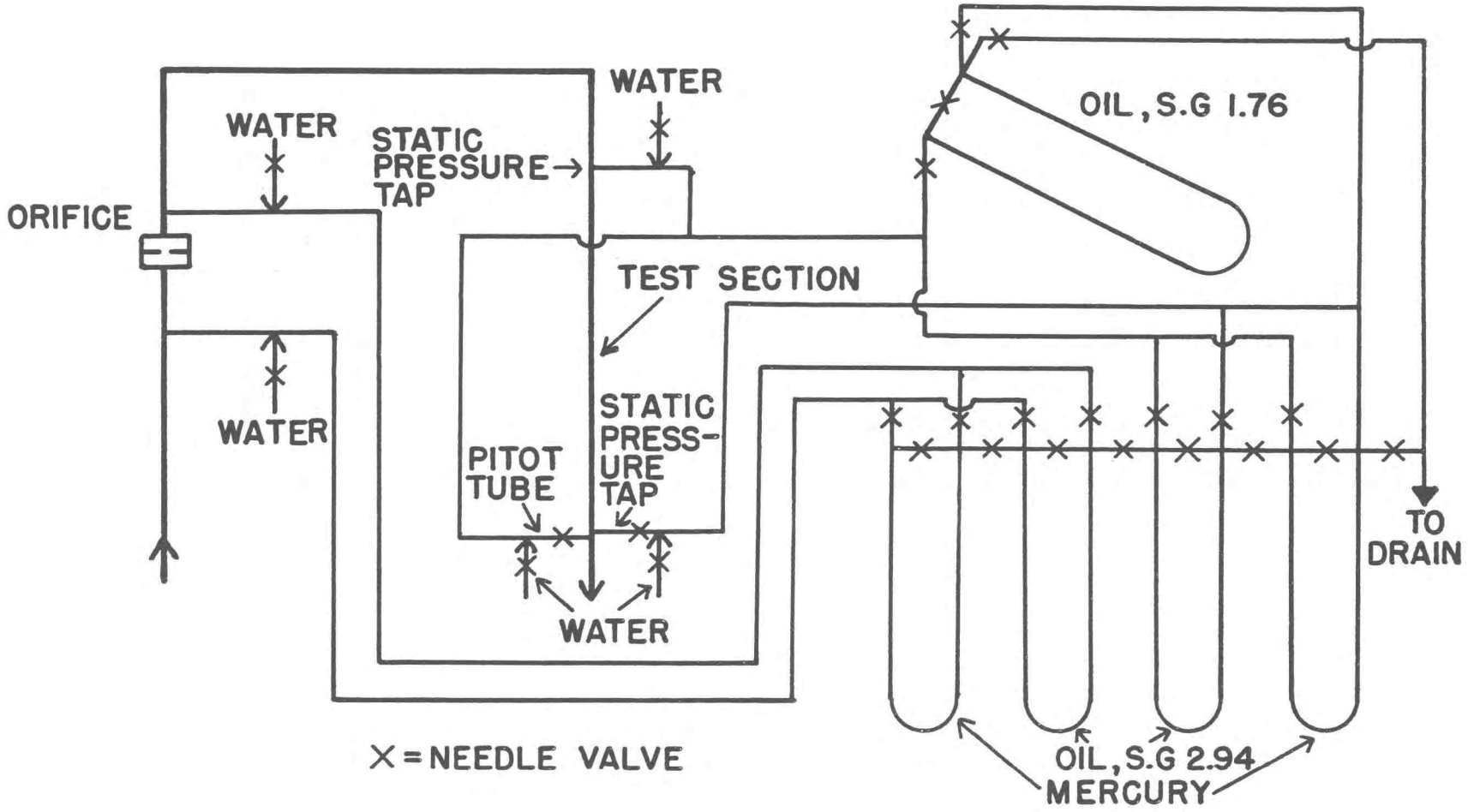

FIGURE 6 MANOMETER SYSTEM

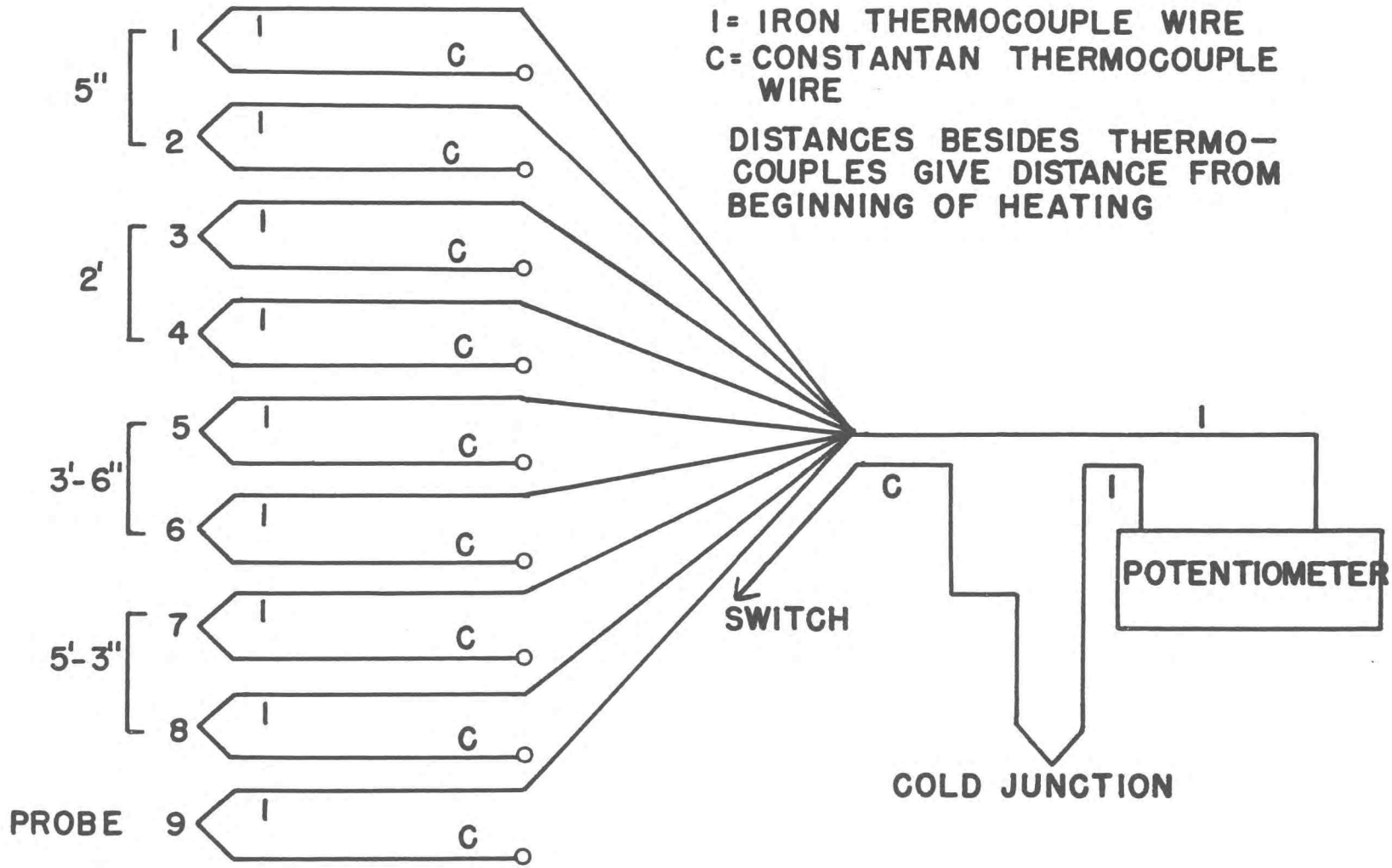

FIGURE 7 THERMOCOUPLE SYSTEM

CHAPTER IV

EXPERIMENTAL PROGRAM

The main purpose of the experiments was to obtain data for calculating the velocity and temperature profiles for turbulent flow of various dispersions of a commercial solvent in water. It was also proposed to measure the pressure drop across the test section, the heat transfer coefficient and to calibrate the orifice. Velocity profile, temperature profile, heat transfer and pressure drop data were also taken with water as a means to determine if the equipment was functioning properly.

Table (1) gives a resume of the various dispersion concentrations and flow rates studied. The Table also gives the actual concentrations of the dispersions used. The run number to be used in further reference to a particular run is also given. For each dispersion studied data were also taken for calculating the friction losses over a flow rate range of 1 lb./sec. to 3 lb./sec. These runs were labelled such that the first two digits referred to the nominal concentration and the third to the run number in that concentration, e.g. 20-4 referred to the fourth run with the 20% dispersion.

For calculating the velocity profile the data taken were (a) the manometer deflection, ΔH_v, due to the difference between the impact and the static pressures and (b) the distance away from the wall, y. These data were taken across the diameter of the tube for

TABLE 1.

Experimental Program

Run No.	Solvent Concentration (Volume %)	Flow Rate (lbs./sec.)	Data taken
w-A	0	1.040	Velocity profile
W-B		1.512	" "
W-C		2.069	" "
W-D		2.102	" "
W-E		3.000	" "
W-F		3.069	" "
W-G		1.026	Temperature profile and heat transfer
W-H		1.066	" " " " "
W-I		2.174	" " " " "
W-J		3.077	" " " " "
W-K		3.015	" " " " "
10-A	8.5	1.007	Velocity profile, temperature profile and heat transfer
10-B	"	1.961	" " " " " " "
10-C	"	2.941	" " " " " " "
20-A	19.6	0.997	" " " " " " "
20-B	"	1.983	" " " " " " "
20-C	"	2.948	" " " " " " "
35-A	34.4	1.000	" " " " " " "
35-B	"	2.020	" " " " " " "
35-C	"	2.956	" " " " " " "
50-A	49.2	1.100	" " " " " " "
50-B	"	2.000	" " " " " " "
50-C	"	2.956	" " " " " " "

isothermal conditions, the temperature being kept at $67^{\circ} \pm 2^{\circ}$ F. Similarly, for calculating the temperature profile the probe thermocouple reading, T_9, at various distances from the wall was noted. This traverse was taken only across half the diameter of the tube. Heat transfer coefficient measurements were made by noting the wall temperatures, T_1 through T_8, and the inlet and outlet bulk temperatures, T_{b1} and T_{b2}, of the dispersions. The friction loss data were taken by noting the manometer deflection, ΔH_T, due to pressure loss across the test section and then noting the flow rate by weighing a sample of the dispersion flowing through the test section. At the same time the deflection of the orifice manometer, ΔH_o, was also noted for calibrating the orifice meter.

CHAPTER V

EXPERIMENTAL PROCEDURE

Before the dispersion was introduced into the system, the whole system was thoroughly flushed with water and drained. Water and solvent were added to the supply tank in the ratio needed to make a dispersion of the desired concentration. The pump and the stirrer were used to mix the two liquids. It usually required about an hour and a half of mixing to form the uniform dispersion. The manometers were flushed to remove any air or solvent that might have entered the manometer lines.

When a uniform dispersion had been obtained data for calibrating the orifice and for calculating the friction loss over the test section were obtained. Flow was adjusted to the lowest value to be studied (about 0.9 lbs./sec.). The deflections on both the orifice manometers, ΔH_O, and the friction loss manometer, ΔH_T, were noted. To obtain the exact flow rate, the flow from the test section was diverted to a weighing tank and the time taken to collect a known weight of the liquid, usually 60 lbs., noted. The liquid collected was returned to the supply tank and the flow rate increased by about 0.2 to 0.3 lbs./sec. This procedure was repeated up to a flow rate of about 3 lbs./sec. During the runs the manometers were periodically flushed. The temperature of the mixture was kept at $67^\circ \pm 2^\circ$ F. by controlling the cooling water rate. After the data had been taken two 500 ml. samples of the mixture were taken, one

each from the supply tank and the hose where the liquid returns to the tank. These were allowed to separate overnight so that the exact concentration of the dispersion could be obtained. In no case was there any difference in the concentrations of the samples taken from the two points thus showing that the dispersions were uniform in concentration.

Velocity profile data were collected for isothermal conditions, the temperature being kept at $67^{\circ} \pm 2^{\circ}$ F. After the liquids had been thoroughly mixed and the manometers flushed, the flow was adjusted to the required value. Then the velocity probe was moved till the manometer deflection, ΔH_v, was zero. This gave the position where the hole in the probe was just outside the tube. In this way the position of the tube wall was fixed. It was found that this method of positioning the probe was quite accurate: zero readings could be duplicated to about 0.003 in. The probe was then moved into the stream and the manometer deflection, ΔH_v, and the distance y noted. This distance was given by the reading on the dial gage. It took from 3 to 10 minutes for the manometer to become steady. The greater time was taken for the low flow rates. The 1.75 specific gravity oil inclined manometer was used for the 1 lb./sec. flow rates and the 2.94 specific gravity oil manometer for the higher rates. The velocity traverse was taken across the diameter of the tube and in each traverse about 25 point velocities were measured. During the traverse the manometers were flushed occasionally. The position of the other wall was also found by

noting the position of zero deflection. The difference between the position of these two zero readings gives the diameter of the tube plus the diameter of the probe hole. The diameter of the tube calculated this way varied from 0.829 in. to 0.832 in. comparing very well with the measured value of 0.830 in.

After completing the velocity profile run, steam was introduced into the steam jacket. The cooling water rate and the steam rate were adjusted such that the outlet temperature, T_{b2}, was about 105° F. It was assumed that steady state conditions had been attained when the temperatures T_{b1} and T_{b2} did not change by more than 0.2° F. in 10 minutes. It took about an hour and a half from the introduction of steam to reach steady state. The temperature profile data was taken after steady state had been attained. The temperature probe was moved such that its tip was adjacent to the tube wall farthest away from the point where the probe was introduced into the tube. This was done by loosening the probe from the block of the traversing mechanism and moving it till its tip hit the wall. The probe was then tightened in place in the block. Since the hypodermic tubing was 0.05-in. in diameter it was assumed that in this position the thermocouple was 0.025 in. from the wall. The probe thermocouple reading was taken in this position and then the probe was moved away from the wall and the thermocouple reading was again taken and the probe position noted. This was repeated until the probe had passed the center of the tube. The probe was then moved back to its original position near the wall, readings being

taken at the same values of y. It was found that any two corresponding readings (i.e., readings at the same value of y taken going away from the wall and coming towards it) did not vary by more than 0.2° F. Sometimes it was found that the temperatures T_{b1} and T_{b2} had changed during the traverse. In this case the corresponding readings of the probe differed considerably so the traverse was repeated. After the traverse had been completed the various wall temperatures (T_1 to T_8) and the fluid temperatures (T_{b1} and T_{b2}) were noted. The steam was then shut off and when the dispersion had cooled down, the cooling water, the stirrer and the pump were shut off. The temperature probe was retracted so that it would not interfere with the next velocity profile.

The observed and calculated data are tabulated in the Appendix.

CHAPTER VI

SAMPLE CALCULATIONS

Pressure Drop and Friction Factor

The pressure drop across the test section, ΔP_T, was calculated from the manometer deflection, ΔH_T, and the effective density of the manometer liquid, ρ_m. The expression used was

$$-\Delta P_T = \underline{K} (\Delta H_T) \rho_m$$

where $\underline{K}$ converts ΔH_T to feet. Since the test section was vertical with liquids of different densities in the pressure transmission lines and the test section, part of the pressure drop, ΔP_T, was due to the static pressure difference, ΔP_s. If the length of the test section is L, the density of the liquid in the test section is ρ_e and the density of the pressure transmission liquid (water) is ρ_w, then

$$\Delta P_s = L (\rho_e - \rho_w)$$

Since in this case dispersions were flowing in the test section, ρ_e was simply the density of the solvent and water comprising the dispersion. The friction loss, P_f, was then

$$-\Delta P_f = -\Delta P_T + \Delta P_s = (\Delta H_T) \rho_m \underline{K} + L(\rho_e - \rho_w)$$

The friction factor is calculated by

$$f = \frac{g_c D}{2 \rho_e U^2} \left(- \frac{\Delta P_f}{L} \right)$$

Since the velocity, U, is related to the mass flow rate, w, by

$$U = \frac{4w}{\pi D^2 \rho_e}$$

one can write

$$f = \frac{\pi^2 g_c D^5}{32L} \left(-\frac{\Delta P_f}{w^2} \right) \rho_e . \qquad (57)$$

Since D = 0.830 in. and L = 6 ft.,

$$f = (10^{-3})\ (2.603) \left(-\frac{\Delta P_f}{w^2} \right) \rho_e .$$

A sample calculation for run number 20-3 showing the use of these equations is given below. The temperature of the dispersion was 67° F. and that of the manometer board 73° F. At these temperatures, for the 2.94 oil manometer, ρ_m = 120.55 lbs. per cu. ft., ρ_w = 62.29 lbs. per cu. ft. and ρ_s = 48.85 lbs. per cu. ft. From these values ρ_e was found to be 59.60 lbs. per cu. ft. ΔH_T measured for the run was 19.5 cm. on the 2.94 oil manometer and w was 1.183 lbs. per sec. Then

$$\Delta P_s = 6.0\ (59.60 - 62.29) = -16.13 \text{ lbs./sq. ft.}$$

and $$-\Delta P_T = (0.03281)\ (19.5)\ (120.55) = 77.13 \text{ lbs./sq. ft.}$$

So $$-\Delta P_f = 77.13 - 16.13 = \underline{61.00 \text{ lbs./sq. ft.}}$$

Hence $$f = (10^{-3})\ (2.603) \left[\frac{(61.00)\ (62.29)}{(1.183)\ (1.183)} \right] = \underline{0.00680}.$$

Velocity profile

The terms to be calculated for presenting the velocity profile data were u^+, $y^+ \mu_m$, $\frac{u}{u_m}$ and $\frac{y}{r_w}$. The point velocity, u, is given by

$$\frac{u^2 \rho_e}{2g_c} = c^2 \rho_m \underline{K} \Delta H_v \quad \text{or} \quad u = c \sqrt{2g_c \underline{K} \frac{\rho_m}{\rho_e} \Delta H_v} \qquad (58)$$

where c is the calibration constant and $\underline{K}$ converts ΔH_v to feet. The

calibration constant was found by dividing the observed average velocity, U, with the calculated average velocity, U_c.

$$U_c = \frac{1}{A_c} \int_0^{r_w} 2\pi r u dr = \frac{2}{r_w^2} \int_0^{r_w} urdr = 11.61 \int_0^{r_w} urdr$$

with r and r_w expressed in inches.

The Reynolds number was calculated by

$$Re = \frac{DG}{\mu_m} = \frac{4w}{D\mu_m} = (10^4)\ (2.741)\ \frac{w}{\mu_m}$$

where the viscosity μ_m is expressed in centipoises. The expressions used for calculating u^+ and $y^+ \mu_m$ were

$$u^+ = \frac{u}{U\sqrt{\frac{f}{2}}} \qquad (22)$$

and $$y^+ \mu_m = \frac{Re\sqrt{f/2}\ \mu_m}{D}\, y = \frac{(10^4)\ (2.741)\ (w)\sqrt{f/2}}{D}\, y \qquad (59)$$

The friction factors were read off from Figure (11). The evaluation of $\frac{u}{u_m}$ and $\frac{y}{r_w}$ is straight forward.

The calculations for these terms were made with the aid of the ALWAC-III digital computer. The integration for evaluating U_c was also performed by the computer. The trapezoidal rule was used to evaluate the integral numerically. For each run the terms $\sqrt{2g_c K \frac{\rho_m}{\rho_e}}$, $\frac{(10^4)\ (2.741)\ (w)\sqrt{f/2}}{D}$, $\frac{1}{U\sqrt{f/2}}$ and the whole set of ΔH_v and y values were supplied to the computer. Using the expressions given above the computer gave the quantities, $\frac{u}{u_m}$, $\frac{y}{r_w}$, $\frac{u}{c}$, $y^+ \mu_m$ and U_c. From the calculated U_c value the constant c was

evaluated and the values u^+ obtained. All the observed data and the calculated results are given in the Appendix.

Heat transfer and temperature profile

The average heat transfer coefficient, h, was calculated from the expression

$$q = h\,A\,(\Delta T)_m$$

where $(\Delta T)_m$ is the mean temperature difference between the wall and the fluid. The heat transferred, q, was found by the expression

$$q = 3600\ w\ C_{pe}\ (T_{b2} - T_{b1})$$

where C_{pe}, the heat capacity of the dispersion was evaluated from the weighted average of the heat capacities of the solvent, C_{ps}, and water, C_{pw}. Substituting the numerical value for A the expression for h becomes

$$h = 2761\ C_{pe}\ \frac{w(T_{b2} - T_{b1})}{(\Delta T)_m}$$

The Stanton number was calculated from

$$St = \frac{h}{GC_{pe}} = \frac{h\,\pi\,D^2}{14400\ w\ C_{pe}} = (10^{-3})\ (2.882)\ \left[\frac{(T_{b2} - T_{b1})}{(\Delta T)_m}\right]$$

The above shows that no physical properties were involved in the evaluation of the Stanton number.

The mean temperature difference was evaluated by taking the weighted average temperature difference between the wall and the fluid. For this calculation it was assumed, as an approximation, that the temperature rise in the fluid was linear with distance.

The thermocouples, T_1 and T_2 gave the wall temperature at a distance L_1 from the beginning of heating; T_3 and T_4 gave the temperature at a distance L_2; T_5 and T_6 gave the temperature at a distance L_3; and T_7 and T_8 gave the temperature at a distance L_4. The average of each set of these temperature readings was called T_A, T_B, T_C and T_D respectively. As an approximation it was assumed that the wall temperature at the start of the heating section was T_A and that at the end was T_D. Knowing the temperature of the fluid at the beginning and the end of the test section, the temperature of the fluid at the points L_1, L_2, L_3 and L_4 was found by linear interpolation. These temperatures were called, respectively, T_{m1}, T_{m2}, T_{m3} and T_{m4}. The mean temperature was then evaluated by

$$(\Delta T)_m = \frac{L_1}{2L}\left[(T_A - T_{b1}) + (T_A - T_{m1})\right]$$
$$+ \frac{(L_2 - L_1)}{2L}\left[(T_A - T_{m1}) + (T_B - T_{m2})\right]$$
$$+ \frac{(L_3 - L_2)}{2L}\left[(T_B - T_{m2}) + (T_C - T_{m3})\right]$$
$$+ \frac{(L_4 - L_3)}{2L}\left[(T_C - T_{m3}) + (T_D - T_{m4})\right]$$
$$+ \frac{(L - L_4)}{2L}\left[(T_D - T_{m4}) + (T_D - T_{b2})\right]$$

After substituting the numerical values for the various lengths this became

$$(\Delta T)_m = \frac{0.0695}{2}\left[(T_A - T_{b1}) + (T_A - T_{m1})\right]$$
$$+ \frac{0.2639}{2}\left[(T_A - T_{m1}) + (T_B - T_{m2})\right]$$
$$+ \frac{0.250}{2}\left[(T_B - T_{m2}) + (T_C - T_{m3})\right]$$
$$+ \frac{0.2917}{2}\left[(T_C - T_{m3}) + (T_D - T_{m4})\right]$$
$$+ \frac{0.1250}{2}\left[(T_D - T_{m4}) + (T_D - T_{b2})\right]$$

There was considerable difference between the wall temperatures from the beginning to the end of the heated section. T_1 and T_2 were of the order of 160° F. while T_7 and T_8 were of the order of 125° F. The difference between temperatures read by any two thermocouples at the same wall position, except for T_1 and T_2, was of the order of 1° to 2° F. However the difference between T_1 and T_2 was usually higher, being of the order of 3° to 4° F.

The Reynolds number was calculated, as shown above, by

$$Re = (2.741)\ (10^4)\left(\frac{w}{\mu_m}\right)$$

The viscosity used was that calculated from the velocity profile data. The procedure for this will be explained later.

The Prandtl number used was that of water at the film temperature. It was assumed that the film temperature was 120° F. for all runs. This was the approximate arithmetic mean of the average fluid and the wall temperature. At this temperature the Prandtl number for water is 3.66.

For presenting the temperature profile data

the terms $(T - T_w)/(T_c - T_w)$ and y/r_w were evaluated. The calculation of these terms was straight forward. The wall temperature used was the average of T_7 and T_8.

An example showing the numerical calculation of the heat transfer coefficient, the Stanton number and the Reynolds number is given below. The run considered is number 20-A. The observed data were: $w = 0.997$ lbs./sec., $T_1 = 163.7^\circ$ F., $T_2 = 167.1^\circ$ F., $T_3 = 154.5^\circ$ F., $T_4 = 152.0^\circ$ F., $T_5 = 143.5^\circ$ F., $T_6 = 145.1^\circ$ F., $T_7 = 121.0^\circ$ F., $T_8 = 123.4^\circ$ F., $T_{b1} = 80.3^\circ$ F. and $T_{b2} = 105.8^\circ$ F. From the inlet and outlet fluid temperatures the fluid temperatures at various points in between were evaluated. These temperatures were:

$T_{m1} = 82.1^\circ$ F., $T_{m2} = 88.8^\circ$ F., $T_{m3} = 95.2^\circ$ F. and $T_{m4} = 102.7^\circ$ F.

$$\text{Then } (\Delta T)_m = 0.0695 \left(\frac{85.1 + 83.3}{2}\right) + 0.2639 \left(\frac{83.3 + 64.5}{2}\right)$$
$$+ 0.250 \left(\frac{64.5 + 49.1}{2}\right) + 0.2917 \left(\frac{49.1 + 19.5}{2}\right)$$
$$0.125 \left(\frac{19.5 + 16.4}{2}\right) = \underline{51.8^\circ \text{ F.}}$$

for the 20% dispersion

$$C_{pe} = (0.161)\ (0.479) + (1 - 0.161)\ (1.00) = 0.916 \text{ BTU/lb. } ^\circ\text{F.}$$

$$\text{Then } h = (2761)\ (0.997)\ (0.916) \left[\frac{(105.8 - 80.3)}{51.8}\right]$$

$$= \underline{1240 \text{ BTU/hr. sq. ft. } ^\circ\text{F.}}$$

$$St = (10^{-3})\ (2.883) \left[\frac{(105.8 - 80.3)}{51.8}\right] = \underline{(1.418)\ 10^{-3}}$$

$$St(Pr)^{2/3} = (1.418)\ (10^{-3})\ (2.41) = \underline{(3.417)\ 10^{-3}}$$

The calculated viscosity was 1.69 cp.

$$\text{So} \quad Re = (2.741)\ (10^4) \left(\frac{0.997}{1.69} \right) = \underline{(1.618)\ 10^4}$$

All the observed and calculated heat transfer data are given in the Appendix.

Estimation of Experimental Errors

The experimental errors involved in calculating the various quantities given above can be estimated by taking the differentials of the quantities involved. The error in the friction factor is estimated by taking the differential of equation (57), assuming there is negligible error involved in measuring ρ_e and L.

$$df = \frac{\pi^2 g_c \rho_e}{32L} \left\{ \left[\left(-\frac{\Delta P_f}{w^2} \right) 5D^4 dD \right] + \left[D^5 \left(\frac{d(-\Delta P_f)}{w^2} \right) \right] - 2\, D^5 \left(-\Delta P_f \frac{dw}{w^3} \right) \right\}$$

$$\text{or} \quad \frac{df}{f} = \frac{5dD}{D} + \frac{d(-\Delta P_f)}{-\Delta P_f} - 2\frac{dw}{w}$$

The error in measuring D was of the order of $\pm$ 0.004 in. or about $\pm$ 1/2% since D = 0.830 in. The scales used to weigh the samples were accurate to $\pm$ 1/2%, hence the error in w, 100(dw/w), was approximately $\pm$ 1/2%. The error in the manometer readings and hence in P_f may be assumed to be about $\pm$ 1%. So

$$\frac{df}{f} = \pm (.025 + .01 \pm .01) = \underline{\pm .045}$$

In other words the error in calculating f is of the order of $\pm$ 4.5%.

From equation (58) it is seen that the error in u/u_m can be estimated by

$$\frac{u}{u_m} = \left(\frac{\Delta H_v}{\Delta H_{vm}} \right)^{1/2}$$

where ΔH_{vm} is the maximum value of ΔH_v. The error in observing ΔH_v was of the order of $\pm 1\%$. So the error in the reduced velocity is

$$\frac{d(u/u_m)}{u/u_m} = \frac{1}{2}\frac{d(\Delta H_v)}{\Delta H_v} - \frac{1}{2}\frac{d(\Delta H_{vm})}{\Delta H_{vm}} = \pm\frac{1}{2}(.01 + .01) = \pm \underline{\underline{0.01}}$$

The error in observing y was about $\pm$ 0.002 in. while the error in measuring r_w was, as stated above, about $\pm 1/2\%$. So the error in y/r_w is given by

$$\frac{d(y/r_w)}{y/r_w} = \frac{0.002}{r_w(y/r_w)} - \frac{dr_w}{r_w} = \pm\left(\frac{0.0048}{y/r_w} + 0.005\right)$$

This shows that the error depends on y/r_w. For small values of y/r_w the error is large while for large y/r_w values the error is small, e.g., for $y/r_w = 0.1$ the error is about $\pm 5\ 1/2\%$ while for $y/r_w = 0.9$ it is about $\pm 1\%$.

The error in calculating u is also given by equation (58). The error in calculating c is of the order of 2%. So

$$\frac{du}{u} = \frac{dc}{c} + \frac{1}{2}\frac{d(\Delta H_v)}{\Delta H_v} = \pm(0.02 + 0.005) = \pm \underline{\underline{0.025}}$$

The error in u^+ is then given by

$$\frac{du^+}{u^+} = \frac{du}{u} - \frac{du}{U} - \frac{1}{2}\frac{df}{f} \approx \pm(0.025 + 0.003 + 0.020) \approx \pm \underline{\underline{0.05}}$$

The variables involved in calculating the heat transfer coefficient and the Stanton number are w, $(T_{b2} - T_{b1})$ and $(\Delta T)_m$. The error in measuring w was, as stated before, of the order of $\pm 1/2\%$. The error in $(T_{b2} - T_{b1})$ was of the order of $\pm 0.4^\circ$ F. Since $(T_{b2} - T_{b1})$ was usually 20° F., the percentage error in

$(T_{b2} - T_{b1})$ was $\pm 2\%$. The wall temperatures were in error by about $\pm 2.5^\circ$ F. Since usually $(\Delta T)_m$ was about 50° F., the percentage error in $(\Delta T)_m$ was $\pm 5\%$. So the error in h is

$$\frac{dh}{h} = \frac{dw}{w} + \frac{d(T_{b2} - T_{b1})}{T_{b2} - T_{b1}} - \frac{d(\Delta T)_m}{(\Delta T)_m}$$

$$= \pm (0.005 + 0.02 + 0.05) = \pm \underline{0.075}$$

The error in the Stanton number is

$$\frac{d(St)}{St} = \frac{d(T_{b2} - T_{b1})}{T_{b2} - T_{b1}} - \frac{d(\Delta T)_m}{(\Delta T)_m} = \pm (0.02 + 0.05) = \pm \underline{0.07}$$

The error in calculating the reduced temperature, $(T - T_w)/(T_c - T_w)$, is given by

$$\frac{d\left[(T - T_w)/(T_c - T_w)\right]}{(T - T_w)/(T_c - T_w)} = \frac{dT}{T - T_w} - \frac{d\,T_w}{T - T_w} - \frac{d\,T_c}{T_c - T_w} + \frac{d\,T_w}{T_c - T_w}$$

Since $(T - T_w)$ is approximately equal to $(T_c - T_w)$, the error can be written as

$$\frac{d\left[(T - T_w)/(T_c - T_w)\right]}{(T - T_w)/(T_c - T_w)} = \frac{dT}{T - T_w} - \frac{d\,T_c}{T_c - T_w}$$

The error in measuring the fluid temperature was about $\pm 0.3^\circ$ F. and since $(T - T_w)$ was of the order of 20° F.

$$\frac{d\left[(T - T_w)/(T_c - T_w)\right]}{(T - T_w)/(T_c - T_w)} = \pm (0.015 + 0.015) = \pm \underline{0.030}.$$

CHAPTER VII

ANALYSIS OF DATA

Velocity Profile and Friction Factor Data

To determine if the apparatus was operating properly velocity profiles and friction factors for water were obtained. The results are shown in Figures (9 and 10) and (8). Friction factors were slightly higher than those predicted by the Nikuradse equation (equation [21]). It should be noted that the friction factor is proportional to the fifth power of the diameter (equation [57]). Hence an error of about 0.4% in measuring the tube diameter results in a 2% error in the calculated friction factor. Curve B in Figure (8) gives friction factors 2% higher than those predicted by equation (21). The water data follows this curve very well. A 0.4% error in measuring the diameter of the tube corresponds to an absolute error of $\pm$ 0.004 in. which is not excessive. The pipe was a commercial pipe and there could easily have been a variation of $\pm$ 0.004 in. in its diameter at various places along its length.

The velocity profile data are shown in Figure (9) as u/u_m vs. y/r_w. Only the data for runs W-A, W-B, W-C and W-E are shown since the remainder of the data fell on the same curve. It is seen that there is no variation with the flow rate. This is due to the fact that the flow rate was fairly high. Figure (9) shows the velocity profile data plotted as u^+ vs. $\log y^+$. Equation (12) is also

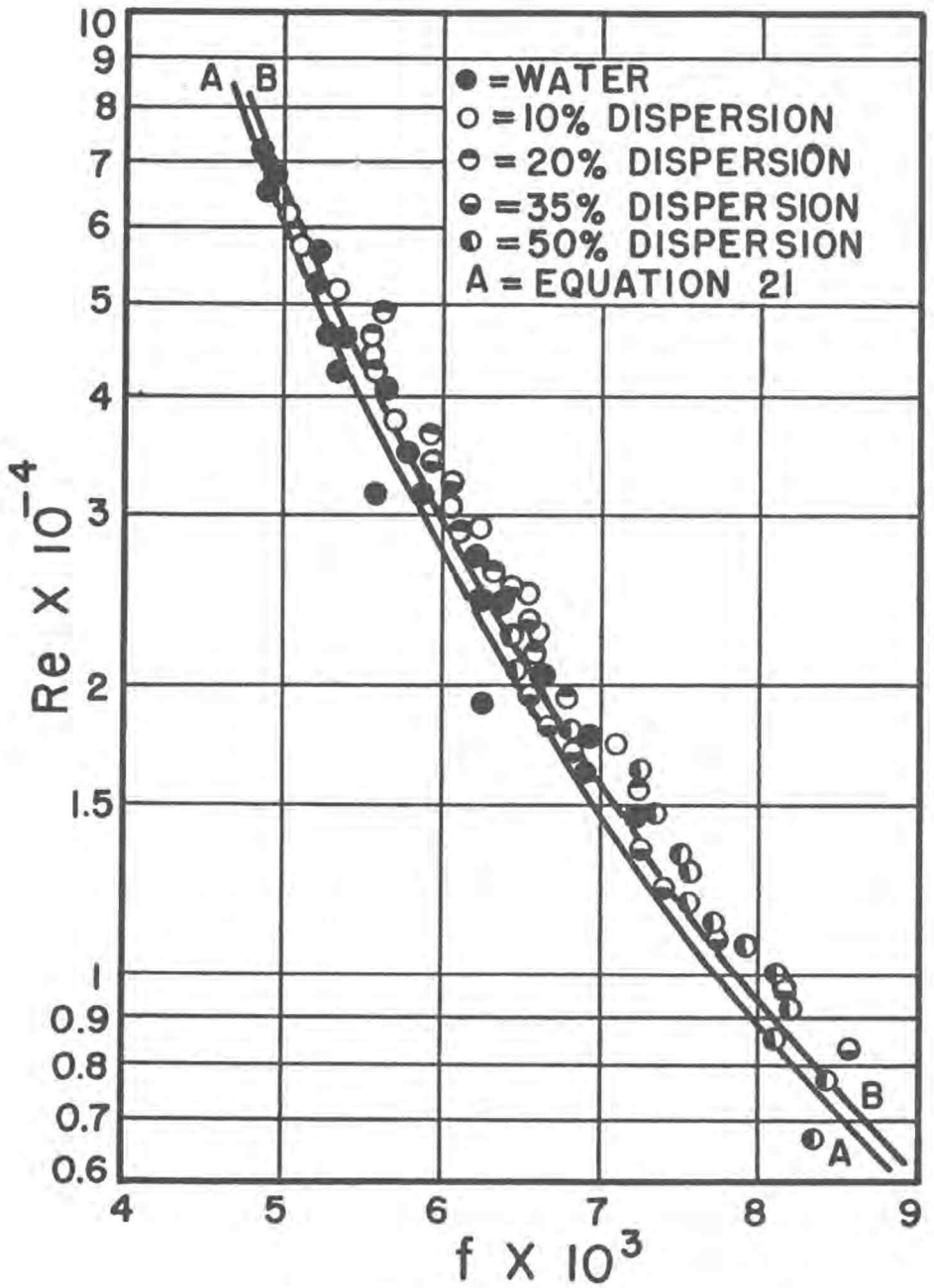

FRICTION FACTOR PLOT

FIGURE 8

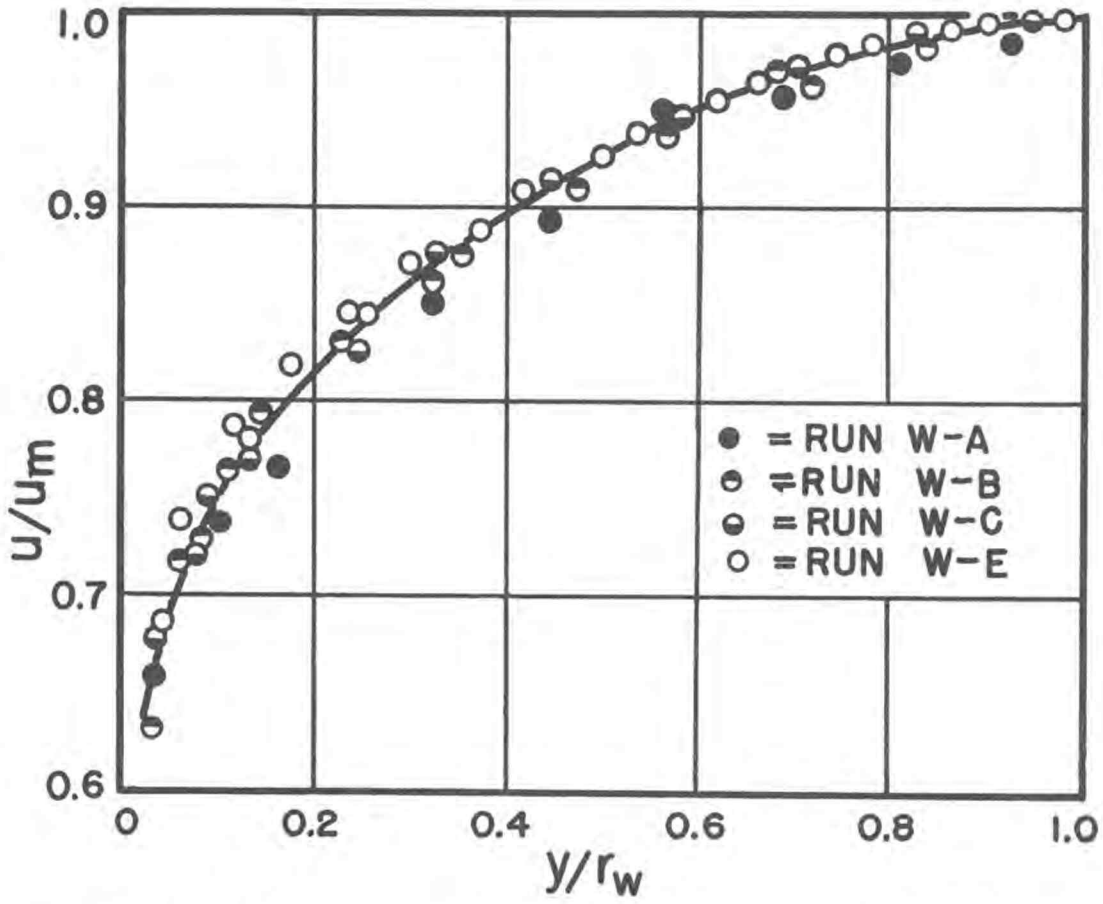

VELOCITY DISTRIBUTION FOR WATER

FIGURE 9

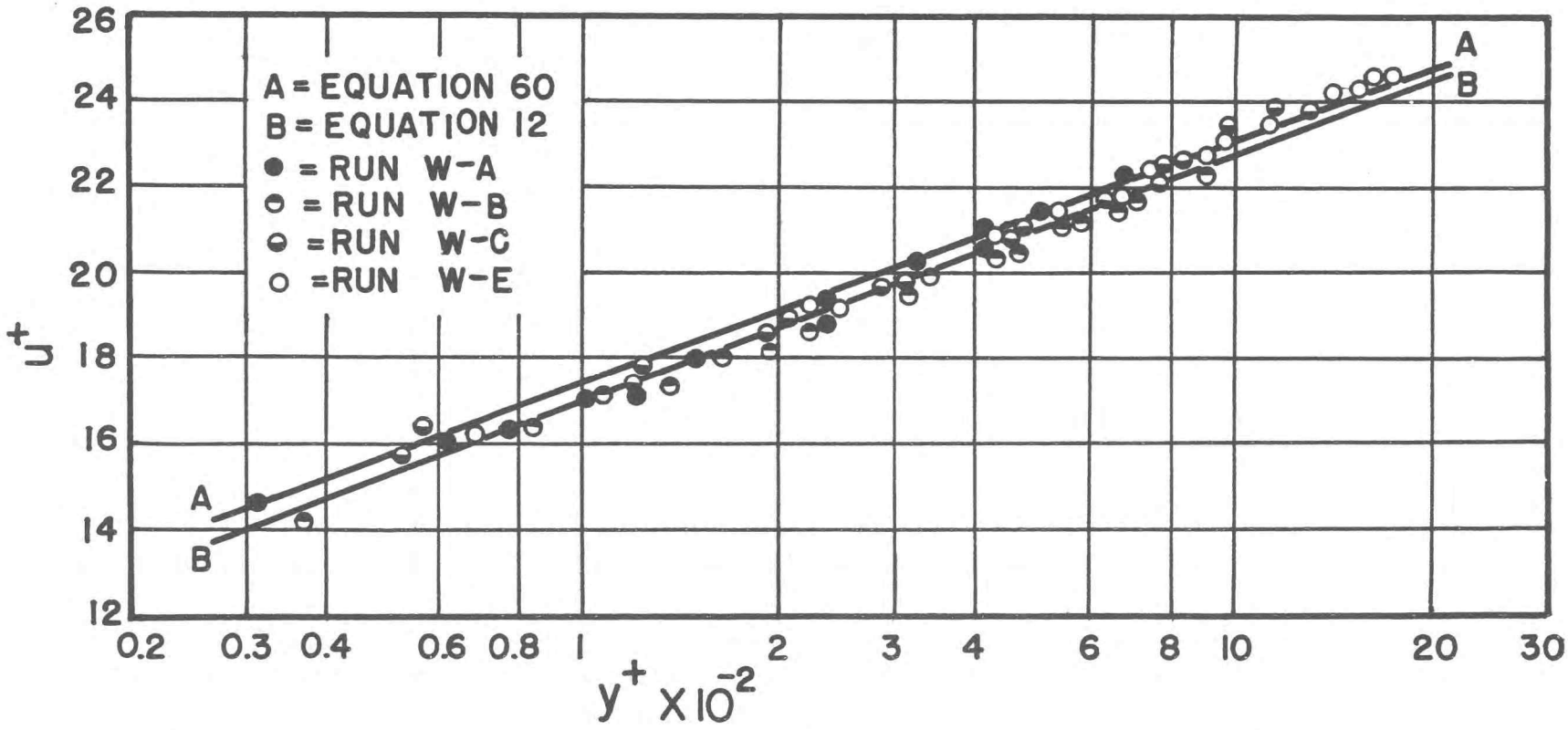

FIGURE 10 VELOCITY PROFILE FOR WATER

plotted in the figure. Data were taken only within the turbulent core of the tube cross-section. A least square analysis of all the water data gave the equation

$$u^+ = 5.61 \log y^+ + 6.10 \qquad (60)$$

This equation is also plotted in Figure (9). The difference between equation (60) and equation (12) is very small over the range of y^+ values covered. This shows that the velocity profile data for water followed the accepted equations very well.

From the analysis of the velocity profile and friction factor data for water it can be concluded that the pressure measuring system and the velocity probe were operating satisfactorily. Coefficients for the velocity probe are given in the Appendix and range between 0.95 and 0.98.

In Figures (12, 13, 14 and 15) the velocity profile data for the various dispersions are shown as u/u_m vs. y/r_w. The curve shown in these figures is that obtained from the water data. All the dispersion data follow this curve very well. There is no apparent effect of the dispersion concentration or flow rate. It is possible that if data had been taken closer to the wall (of the order of 0.005 in.) some effects of flow rate and concentration may have been detected. In Figures (16 and 17) the data for the dispersions are plotted as u^+ vs. $\log y^+ \mu_m$, where the viscosity is in centipoises. As shown in the chapter on sample calculations

$$y^+ \mu_m = \frac{(104)\ (2.741)\ (w)}{D} \left[\sqrt{f/2}\right] y$$

In calculating this term no knowledge of the viscosity was needed. The friction factors were obtained from Figure (11).

Figures (16 and 17) show the effect of the dispersion concentration on the velocity profile data. From these figures it is seen that for each concentration, except possibly the 50%, the average flow rate has no effect on the velocity profile. For the 50% concentration the 1 lb./sec. flow rate data (run 50-A) appears to have a slightly lower slope than the 2 and 3 lb./sec. data (runs 50-B and 50-C). For a particular value of $y^+ \mu_m$ the observed u^+ decreases with the dispersion concentration.

If the dispersions behaved as Newtonian fluids at the flow rates studied, the velocity profile could be correlated by equation (12). From Figures (16 and 17) it is evident that the data for each concentration (except the 50%) can be correlated by straight lines, i.e., with equations of the form

$$u^+ = A \log (y^+ \mu_m) + B \qquad (61)$$

where B certainly and A possibly may be functions of the concentration. For the 50% concentration it appears that runs 50-B and 50-C can be correlated by one equation of the form of equation (61). The data for run 50-A can be correlated by a similar equation with a slightly lower slope than that for runs 50-B and 50-C. By a least square analysis of the data for each concentration the values of the constants were determined. The equations thus become

For 10% dispersion $u^+ = 4.44 + 5.86 \log (y^+ \mu_m)$ (62)

For 20% dispersion $u^+ = 5.25 + 5.34 \log (y^+ \mu_m)$ (63)

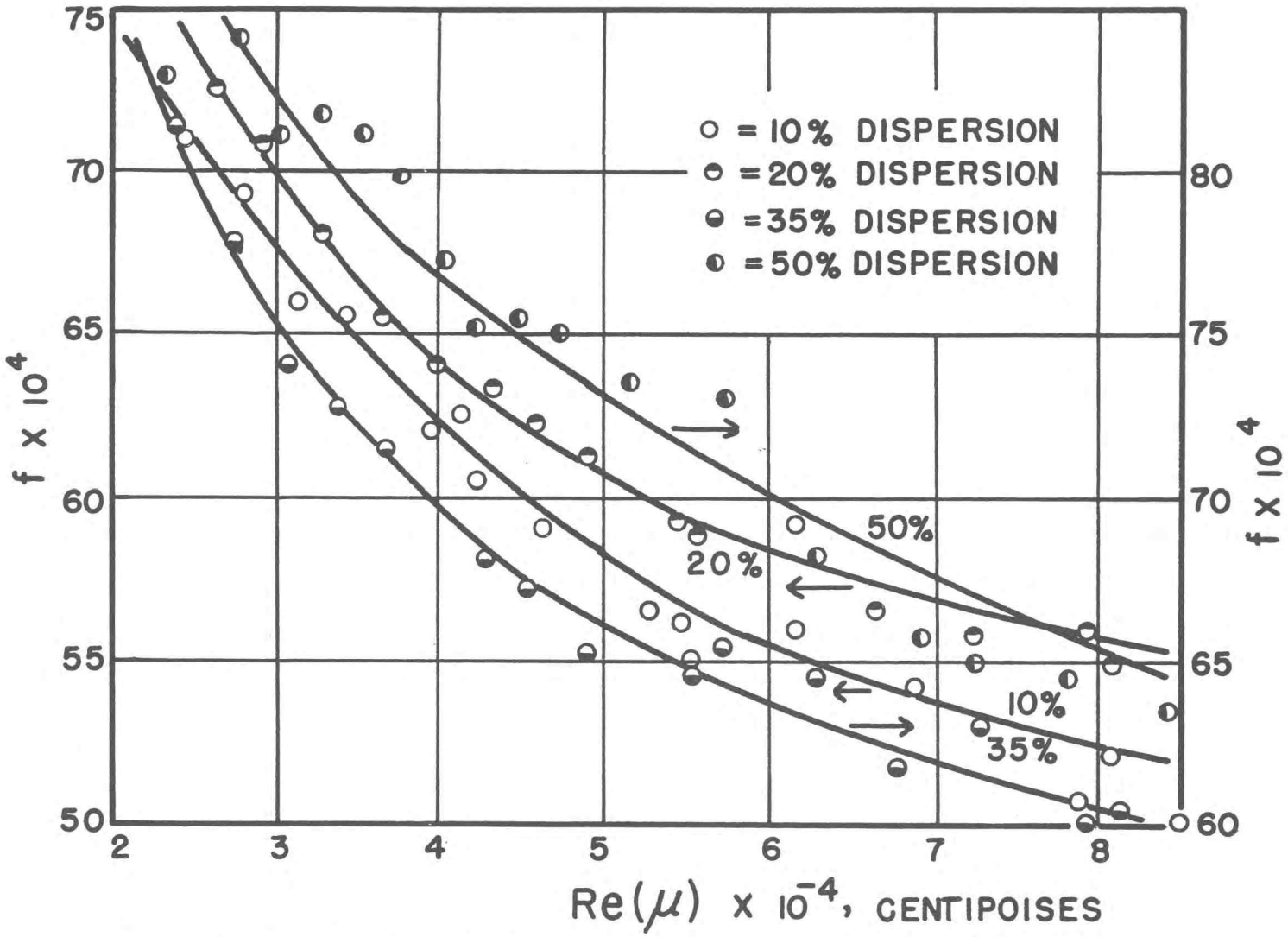

FIGURE II FRICTION FACTORS FOR DISPERSIONS

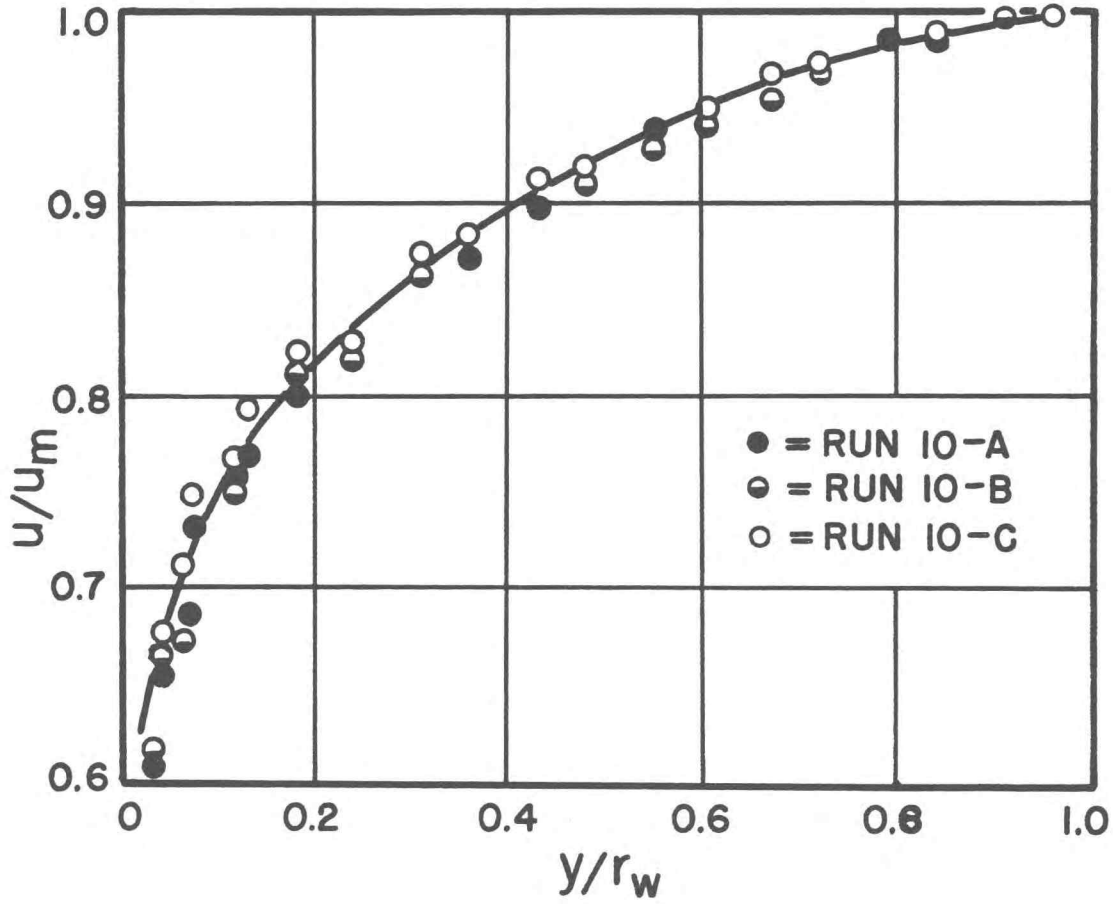

VELOCITY DISTRIBUTION FOR 10% DISPERSION

FIGURE 12

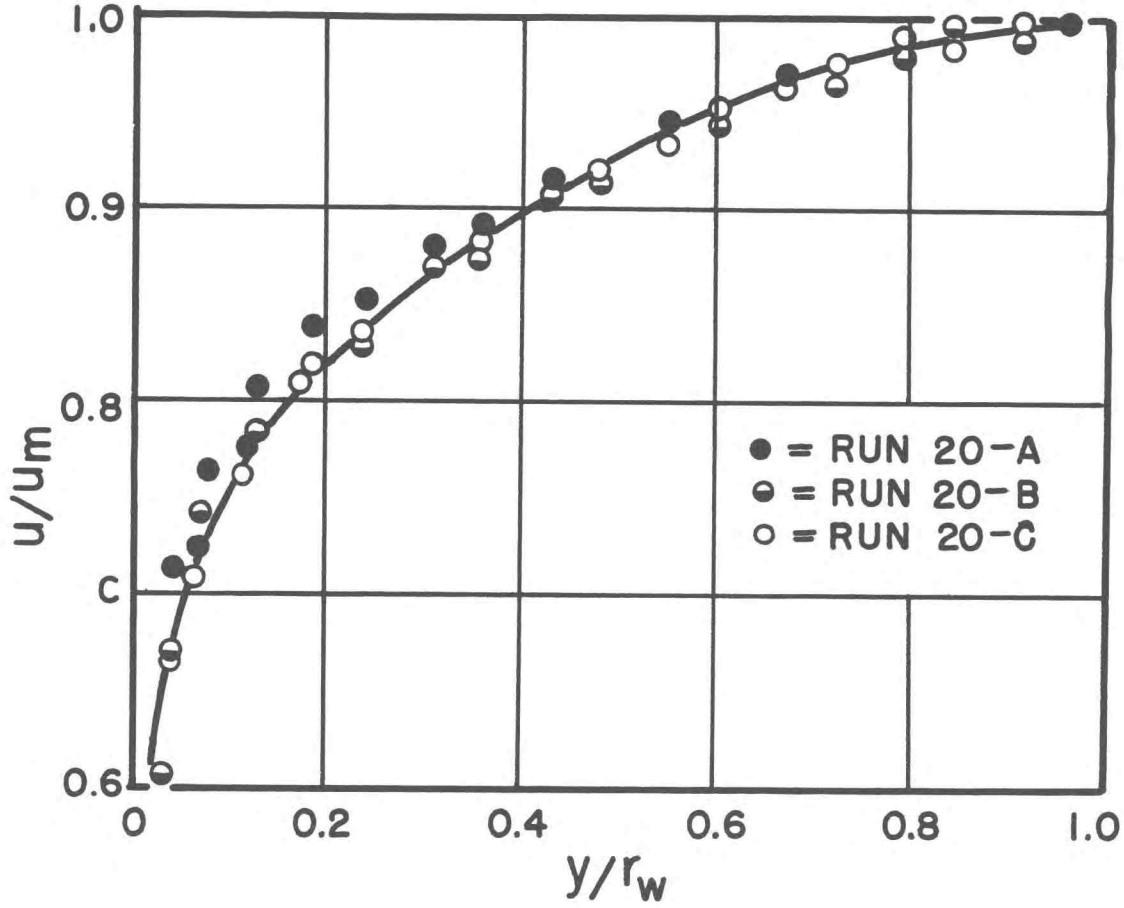

VELOCITY DISTRIBUTION FOR 20% DISPERSION

FIGURE 13

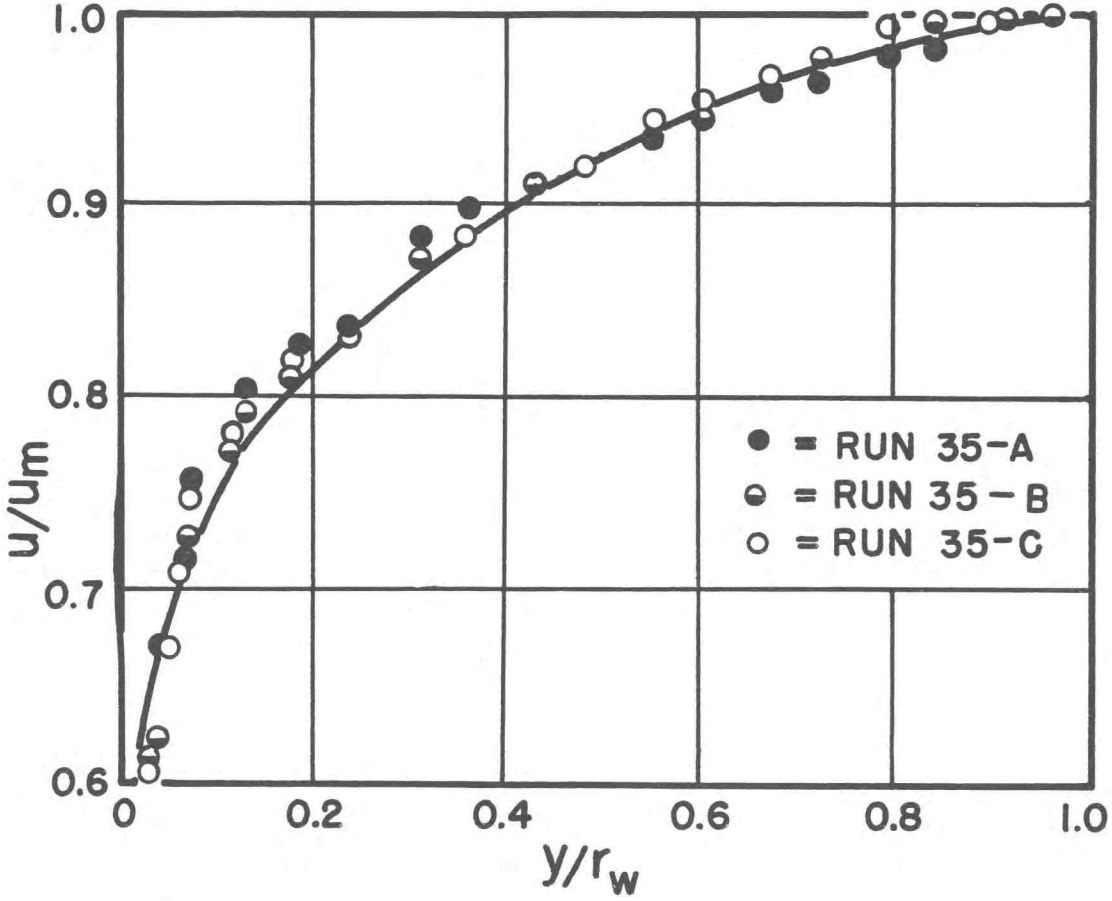

VELOCITY DISTRIBUTION FOR 35% DISPERSION

FIGURE 14

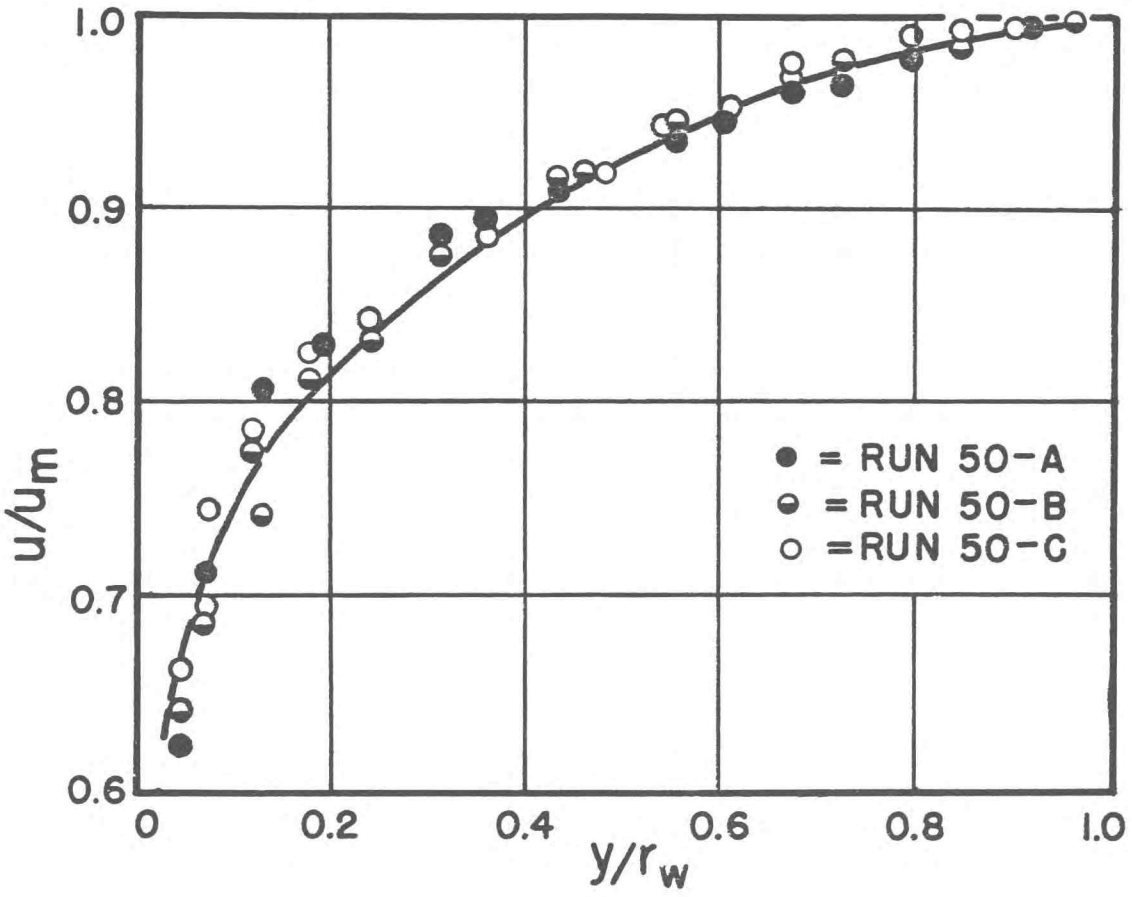

VELOCITY DISTRIBUTION FOR 50% DISPERSION

FIGURE 15

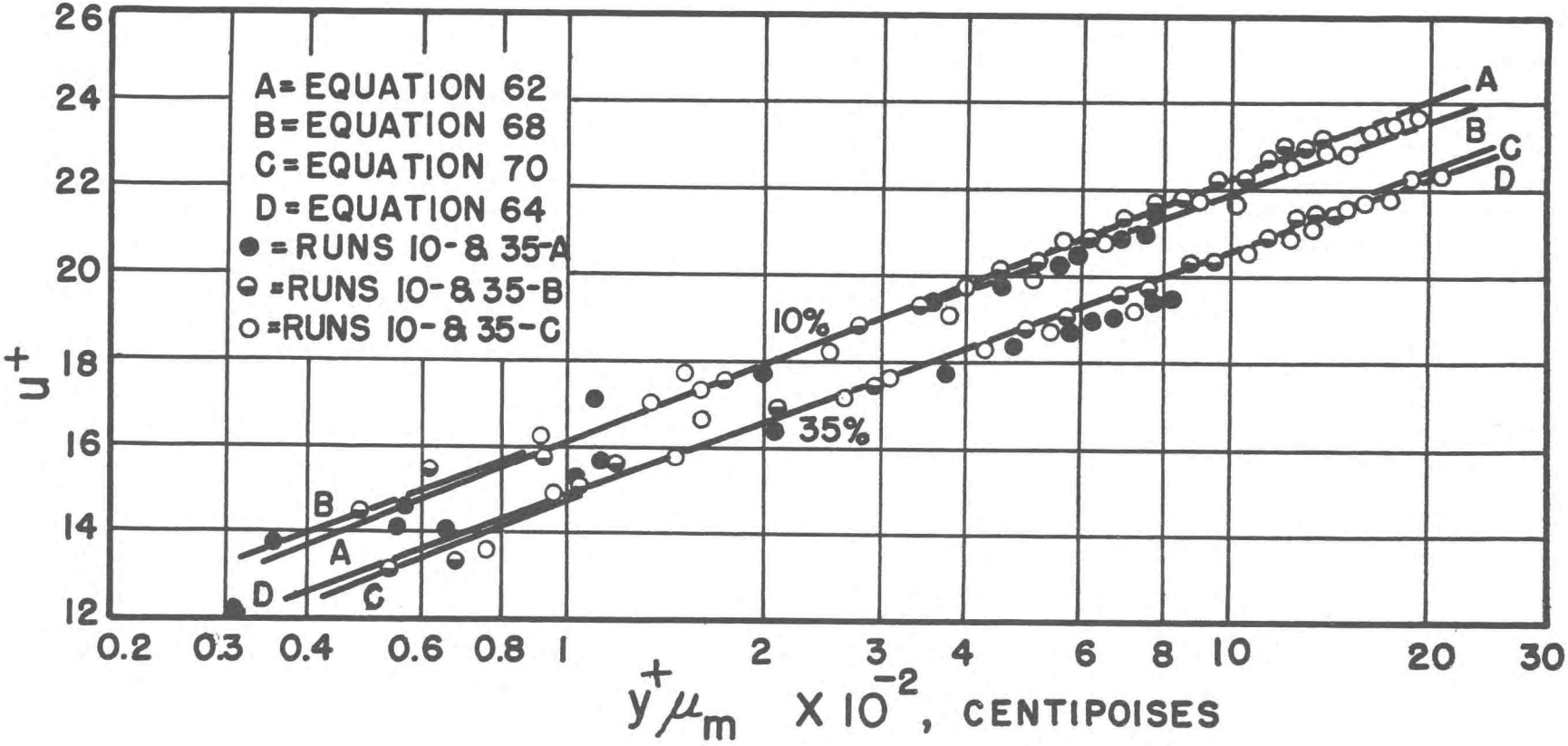

FIGURE 16 VELOCITY PROFILES FOR 10 & 35% DISPERSIONS

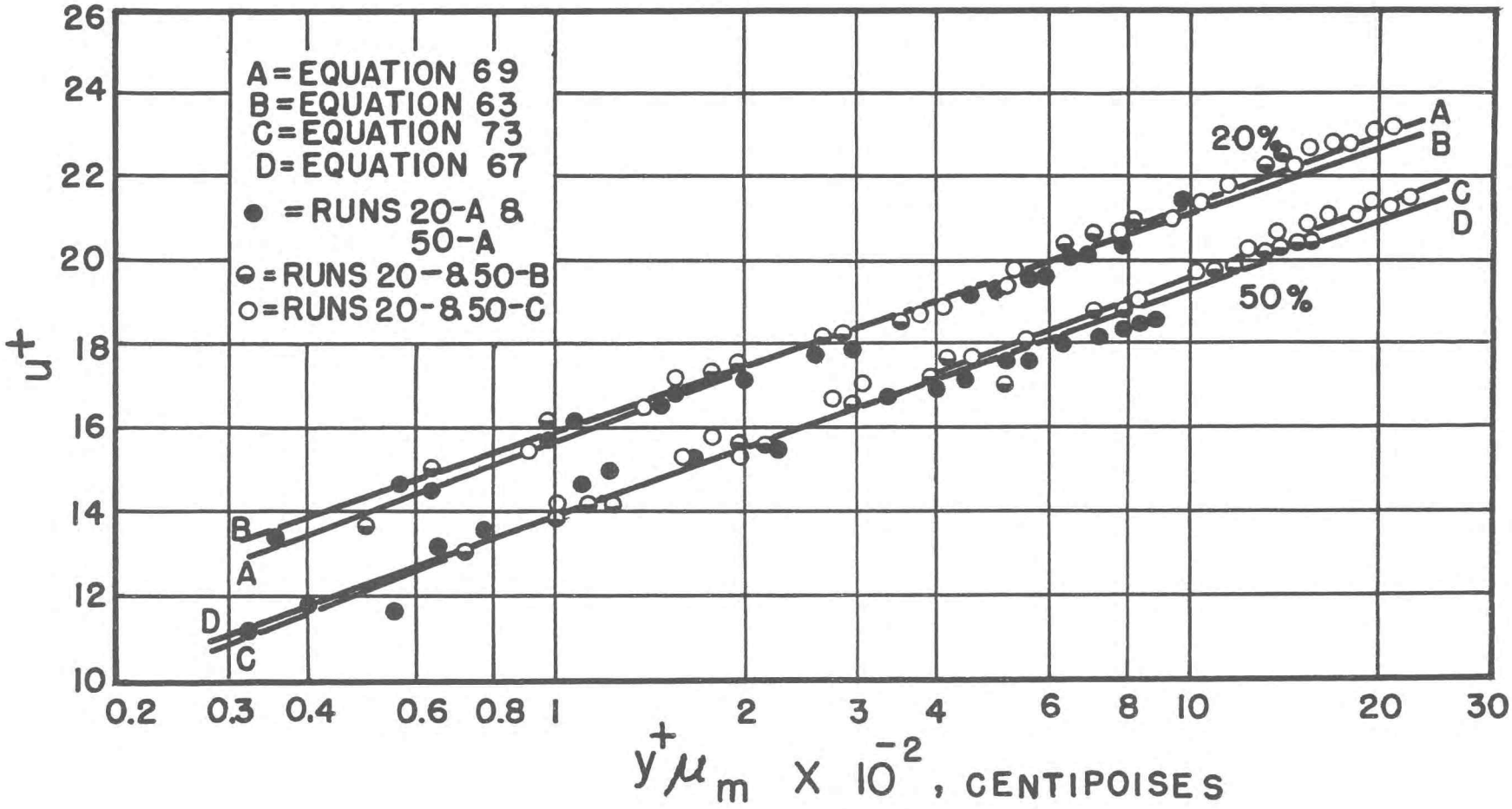

FIGURE 17 VELOCITY PROFILES FOR 20 & 50% DISPERSIONS

For 35% dispersion $u^+ = 3.80 + 5.53 \log (y^+ \mu_m)$ (64)

For 50-B and 50-C $u^+ = 2.26 + 5.78 \log (y^+ \mu_m)$ (65)

for 50-A $u^+ = 4.40 + 4.82 \log (y^+ \mu_m)$ (66)

The equations for the 50% dispersions are fairly close together and the maximum difference in u^+ predicted by the two equations over the range of values covered is about 5%. This is the same as the estimated error in calculating u^+. Therefore it was concluded that with the present data a distinction between the equations obtained for run 50-A and runs 50-B and 50-C was not warranted and a single equation was used to correlate all the 50% data. A least square analysis of all the 50% data gave the equation

$$u^+ = 2.79 + 5.56 \log (y^+ \mu_m) \quad (67)$$

Equations (62, 63, 64 and 67) are shown in Figures (16 and 17).

From equations (62, 63, 64 and 67) it is apparent that there is no definite trend in the values of the slopes obtained. Equations (12) and (25 and 29) show that the value of the slope should be 5.75 for Newtonian fluids and $5.66/(n)^{0.75}$ for non-Newtonian fluids. Since the calculated values of the slopes were very close to 5.75 it was decided to obtain equations using this value of the slope. By the method of least square analysis the equations obtained were

For 10% dispersion $u^+ = 4.69 + 5.75 \log (y^+ \mu_m)$ (68)

For 20% dispersion $u^+ = 4.19 + 5.75 \log (y^+ \mu_m)$ (69)

For 35% dispersion $u^+ = 3.22 + 5.75 \log (y^+ \mu_m)$ (70)

For 50-B and 50-C $u^+ = 2.49 + 5.75 \log (y^+ \mu_m)$ (71)

For 50-A $$u^+ = 2.07 + 5.75 \log (y^+ \mu_m) \qquad (72)$$

Again it is seen that the difference between the values of u^+ predicted for the equations for runs 50-B and 50-C and run 50-A is within the estimated error in calculating u^+. So only one equation was used to represent all the data for the 50% dispersion. The equation obtained was

$$u^+ = 2.35 + 5.75 \log (y^+ \mu_m) \qquad (73)$$

Equations (68, 69, 70 and 73) are also plotted in Figures (16 and 17.)

From the figures it is apparent that over the range of values of u covered there is practically no difference between the equations (62, 63, 64 and 67) and the corresponding one in the set (68, 69, 70 and 73). The maximum difference in the u^+ predicted by the two equations was about 3% for the 20% dispersion. This was within the error of calculating u^+.

Hence it can be stated that the dispersions behaved as Newtonian liquids over the range of flow rates covered. The slight differences in the equations for the 50% dispersion noted above could have been due to non-Newtonian behavior of the dispersion at low flow rates. However considering the errors involved in measuring u^+ this variation is not large enough to warrant making the conclusion that the 50% dispersion behaved as a non-Newtonian fluid at this flow rate.

The viscosity of the dispersion can be evaluated from the value of the constant B. Comparing equation (12) with equation (61) it is noted that

$$5.75 \log \mu_m + B = 5.50 \qquad (74)$$

Using this expression the values of viscosity calculated for the various dispersions are given below.

TABLE 2.

Apparent Viscosity of Dispersions

Vol. % Solvent	Calculated viscosity at 67 ± 2°F., cp.	Viscosity obtained by Cengel at 70 ± 1° F., cp.
8.5	1.38	1.12
19.6	1.69	1.43
34.4	2.50	2.64
49.2	3.53	5.70

Using these calculated viscosities all the velocity profile data for the various concentrations can be correlated by equation (12).

The viscosities calculated from Cengel's correlation (4, p. 65-69) are also given in Table (2). Cengel calculated the viscosities from the friction factor data. Both the present and Cengel's results show that the viscosity increases with the dispersion concentration. The viscosities obtained from the present results compare quite well with those obtained by Cengel for dispersion concentrations up to 35%. For the 50% dispersion there is a marked difference between the two values. There is considerable scatter in the friction factor data as plotted by Cengel and the curve drawn by him through these points to calculate the viscosities is

quite arbitrary. Another factor contributing to the differences in the viscosities is that in both cases the term calculated is log μ_m. Slight differences in log μ_m, for large μ_m values, show up as comparatively large differences in μ_m. Cengel has made a thorough literature survey of the dependence of the viscosity of Newtonian suspensions and emulsions on the concentration of the dispersed phase.

The friction factor data for the dispersions are presented in Figure (11) as a function of the flow rate. In Figure (8) the friction factor is plotted against log Re. The Reynolds number is based on the viscosities given above in Table (2). Again it is noted that the points lie slightly above the line representing equation (21). However the data correspond better with curve B in Figure (8). As stated before this could be due to non-uniformity in the diameter of the pipe. It should be noted that this slight discrepency in measuring the diameter of the tube does not affect the other results materially.

The results show that by the use of the viscosities given in Table (2), the friction factor data for the dispersions can be correlated by equation (21). At these flow rates the dispersions may be treated as single phase Newtonian fluids.

As stated before Finnigan (10) and later Cengel (4) and Wright (30) observed some non-Newtonian characteristics in the dispersion used in this study. The most marked deviation from Newtonian behavior was at flow rates less than 1 lb./sec. The deviation was

also most marked for the higher concentration dispersions. It is possible for liquids to behave as non-Newtonian at low shear rates and as Newtonian at high shear rates or vice versa. Alves, Boucher and Pigford (1) and Merrill (17) have observed that the exponent n in equation (6) is, in some cases, a function of the rate of shear. It is also possible that at the low flow rates studied by Finnigan, Cengel and Wright there was some phase separation of the solvent and the water.

Temperature Profiles and Heat Transfer Coefficients

The operation of the temperature measuring portion of the equipment was also tested by measuring temperature profiles and heat transfer coefficients for water. The temperature profiles obtained are shown in Figure (18). The temperature is plotted as $(T - T_w)/(T_c - T_w)$ the wall temperature being that at the point where the probe was inserted. Also in Figure (18) the temperature profiles calculated by Martinelli's correlation (equation [41]) for Prandtl numbers of 3.66, 7.5 and 20 and a Reynolds number of 38,500 are plotted. Results calculated from Sleicher's equation (42) for a Prandtl number of 7.5 and Reynolds number of 38,500 are also given. As stated before at these high Reynolds numbers the temperature profiles do not change appreciably with the flow rate.

It is seen that the data follow quite closely the curve predicted by Martinelli's equation for a Prandtl number of 3.66. This is the Prandtl number of water at the film temperatures

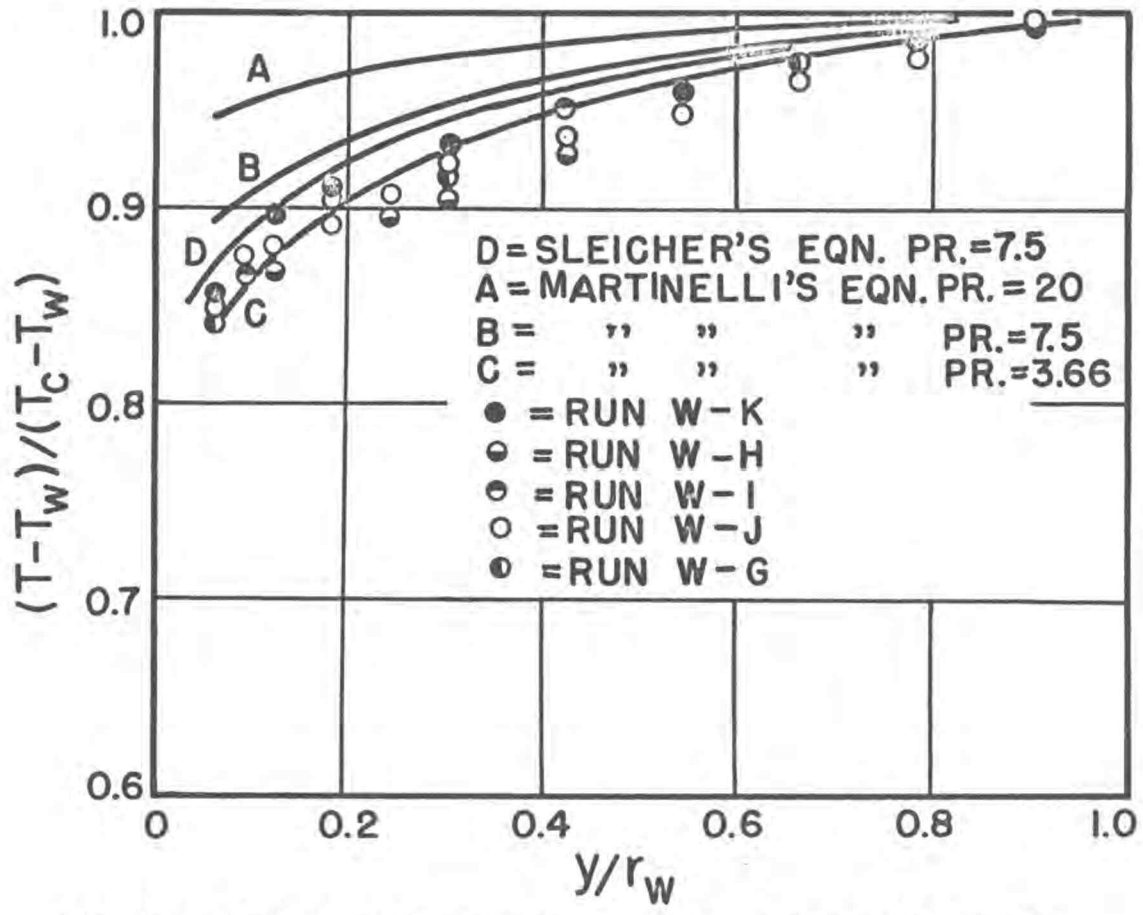

TEMPERATURE PROFILES FOR WATER

FIGURE 18

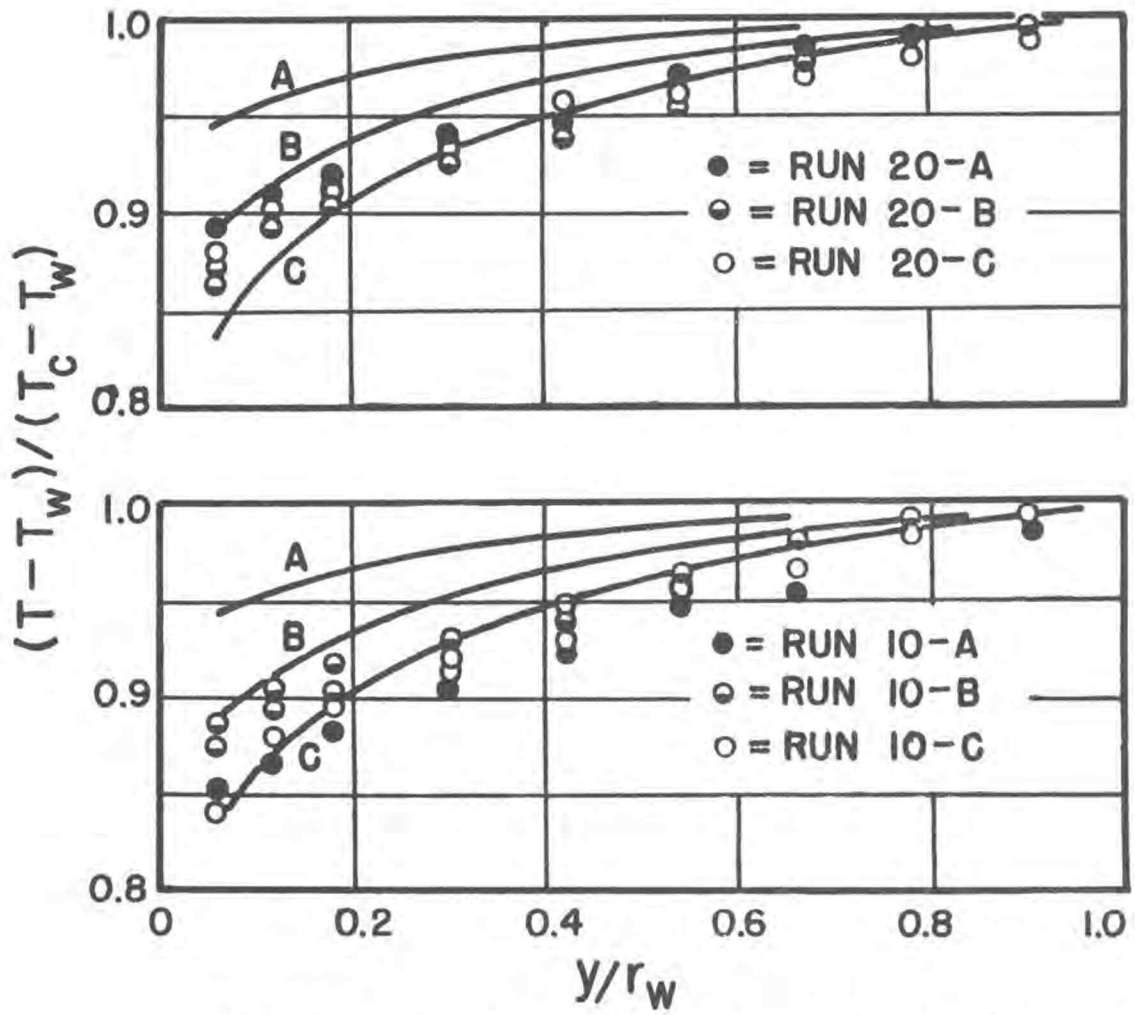

TEMPERATURE PROFILES FOR
10 AND 20% DISPERSIONS

FIGURE 19

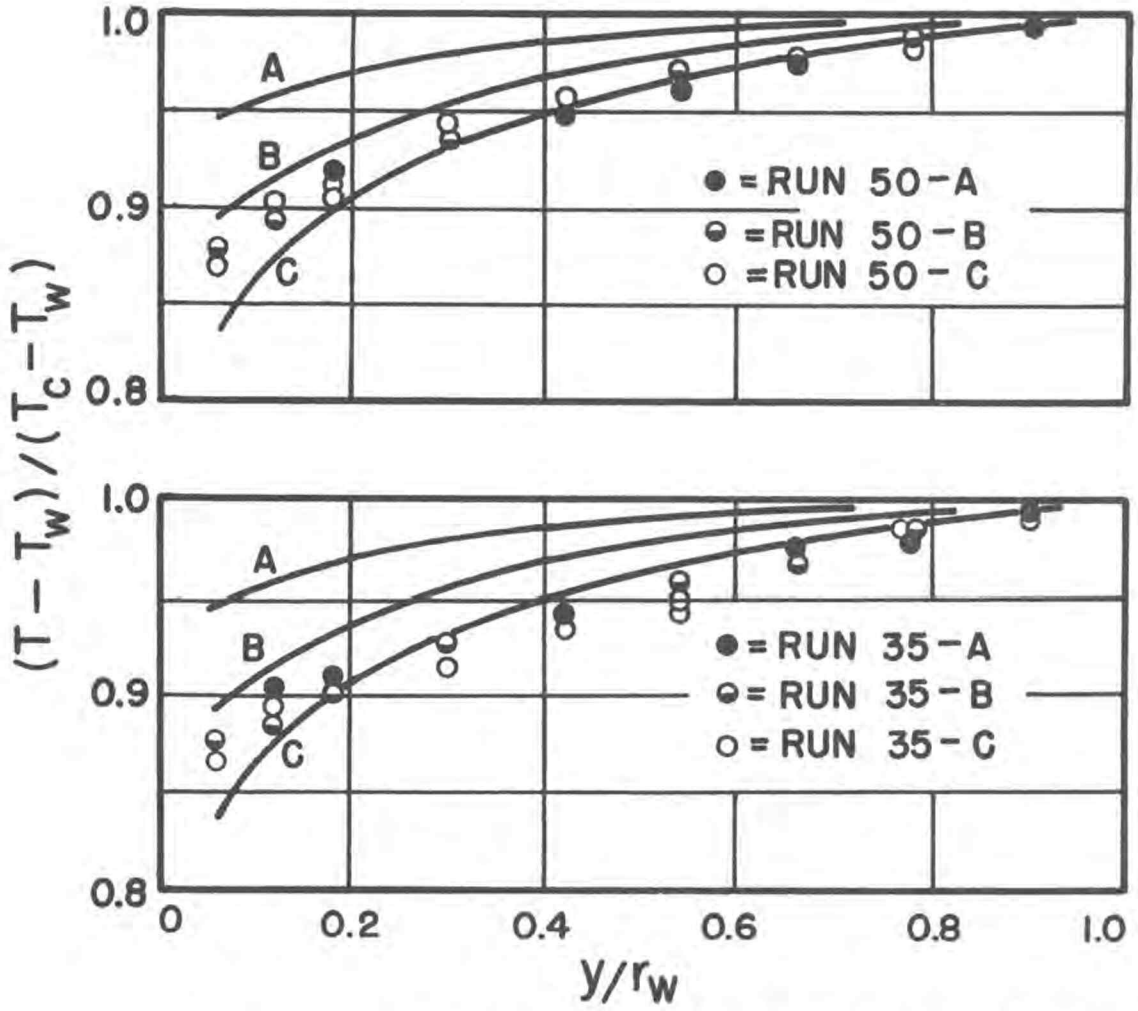

TEMPERATURE PROFILES FOR
35 AND 50% DISPERSIONS

FIGURE 20

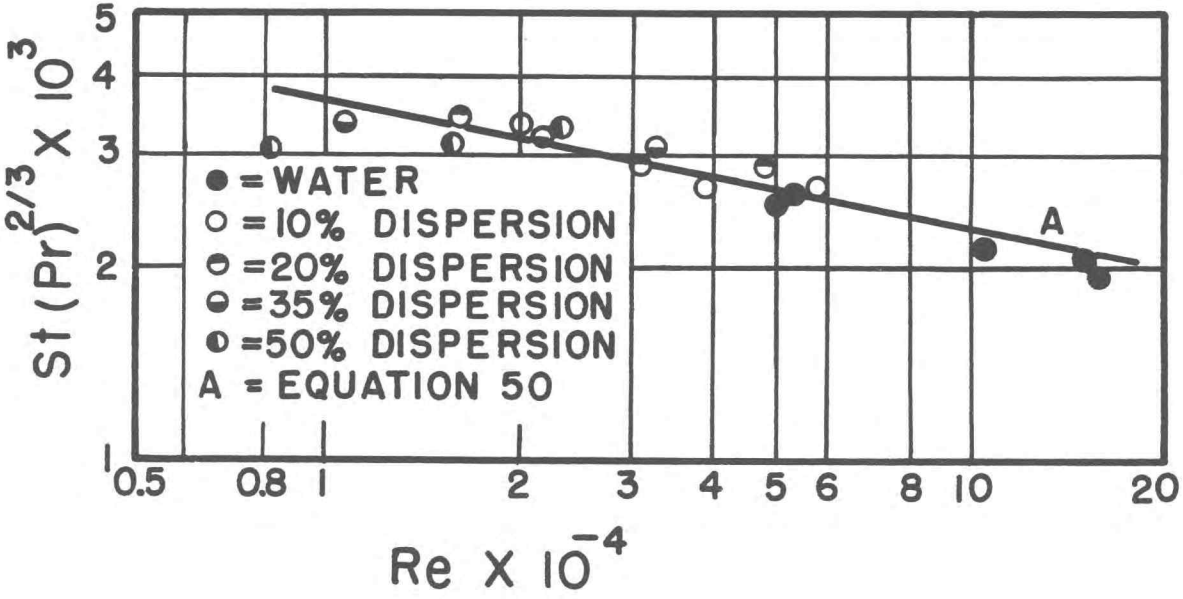

HEAT TRANSFER RESULTS

FIGURE 21

encountered in the experiments. Since the temperature profiles are quite flat at these high Prandtl numbers a slight difference in the measured fluid temperature, T, appears quite exaggerated when plotted as $(T - T_w)/(T_c - T_w)$. The greatest variations between this dimensionless temperature for water are of the order of 3%.

The heat transfer data are plotted as log $St(Pr)^{2/3}$ vs. log Re. in Figure (21). Colburn's equation (50) is also plotted in this figure. It is seen that the experimental data for water follows Colburn's equation very well. These test runs showed that the temperature measuring part of the equipment was functioning satisfactorily.

The temperature profiles for the various dispersions are plotted in Figures (19 and 20) as $(T - T_w)/(T_c - T_w)$ vs. y/r_w. Results calculated from Martinelli's equation (41) for Prandtl numbers of 3.66, 7.5 and 20 and a Reynolds number of 38,500 are also shown in these figures. It can be seen from these figures that the dispersion concentration and the flow rates have no effect on the profiles. All the profiles are similar to those obtained for water.

In the case of dispersions or suspensions flowing in pipes the continuous phase will form a film adjacent to the pipe wall. For the case of solid particles flowing in a turbulent gas stream, Soo and Tien (28) have stated that near the wall the solid particles tend to move away from the wall owing to a spinning force on the particles. They have stated that statistically a small portion of the particles may strike the wall but a great majority of them will

be turned away from it. This means that there would be a film of the continuous phase adjacent to the wall. This film would constitute the laminar sub-layer.

In turbulent flow heat transfer to liquids (i.e., high Prandtl number fluids) the greatest part of the temperature drop occurs in the laminar sub-layer. So the temperature profile and the heat transfer coefficient should depend on the Prandtl number calculated at the film properties. The equation given by Friend and Metzner (equation [54]) for high Prandtl number liquids uses the Prandtl number based on properties determined at the wall film temperature. Based on the viscosity of the dispersion, the Prandtl number for the 50% dispersion would be about 25. The temperature profiles observed for the 50% dispersion definitely do not correspond to those of such a high Prandtl number. It, therefore, appears that a Prandtl number other than that based on the dispersion properties should be used to correlate the heat transfer data of dispersions. The Prandtl number to be used would appear to be that of the continuous phase at the film temperature since temperature profiles for the dispersion are very similar to those for water at the film temperature.

The heat transfer results are given in Figure (21) as $\log St(Pr)_c^{2/3}$ vs. $\log Re$. The Prandtl number is based on the properties of the continuous phase (water) at the film temperature. The points follow the Colburn equation very well except the point for run 50-A which is about 25% below Colburn's equation. This

could have been due to phase separation or non-Newtonian behavior of the dispersion at this low flow rate. The satisfactory conformity of the data with Colburn's equation again shows that the heat transfer mechanism is governed by the Prandtl number of the continuous phase.

The heat transfer results are also compared with the observed friction factors at the same flow rates. In Table (3) the group $St(Pr)_c^{2/3}$ is compared with Colburn's j_H factor (equation [52]). This is based on the friction factors obtained from Figure (11). Again except for the run 50-A, the predicted and the observed groups compare quite well. Further, Friend and Metzner's equation (54) was used to calculate the effective Prandtl numbers of the dispersions. These are also given in Table (3). It is seen that most of the calculated Prandtl numbers fall close to 4.0. There is no consistant variation in the calculated Prandtl numbers with the concentration.

Orr and Dallavalle (20) in their correlation have used a Prandtl number based on the properties of the suspensions. However the volumetric concentrations of their suspensions were not very high so there was not a very great variation in the apparent viscosity of the suspension. Moreover although there is an increase in the apparent viscosity there is also an increase in the apparent thermal conductivity and a decrease in the heat capacity of the suspension compared to that of the continuous phase, so that effectively the Prandtl number of the suspension

TABLE 3.

Calculated Prandtl Number and Comparison of $St(Pr)_c^{2/3}$ with j_H

Run No.	$St(Pr)_c^{2/3} \times 10^3$	$j_H \times 10^3$	Calculated Pr
10-A	3.376	3.45	3.85
10-B	2.706	2.83	4.45
10-C	2.670	2.56	3.95
20-A	3.417	3.57	3.95
20-B	2.964	2.98	4.00
20-C	2.772	2.80	4.20
35-A	3.352	3.86	5.20
35-B	3.205	3.25	3.90
35-C	3.034	3.00	3.85
50-A	3.041	4.15	6.00
50-B	3.140	3.59	4.65
50-C	3.439	3.20	3.35

does not differ greatly from that of the continuous phase. For instance for their run number 32, the Prandtl number calculated from the suspension properties is (0.856)(1.05)/(0.411) = 2.13 while the Prandtl number of water at 180° F. (the film temperature) is 2.15. So most of their results could also have been correlated with a Prandtl number based on the continuous phase.

As stated before Finnigan's (10) and Wright's (30) results are

based on a Prandtl number calculated with the suspension heat capacity and continuous phase thermal conductivity. This gives rise to Prandtl numbers as high as 40 for the 50% dispersion. Hence their results do not agree with those presented in this work. It should be noted that they were heating their test section electrically and the driving temperature, $(\Delta T)_m$, in their experiments was quite small, in some cases only 3 or 4° F. Therefore a small error in measuring the temperatures would result in a large error in the heat transfer coefficient. If Wright's results are plotted using the Prandtl number of water the points would fall as much as 60% below equation (50). As stated above this could be due to errors in measuring the wall temperature.

In Figure (22) the heat transfer coefficients calculated are plotted against the flow rates. It is seen that the dispersions give higher heat transfer coefficients than the single phase fluid at the same mass flow rate. This has also been observed by Orr and Dallavalle (20). This could have been caused by the dispersed phase droplets causing more turbulence and effectively reducing the thickness of the laminar sub-layer.

From the heat transfer results and temperature profiles obtained in this work it can be concluded that heat transfer to a liquid-liquid dispersion in turbulent flow can be treated by relationships developed for heat transfer to a single phase fluid. The dispersions studied behaved as a fluid with a Prandtl number equal to that of the continuous phase at the film.

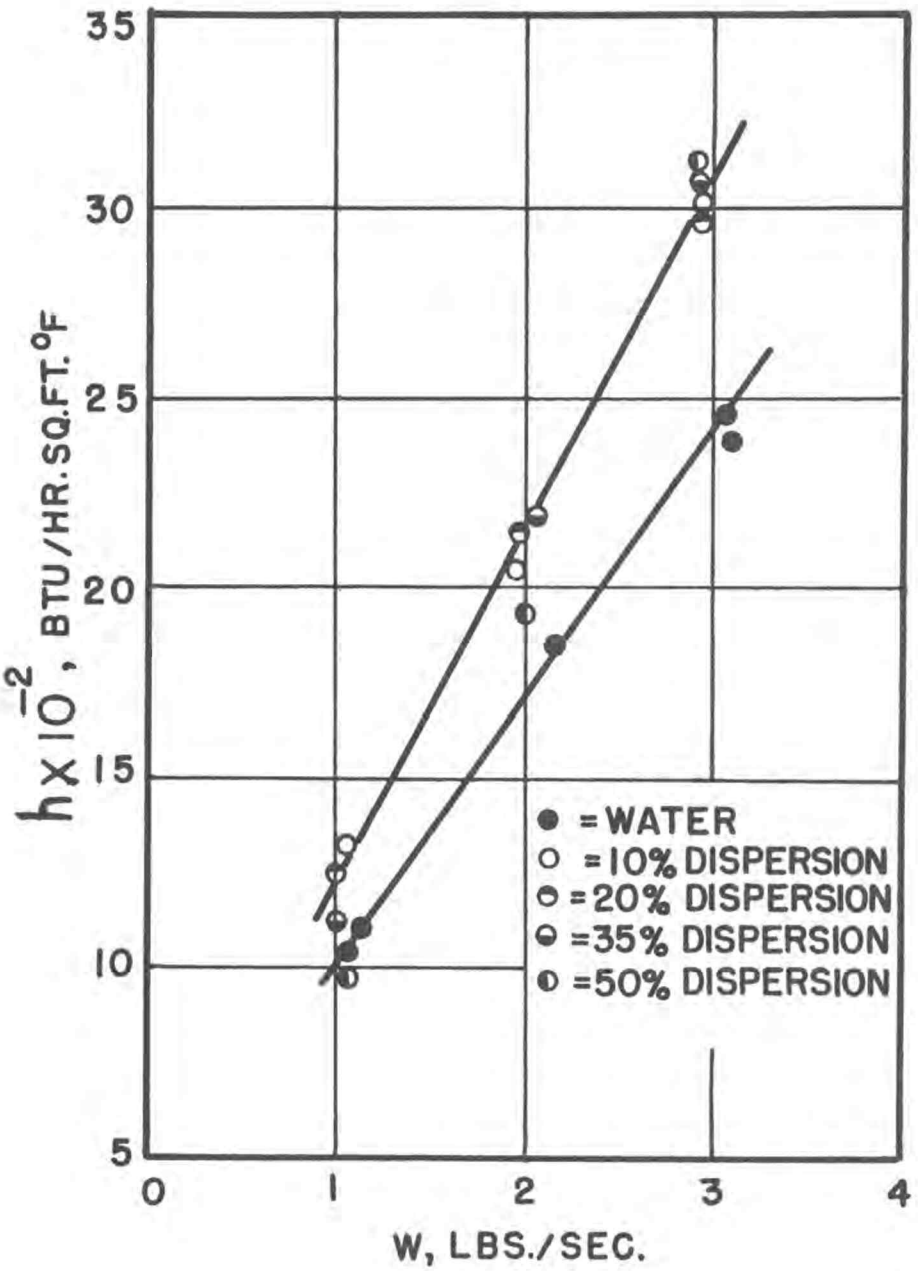

VARIATION OF HEAT TRANSFER COEFFICIENTS WITH FLOW RATE

FIGURE 22

CHAPTER VIII

CONCLUSIONS

The conclusions of this investigation may be summarized as follows:

(a) In the range of flow rates investigated (1 lb./sec. to 3 lb./sec.) the dispersions studied can be treated as Newtonian liquids.

(b) In this range the friction factor for dispersions can be predicted by equation (21) and the velocity profile in the turbulent core by equation (12). The viscosity of the dispersions is a function of the concentration and can be evaluated by an analysis of the velocity profile data.

(c) The temperature profiles obtained correspond to those of a liquid with a Prandtl number equal to that of the continuous phase at the wall film temperatures. This shows that a film of the continuous phase forms adjacent to the wall. Heat transfer to dispersions is governed by the Prandtl number of this film.

(d) The heat transfer coefficient to the dispersions can be predicted by equation (50) with the Prandtl number based on the properties of the continuous phase at the film and the Reynolds number based on the dispersion viscosity.

CHAPTER IX

RECOMMENDATIONS FOR FURTHER WORK

The present investigation has shown some interesting aspects of the flow of liquid-liquid dispersions. To pursue some of these facets of the overall study the following recommendations for further work are made:

(a) Velocity and temperature profile studies should be made for flow rates less than 1 lb./sec. to determine whether the dispersions behave as non-Newtonian or Newtonian liquids at low flow rates.

(b) It would be desirable to study dispersions of liquids having widely differing viscosities to determine whether these could also be treated as Newtonian liquids.

(c) Studies should be conducted in tubes of widely varying diameters. As yet studies have been conducted only in tubes of approximately an inch in diameter.

(d) Photographic studies of the flow of dispersions should be made to determine the size of the dispersed phase droplets at various flow rates and concentrations. It is possible that the abnormally high friction factors obtained by Cengel (4) at low flow rates could be due to changes in the dispersed phase droplet size.

(e) Visual studies should be made to determine whether a film of the continuous phase exists at the tube wall.

BIBLIOGRAPHY

1. Alves, George E., D. F. Boucher and R. L. Pigford. Pipe-line design for non-Newtonian solutions and suspensions. Chemical Engineering Progress 48:385-393. 1952.

2. Baron, Thomas, C. S. Sterling and A. P. Schueler. Viscosity of suspensions - Review and application to two-phase flow. Midwestern Conference on Fluid Mechanics. Proceedings 3:103-123. 1953.

3. Batchelor, G. K. Kolmogoroff's theory of locally isotropic turbulence. Proceedings of the Cambridge Philosophical Society 43:533-559. 1947.

4. Cengel, John A. Viscosity of liquid-liquid dispersions in laminar and turbulent flow. Master's thesis. Corvallis, Oregon State College, 1959. 110 numb. leaves.

5. Charles, M. E., G. W. Govier and G. W. Hodgson. The horizontal pipeline flow of equal density oil-water mixtures. The Canadian Journal of Chemical Engineering 39:27-36. 1961.

6. Clayton, William. The theory of emulsions and their technical treatment. 5th ed. New York, Blakiston, 1954. 669 p.

7. Colburn, Allan P. A method of correlating forced convection heat transfer data and a comparison with fluid friction. Transactions of the American Institute of Chemical Engineers 29:174-208. 1933.

8. Deissler, Robert G. Analysis of turbulent heat transfer, mass transfer and friction in smooth tubes at high Prandtl and Schmidt numbers. Washington, 1954. 53 p. (U.S. National Advisory Committee for Aeronautics. Technical Note no. 3145)

9. Dodge, D. W. and A. B. Metzner. Turbulent flow of non-Newtonian systems. American Institute of Chemical Engineers. Journal 5: 189-204. 1959.

10. Finnigan, Jerome W. Pressure losses and heat transfer for the flow of mixtures of immiscible liquids in circular tubes. Ph.D. thesis. Corvallis, Oregon State College, 1958. 154 numb. leaves.

11. Friend, W. L. and A. B. Metzner. Turbulent heat transfer inside tubes and the analogy among heat, mass and momentum transfer. American Institute of Chemical Engineers. Journal 4:393-402. 1958.

12. Knudsen, James G. and Donald L. Katz. Fluid dynamics and heat transfer. New York, McGraw-Hill, 1958. 576 p.

13. _____. Velocity profiles in annuli. Midwestern Conference on Fluid Dynamics. Proceedings 1:175-203. 1951.

14. Leeds and Northrup Company. Standard conversion tables for Leeds and Northrup thermocouples. Philadelphia, n.d., 43 p.

15. Martinelli, R. C. Heat transfer to molten metals. Transactions of the American Society of Mechanical Engineers 69: 947-959. 1947.

16. Maude, A. D. and R. L. Whitmore. The turbulent flow of suspensions in tubes. Transactions of the Institution of Chemical Engineers 36:296-304. 1958.

17. Merrill, E. W. Viscometric classification of polymer solutions. Industrial and Engineering Chemistry 51:868-870. 1959.

18. Metzner, A. B. and P. S. Friend. Heat transfer to turbulent non-Newtonian fluids. Industrial and Engineering Chemistry 51:879-882. 1959.

19. Metzner, A. B. and J. C. Reed. Flow of non-Newtonian fluids - Correlation of the laminar, transition and turbulent flow regions. American Institute of Chemical Engineers. Journal 1:34-40. 1955.

20. Orr, Clyde, Jr. and J. M. Dallavalle. Heat transfer properties of liquid-solid suspensions. In: Heat transfer - Research studies for 1954. Chemical Engineering Progress Symposium Series no. 9(vol. 50):29-45. 1954.

21. Prandtl, L. Report on investigation of developed turbulence. Washington, 1959. 7 p. (U.S. National Advisory Committee for Aeronautics. Technical Memorandum no. 1231)

22. Reichardt, H. The principles of turbulent heat transfer. Washington, 1957. 54 p. (U.S. National Advisory Committee for Aeronautics. Technical Memorandum no. 1408)

23. Russell, T. W. F., G. W. Hodgson and G. W. Govier. Horizontal pipeline flow of mixtures of oil and water. The Canadian Journal of Chemical Engineering 37:9-17. 1959.

24. Shaver, Robert G. and Edward W. Merrill. Turbulent flow of pseudoplastic polymer solutions in straight cylinderical tubes. American Institute of Chemical Engineers. Journal 2:181-188. 1959.

25. Sleicher, Charles A., Jr. Heat transfer in a pipe with turbulent flow and arbitrary wall-temperature distribution. Ph.D. thesis. Ann Arbor, University of Michigan, 1955. 156 numb. leaves (microfilm).

26. Sleicher, C. A., Jr. and M. Tribus. Heat transfer in a pipe with turbulent flow and arbitrary wall-temperature distribution. In: Heat Transfer and Fluid Mechanics Institute, Stanford University, Stanford, California. Preprints of Papers, 1956, p. 59-78.

27. Soo, S. L. and J. A. Regalbuto. Concentration distribution in two-phase pipe flow. The Canadian Journal of Chemical Engineering 38:160-166. 1960.

28. Soo, S. L. and C. L. Tien. Effect of the wall on two-phase turbulent motion. Transactions of the American Society of Mechanical Engineers, Journal of Applied Mechanics 82:5-13. 1960.

29. Stanton, T. E., Dorothy Marshall and C. N. Bryant. On the conditions of the boundary of a fluid in turbulent motion. Proceedings of the Royal Society of London, Series A, 97:413-434. 1920.

30. Wright, Charles H. Pressure drop and heat transfer for liquid-liquid dispersions in turbulent flow in a circular tube. Master's thesis. Corvallis, Oregon State College, 1959. 120 numb. leaves.

APPENDIX I

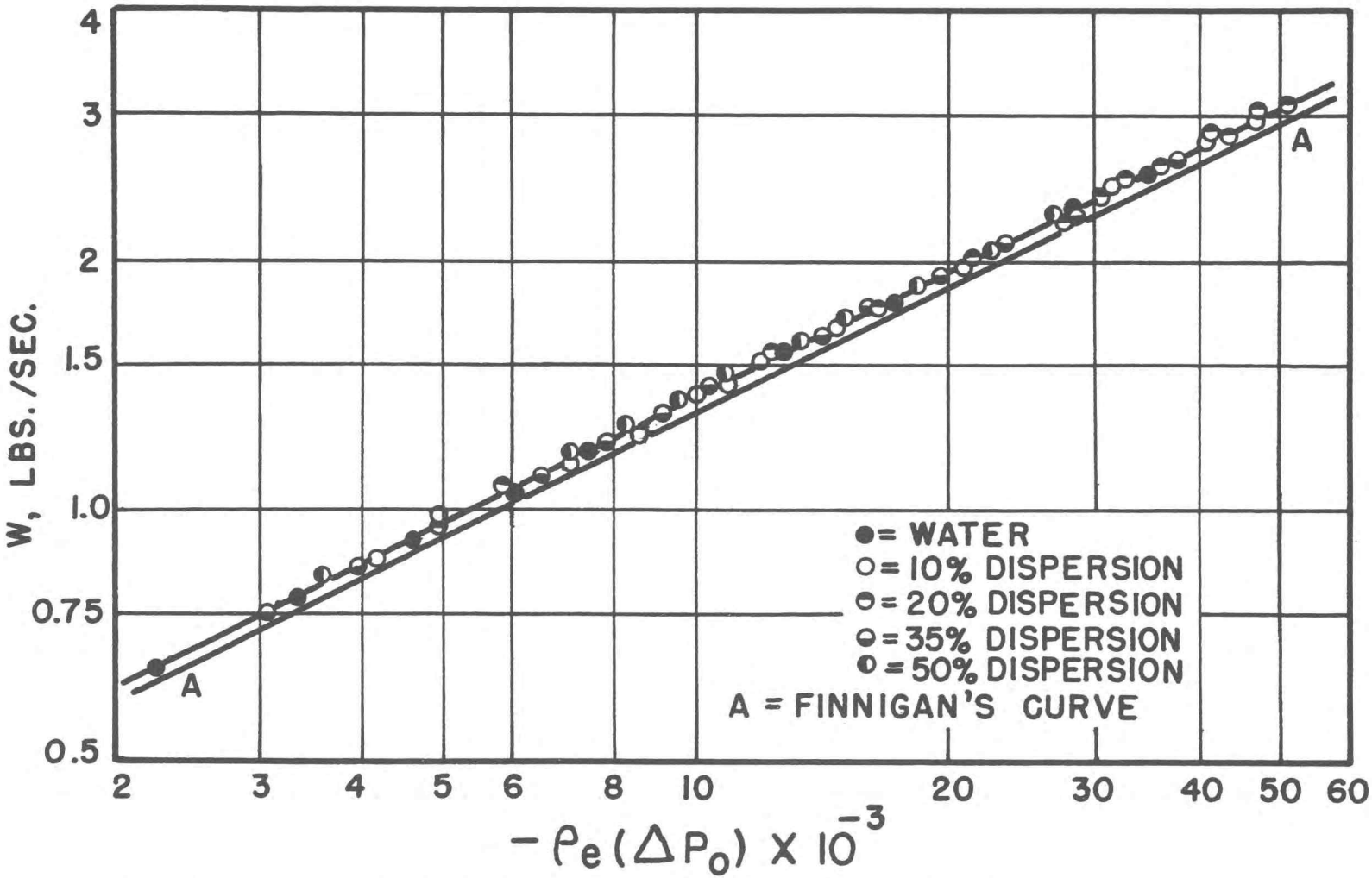

FIGURE 23 ORIFICE CALIBRATION CURVE

CALIBRATION OF THE ORIFICE

Finnigan (10, p. 16-22) has shown that the discharge through a sharp edged orifice in a pipe is related to the pressure drop across the orifice, $\Delta P'$. If the pipe is of diameter D, and is vertical and if the orifice is of diameter D_o, then

$$w = c_o A_o \left[\frac{2 g_c \rho_e (-\Delta P' - \rho_e g \Delta Z'/g_c)}{1 - (D_o / D_1)^4} \right]^{1/2}$$

where c_o = the discharge coefficient of the orifice

A_o = the area of cross-section of the orifice

$\Delta Z'$ = the distance between the pressure taps across the orifice.

Since $\Delta Z'$ is a constant and ρ_e is another constant for each fluid used so $(-\Delta P' - \rho_e g \Delta Z'/g_c)$ can be written as $-\Delta P_o$. If log w is plotted against log $\rho_e(-\Delta P_o)$ a straight line is obtained having a slope of 0.5. Such a plot is a calibration curve of the orifice. The calibration curve obtained from the present investigation is shown in Figure (23). The calibration curve obtained by Finnigan is also given in Figure (23). It is seen that there is a difference of approximately 2% in the two curves. The discharge coefficient obtained by Finnigan was 0.61 while that obtained from the present is about 0.62.

APPENDIX II

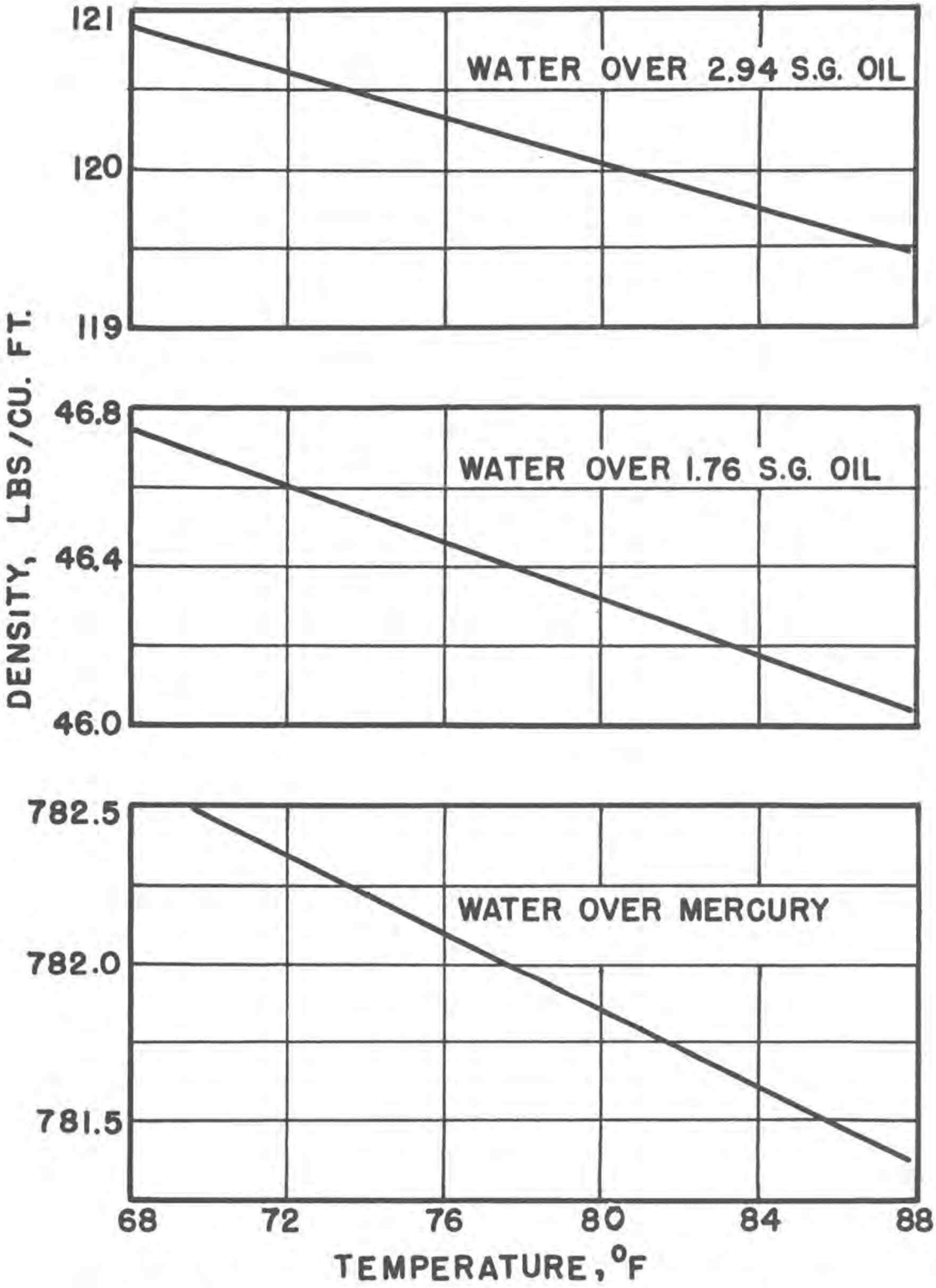

DENSITY OF MANOMETER FLUIDS

FIGURE 24

PHYSICAL PROPERTIES

Equivalent Density of the Manometer Fluids

The manometer oils used were supplied by King Engineering Corporation. The density of the oils was taken from a brochure supplied by the manufacturer. Figure (24) shows the variation of the difference between the density of the two oils used and water with temperature. The density difference between mercury and water is also given in the figure.

Physical Properties of the Solvent

The solvent used was a commercial cleaning solvent manufactured by the Shell Oil Company and marketed under the name "Shellsolv 360". Finnigan (10, p. 129-142) has given a detailed report on the physical properties of this solvent. Table (4) summarizes these properties.

TABLE 4.

Physical Properties of the Solvent

Temp. °F.	Density lb./cu. ft.	Heat capacity BTU/lb. °F.	Thermal conductivity BTU/lb. °F. ft.	Viscosity x 10^4 lb./sec. ft.
50	49.35	0.456	0.128	7.90
55	49.22	0.458	0.124	7.55
60	49.08	0.461	0.119	7.20
65	48.96	0.464	0.115	6.90
70	48.82	0.467	0.111	6.60
80	48.50	0.473	0.101	
90	48.30	0.480		

APPENDIX III

TABULATED DATA

The temperature of the fluid during the runs tabulated in Table (5) were:

W-1 to W-15	55° F.
10-1 to 10-11	68° F.
20-1 to 20-14	67° F.
35-1 to 35-18	65° F.
50-1 to 50-17	65° F.

TABLE 5.

Observed Friction Factor and Orifice Calibration Data

Run No.	ΔH_T (Cm. 2.94 Oil)	ΔH_T (Cm. Hg.)	ΔH_o (Cm. 2.94 Oil)	ΔH_o (Cm. Hg.)	w (lbs./sec.)
W-1	4.6		9.1		0.638
W-2	6.6		13.4		0.781
W-3	8.7		18.6		0.916
W-4	11.1		24.4		1.055
W-5	13.6		30.5	4.8	1.174
W-6	16.2		37.2	5.9	1.313
W-7	19.0		45.2	7.0	1.439
W-8	21.6		51.6	8.2	1.546
W-9	24.6		60.3	9.4	1.667
W-10	28.1		70.3	10.9	1.786
W-11	33.8	5.2		13.4	2.020
W-12	42.8	6.6		17.6	2.299
W-13	50.9	7.9		21.5	2.521
W-14	60.5	9.3		26.1	2.804
W-15	69.1	10.6		30.4	3.000
10-1	10.7		17.0		0.874
10-2	15.7		29.0		1.141
10-3	18.1		35.0		1.242
10-4	20.6		41.3		1.353
10-5	24.3		51.5	8.0	1.523
10-6	28.3		62.6	9.7	1.671
10-7	36.8			13.3	1.974
10-8	45.9			17.3	2.222
10-9	55.3	8.6		21.6	2.479
10-10	67.4	10.3		27.0	2.843
10-11		11.8		31.4	3.061
20-1	14.9		20.7		0.956
20-2	16.8		25.2		1.052
20-3	19.5		31.9		1.183
20-4	22.1		38.8		1.298
20-5	25.4		46.1	7.2	1.428
20-6	29.2		54.7	8.5	1.558
20-7	32.3		62.3	9.9	1.657
20-8	35.0		69.9	10.9	1.760
20-9	42.7			14.2	2.013
20-10	51.6			17.7	2.222
20-11	57.2	9.3		20.0	2.400

TABLE 5. (Continued)

Observed Friction Factor and Orifice Calibration Data

Run No.	ΔH_T (Cm. 2.94 Oil)	ΔH_T (Cm. Hg.)	ΔH_o (Cm. 2.94 Oil)	ΔH_o (Cm. Hg.)	w (lbs./sec.)
20-12	66.0	10.1		23.5	2.609
20-13		11.9		27.7	2.830
20-14	53.1			17.9	2.247
35-1	15.2		13.1		0.754
35-2	17.1		17.0		0.859
35-3	19.9		21.2		0.992
35-4	22.1		28.0		1.103
35-5	24.9		34.1		1.212
35-6	28.0		39.9		1.319
35-7	31.5		47.4		1.422
35-8	34.2		54.1	8.3	1.538
35-9	37.3		61.6	9.6	1.635
35-10	41.1		71.2	11.1	1.765
35-11	47.5			13.2	1.899
35-12	54.7	8.5		15.7	2.083
35-13	63.1	9.7		18.8	2.273
35-14		10.7		21.2	2.449
35-15		12.3		25.2	2.620
35-16		13.8		28.9	2.857
35-17		15.8		33.8	3.093
35-18		14.7		31.6	2.941
50-1	20.3		15.6		0.842
50-2	24.6		22.3		0.996
50-3	26.8		26.3		1.087
50-4	30.2		31.5		1.188
50-5	32.8		36.9		1.271
50-6	35.5		42.6		1.361
50-7	38.3		48.9		1.453
50-8	40.4		54.0	8.3	1.523
50-9	44.1		60.0	9.3	1.613
50-10	48.3		67.7	10.6	1.709
50-11	54.4		12.8	1.863	
50-12	62.1	9.6		15.7	2.069
50-13		11.0		18.7	2.273
50-14		12.6		22.6	2.500
50-15		13.6		24.9	2.632
50-16		15.4		28.8	2.830
50-17		17.2		32.8	3.030

TABLE 6.

Calculated Friction Factor and Orifice Calibration Data

Run No.	$-\Delta P_f$ (lbs_f/ sq. ft.)	$f \times 10^3$	$Re \times 10^{-4}$	$-\Delta P_o \rho_e \times 10^{-3}$ $\frac{lbs_m \ lbs_f}{ft^5}$	$Re\ (\mu_m) \times 10^{-4}$
W-1	18.2	7.27	1.454	2.246	
W-2	26.1	6.94	1.781	3.313	
W-3	34.4	6.66	2.088	4.599	
W-r	44.0	6.42	2.405	6.028	
W-5	53.9	6.35	2.677	7.538	
W-6	64.2	6.05	2.993	9.192	
W-7	75.2	5.90	3.280	11.17	
W-8	85.5	5.81	3.526	12.75	
W-9	97.4	5.69	3.800	14.90	
W-10	111.2	5.66	4.071	17.36	
W-11	133.8	5.32	4.606	21.47	
W-12	169.5	5.21	5.241	28.20	
W-13	201.5	5.15	5.748	34.45	
W-14	239.6	4.95	6.392	41.82	
W-15	273.6	4.94	6.840	48.72	
10-1	34.3	7.11	1.755	4.118	2.420
10-2	54.0	6.59	2.292	7.010	3.162
10-3	63.5	6.55	2.495	8.457	3.442
10-4	73.4	6.25	2.992	9.975	4.127
10-5	88.0	6.05	3.060	12.43	4.221
10-6	103.9	5.91	3.357	15.11	4.631
10-7	137.5	5.62	3.966	20.83	5.471
10-8	173.5	5.58	4.465	27.09	6.158
10-9	210.7	5.43	4.981	33.82	6.870
10-10	258.5	5.08	5.712	42.27	7.879
10-11	294.9	5.00	6.150	49.15	8.483
20-1	42.8	7.27	1.568	4.919	2.649
20-2	50.3	7.08	1.726	5.980	2.416
20-3	61.0	6.80	1.941	7.560	3.279
20-4	71.3	6.54	2.129	9.186	3.597
20-5	84.3	6.40	2.343	10.91	3.958
20-6	99.4	6.33	2.556	12.34	4.318
20-7	111.6	6.23	2.718	14.73	4.592
20-8	122.3	6.13	2.888	16.52	4.878
20-9	152.8	5.87	3.303	21.77	5.579
20-10	188.0	5.92	3.646	27.12	6.158

TABLE 6. (Continued)

Calculated Friction Factor and Orifice Calibration Data

Run No.	$-\Delta P_f$ (lbs_f/sq.ft.)	$f \times 10^3$	$Re \times 10^{-4}$	$-\Delta P_o \rho_e \times 10^{-3}$ $\frac{lbs_m \ lbs_f}{ft^5}$	$Re\ (\mu_m) \times 10^{-4}$
20-11	210.1	5.66	3.937	30.64	6.651
20-12	244.9	5.58	4.281	36.00	7.231
20-13	288.9	5.59	4.643	42.44	7.843
20-14	193.9	5.94	3.686	27.43	6.227
35-1	32.4	8.56	0.836	3.053	2.090
35-2	39.9	8.13	0.952	3.943	2.381
35-3	50.9	7.77	1.100	4.900	2.749
35-4	59.6	7.40	1.223	6.451	3.057
35-5	70.7	7.28	1.344	7.842	3.359
35-6	83.0	7.15	1.462	9.164	3.656
35-7	96.8	7.21	1.576	10.88	3.941
35-8	107.5	6.81	1.705	12.40	4.262
35-9	119.7	6.73	1.812	14.11	4.531
35-10	134.7	6.53	1.957	16.30	4.892
35-11	160.0	6.66	2.105	19.62	5.263
35-12	188.5	6.54	2.309	23.32	5.773
35-13	221.7	6.46	2.520	27.92	6.299
35-14	247.0	6.18	2.715	31.47	6.787
35-15	288.1	6.30	2.904	37.40	7.261
35-16	326.6	6.00	3.167	42.88	7.918
35-17	378.0	5.94	3.429	50.14	8.572
35-18	349.7	6.07	3.260	46.88	8.151
50-1	40.7	8.32	0.663	3.530	2.333
50-2	57.7	8.44	0.784	5.007	2.760
50-3	66.4	8.11	0.856	5.889	3.013
50-4	79.9	8.18	0.935	7.035	3.292
50-5	90.2	8.11	1.000	8.225	3.523
50-6	100.8	7.90	1.071	9.482	3.772
50-7	111.9	7.72	1.144	10.87	4.027
50-8	119.9	7.53	1.199	11.99	4.221
50-9	134.9	7.54	1.269	13.32	4.470
50-10	151.5	7.51	1.345	15.01	4.736
50-11	175.6	7.36	1.466	18.40	5.163
50-12	215.1	7.28	1.628	22.54	5.734
50-13	242.8	6.83	1.789	26.84	6.299
50-14	283.9	6.59	1.968	32.41	6.929
50-15	309.6	6.49	2.071	35.70	7.294

TABLE 6. (Continued)

Calculated Friction Factor and Orifice Calibration Data

Run No.	$-\Delta P_f$ (lbs_f/ sq.ft.)	f x 10^3	Re x 10^{-4}	$-\Delta P_o \rho_e \times 10^{-3}$ $\frac{lbs_m \ lbs_f}{ft^5}$	Re (μ_m) x 10^{-4}
50-16	355.8	6.44	2.227	41.28	7.843
50-17	402.0	6.35	2.385	47.00	8.397

In Table (7) the following new symbols are used:

$$G = (2g_c \frac{K}{} \rho_m / \rho_e)^{1/2}$$

$$H = \frac{Re \sqrt{f/2}}{D} \quad \text{(for water)}$$

$$= \frac{Re\, \mu_m \sqrt{f/2}}{D} \quad \text{(for dispersions)}$$

$$I = \frac{1}{U \sqrt{f/2}}$$

TABLE 7.

Constants Used for Evaluating the Velocity Profile Data

Run No.	T_m (°F.)	T_a (°F.)	w (lbs./sec.)	U (ft./sec.)	G	H	I	c
W-A	64	74	1.040	4.448	1.208	1766	4.095	0.969
W-B	60	69	1.512	6.462	2.022	2348	2.926	0.972
W-C	66	75	2.069	8.840	2.018	3347	2.235	0.948
W-D	65	74	2.102	8.980	2.022	3358	2.205	0.962
W-E	60	73	3.000	12.85	2.020	4334	1.589	0.958
W-F	67	73	3.069	13.13	2.020	4613	1.564	0.960
10-A	68	71	1.007	4.407	1.254	1952	3.865	
10-B	67	72	1.961	8.582	2.044	3445	2.190	0.946
10-C	69	71	2.941	12.87	2.044	5002	1.509	0.955
20-A	67	73	0.997	4.461	1.268	1966	3.755	
20-B	67	72	1.983	8.874	2.066	3575	2.064	0.956
20-C	69	75	2.948	13.19	2.066	5149	1.433	0.962
35-A	65	73	1.000	4.622	1.288	2052	3.484	
35-B	65	75	2.020	9.337	2.100	3802	1.879	0.967
35-C	67	76	2.956	13.66	2.100	5349	1.336	0.971
50-A	65	75	1.049	5.079	1.311	2231	3.057	
50-B	67	74	2.000	9.684	2.138	3955	1.724	0.979
50-C	67	77	2.956	14.31	2.138	5535	1.232	0.980

In Table (8) ΔH_v is given in ins. of the inclined manometer readings for the 1-lb. runs (runs W-A, 10-A, 20-A, 35-A and 50-A) and in cm. of the 2.94 specific gravity oil manometer for the remaining runs.

TABLE 8.

Velocity Profile Data

Run No. W-A

y (in.)	ΔH_v	u (ft./sec.)	y/r_w	u/u_m	u^+	y^+
0.017	9.3	3.570	0.041	0.658	14.61	30.2
0.035	11.3	3.935	0.084	0.725	16.10	62.2
0.060	12.7	4.172	0.145	0.769	17.08	106.6
0.085	13.9	4.364	0.205	0.804	17.86	151.0
0.135	15.5	4.609	0.325	0.849	18.86	239.8
0.185	17.1	4.840	0.446	0.892	19.81	328.6
0.235	18.5	5.035	0.566	0.928	20.61	417.4
0.285	19.8	5.208	0.687	0.960	21.32	506.2
0.335	20.5	5.299	0.807	0.976	21.69	595.0
0.385	21.0	5.364	0.928	0.988	21.95	683.7
0.044	11.7	4.004	0.106	0.738	16.40	78.1
0.069	12.6	4.155	0.166	0.766	17.02	122.5
0.084	14.0	4.380	0.202	0.807	17.94	149.2
0.134	16.1	4.697	0.323	0.865	19.23	238.0
0.184	17.7	4.924	0.443	0.907	20.16	326.8
0.234	19.3	5.142	0.564	0.947	21.06	415.6
0.284	20.2	5.261	0.684	0.969	21.54	504.4
0.334	20.8	5.338	0.805	0.984	21.86	593.2
0.384	21.3	5.402	0.925	0.995	22.12	682.0

TABLE 8. (Continued)

Velocity Profile Data

Run No. W-B

y (in.)	ΔH_v	u (ft./sec.)	y/r_w	u/u_m	u^+	y^+
0.016	6.9	5.167	0.039	0.632	14.15	37.5
0.036	9.2	5.967	0.087	0.729	16.35	84.6
0.059	10.4	6.344	0.142	0.775	17.38	138.5
0.084	11.3	6.613	0.202	0.808	18.11	197.2
0.134	12.8	7.038	0.323	0.861	19.44	314.6
0.184	14.2	7.413	0.443	0.906	20.31	432.0
0.234	15.2	7.670	0.564	0.937	21.01	546.4
0.284	15.9	7.844	0.684	0.959	21.49	666.8
0.334	16.7	8.039	0.805	0.982	22.02	784.2
0.384	17.1	8.135	0.925	0.994	22.28	901.6
0.025	8.9	5.869	0.060	0.717	16.07	58.9
0.046	10.1	6.252	0.111	0.764	17.13	108.0
0.071	11.1	6.554	0.171	0.801	17.95	166.7
0.096	11.9	6.786	0.231	0.829	18.59	225.4
0.146	13.2	7.147	0.352	0.874	19.89	342.8
0.196	14.3	7.440	0.472	0.909	20.38	460.2
0.246	15.3	7.695	0.593	0.940	21.08	577.6
0.296	16.1	7.894	0.713	0.965	21.62	695.0
0.346	16.7	8.040	0.834	0.983	22.02	812.4
0.396	17.0	8.135	0.954	0.994	22.28	929.8

TABLE 8. (Continued)

Velocity Profile Data

Run No. W-C

y (in.)	ΔH_v	u (ft./sec.)	y/r_w	u/u_m	u^+	y^+
0.016	13.6	7.055	0.039	0.658	15.85	53.5
0.036	16.4	7.747	0.087	0.723	17.41	120.1
0.058	18.8	8.295	0.140	0.774	18.64	194.1
0.093	21.5	8.870	0.224	0.827	19.93	311.3
0.143	24.0	9.372	0.345	0.875	21.06	478.6
0.193	26.2	9.793	0.465	0.913	22.01	646.0
0.243	28.0	10.12	0.586	0.944	22.75	813.3
0.293	29.6	10.44	0.706	0.974	23.47	980.8
0.343	30.8	10.62	0.827	0.990	23.85	1148
0.393	31.3	10.70	0.947	0.998	24.05	1315
0.017	14.8	7.359	0.041	0.687	16.36	57.2
0.037	17.8	8.071	0.089	0.753	17.95	123.8
0.062	20.0	8.556	0.149	0.798	19.02	207.5
0.087	21.6	8.891	0.210	0.829	19.77	291.2
0.137	24.1	9.392	0.330	0.876	20.88	458.5
0.187	26.2	9.792	0.451	0.913	21.77	625.9
0.237	27.9	10.10	0.571	0.943	22.46	793.2
0.337	30.6	10.58	0.812	0.987	23.53	1128
0.387	31.2	10.68	0.933	0.997	23.75	1295

TABLE 8. (Continued)

Velocity Profile Data

Run No. W-D

y (in.)	ΔH_v	u (ft./sec.)	y/r_w	u/u_m	u^+	y^+
0.017	14.4	7.381	0.041	0.675	16.32	57.2
0.037	17.3	8.090	0.089	0.740	17.88	123.9
0.062	19.6	8.611	0.149	0.788	19.04	207.6
0.087	21.2	8.956	0.210	0.819	19.79	291.3
0.137	23.8	9.489	0.330	0.868	20.98	458.7
0.187	25.8	9.880	0.451	0.904	21.83	626.1
0.237	27.8	10.25	0.571	0.938	22.66	793.5
0.287	29.4	10.54	0.692	0.965	23.31	960.9
0.337	30.6	10.76	0.812	0.984	23.78	1128
0.387	31.4	10.90	0.933	0.997	24.09	1296
0.042	18.3	8.321	0.101	0.761	18.30	140.6
0.067	20.3	8.764	0.161	0.802	19.27	224.3
0.092	21.9	9.102	0.222	0.832	20.01	308.0
0.142	24.5	9.628	0.342	0.881	21.17	475.4
0.192	26.7	10.05	0.463	0.919	22.10	642.8
0.242	28.5	10.38	0.583	0.950	22.84	810.2
0.292	29.9	10.64	0.704	0.973	23.39	977.6
0.342	30.9	10.81	0.824	0.989	23.78	1145
0.392	31.5	10.91	0.945	0.998	24.01	1312

TABLE 8. (Continued)

Velocity Profile Data

Run No. W-E

y (in.)	ΔH_v	u (ft./sec.)	y/r_w	u/u_m	u^+	y^+
0.016	27.5	10.11	0.039	0.654	16.07	69.4
0.034	33.9	11.23	0.082	0.727	17.84	148.4
0.057	39.1	12.06	0.137	0.780	19.16	247.0
0.107	45.6	13.03	0.258	0.843	20.69	463.7
0.157	50.7	13.74	0.378	0.889	21.82	680.4
0.207	54.9	14.29	0.499	0.925	22.71	897.1
0.257	58.4	14.75	0.619	0.954	23.41	1113
0.307	61.4	15.12	0.740	0.978	24.01	1330
0.357	63.1	15.32	0.860	0.991	24.34	1547
0.407	64.1	15.44	0.981	0.999	24.53	1764
0.051	39.7	12.15	0.118	0.786	19.31	221.0
0.074	43.1	12.66	0.178	0.819	20.12	320.7
0.099	46.0	13.08	0.239	0.846	20.79	429.1
0.124	48.6	13.45	0.299	0.870	21.36	537.4
0.174	53.1	14.06	0.419	0.909	22.33	754.1
0.224	56.5	14.50	0.540	0.938	23.03	970.8
0.274	59.5	14.88	0.660	0.963	23.64	1188
0.324	62.0	15.19	0.781	0.983	24.13	1404
0.374	63.6	15.38	0.901	0.995	24.44	1621

TABLE 8. (Continued)

Velocity Profile Data

Run No. W-F

y (in.)	ΔH_v	u (ft./sec.)	y/r_w	u/u_m	u^+	y^+
0.018	27.9	10.23	0.043	0.651	16.00	83.0
0.028	35.8	11.59	0.067	0.737	18.13	129.2
0.053	41.0	12.40	0.128	0.789	19.39	244.5
0.099	47.3	13.32	0.239	0.847	20.83	456.7
0.153	52.7	14.06	0.369	0.894	21.98	705.8
0.203	56.7	14.59	0.489	0.928	22.80	936.4
0.253	60.2	15.03	0.610	0.956	23.50	1167
0.303	63.1	15.39	0.730	0.979	24.06	1398
0.353	65.0	15.62	0.851	0.993	24.43	1628
0.403	65.8	15.71	0.971	0.999	24.66	1859
0.013	26.7	10.01	0.031	0.637	15.65	60.0
0.028	36.3	11.67	0.067	0.742	18.25	129.1
0.053	41.3	12.45	0.128	0.792	19.46	244.5
0.078	44.6	12.94	0.188	0.823	20.23	359.8
0.128	50.0	13.70	0.308	0.871	21.42	590.4
0.178	54.2	14.26	0.429	0.907	22.31	821.1
0.228	58.0	14.75	0.549	0.938	23.07	1052
0.278	61.1	15.14	0.670	0.963	23.67	1282
0.328	63.7	15.46	0.790	0.983	24.17	1513
0.378	65.3	15.65	0.911	0.995	24.47	1744

TABLE 8. (Continued)

Velocity Profile Data

Run No. 10-A

y (in.)	ΔH_v	u (ft./sec.)	y/r_w	u/u_m	u^+	$y^+ \mu_m$ (cp.)
0.014	8.3	3.320	0.034	0.609	12.83	27.3
0.029	10.6	3.752	0.070	0.688	14.50	56.6
0.050	12.9	4.139	0.120	0.759	16.00	97.6
0.100	15.1	4.478	0.241	0.821	17.70	195.2
0.150	17.1	4.766	0.361	0.874	18.82	292.8
0.200	18.6	4.970	0.482	0.911	19.21	390.4
0.250	20.1	5.167	0.602	0.947	19.97	488.0
0.300	21.1	5.293	0.723	0.971	20.46	585.6
0.350	21.9	5.393	0.843	0.989	20.84	683.2
0.400	22.3	5.442	0.964	0.998	21.44	780.8
0.018	9.6	3.570	0.043	0.655	13.79	35.1
0.032	12.0	3.992	0.077	0.732	15.43	62.5
0.055	13.2	4.187	0.133	0.768	16.18	107.3
0.080	14.3	4.358	0.193	0.799	17.38	156.2
0.130	16.4	4.667	0.313	0.856	18.04	253.8
0.180	18.0	4.889	0.434	0.896	19.39	351.4
0.230	19.7	5.115	0.554	0.938	19.77	449.0
0.280	20.7	5.243	0.675	0.961	20.26	546.6
0.330	21.7	5.369	0.795	0.984	20.75	644.2
0.380	22.1	5.418	0.916	0.993	20.93	741.8

TABLE 8. (Continued)

Velocity Profile Data

Run No. 10-B

y (in.)	ΔH_v	u (ft./sec.)	y/r_w	u/u_m	u^+	$y^+ \mu_m$ (cp.)
0.014	11.5	6.578	0.034	0.617	14.42	48.2
0.027	13.7	7.180	0.065	0.674	15.72	93.0
0.050	17.0	7.998	0.120	0.750	17.52	172.2
0.100	20.5	8.783	0.241	0.824	19.23	344.5
0.150	22.9	9.282	0.361	0.871	20.33	516.8
0.200	25.1	9.718	0.482	0.912	21.29	689.0
0.250	26.7	10.02	0.602	0.940	21.95	861.3
0.300	28.3	10.32	0.723	0.968	22.30	1034
0.350	29.3	10.50	0.843	0.985	22.99	1206
0.400	30.1	10.64	0.964	0.998	23.11	1378
0.018	13.4	7.041	0.043	0.666	15.42	62.0
0.080	20.1	8.623	0.193	0.816	18.89	275.6
0.130	22.4	9.103	0.313	0.861	19.94	447.8
0.180	24.3	9.482	0.434	0.897	20.77	620.1
0.230	26.1	9.826	0.554	0.930	21.52	792.3
0.280	27.5	10.09	0.675	0.954	22.09	964.6
0.330	29.3	10.41	0.795	0.985	22.80	1137
0.380	29.8	10.50	0.916	0.993	23.00	1309

TABLE 8. (Continued)

Velocity Profile Data

Run No. 10-C

y (in.)	ΔH_v	u (ft./sec.)	y/r_w	u/u_m	u^+	$y^+\mu_m$ (cp.)
0.018	29.8	10.66	0.043	0.679	16.12	90.0
0.030	36.4	11.78	0.072	0.751	17.71	150.1
0.055	40.8	12.47	0.133	0.795	18.85	275.1
0.080	44.0	12.95	0.193	0.825	19.58	400.2
0.130	49.4	13.72	0.313	0.874	20.75	650.3
0.180	53.7	14.30	0.434	0.912	21.63	900.4
0.280	60.2	15.15	0.675	0.965	22.90	1401
0.330	62.7	15.46	0.795	0.985	23.37	1651
0.380	64.3	15.65	0.916	0.998	23.67	1901
0.027	32.9	11.20	0.065	0.714	16.89	135.1
0.050	38.1	12.05	0.120	0.768	18.18	250.1
0.075	42.1	12.67	0.181	0.807	19.11	375.1
0.100	45.3	13.14	0.241	0.837	19.83	500.2
0.150	50.4	13.87	0.361	0.884	20.92	750.3
0.200	54.6	14.42	0.482	0.919	21.76	1000
0.250	58.2	14.89	0.602	0.949	22.47	1250
0.350	63.1	15.51	0.843	0.988	23.40	1751
0.400	64.5	15.68	0.964	0.999	23.66	2001

TABLE 8. (Continued)

Velocity Profile Data

Run No. 20-A

y (in.)	ΔH_v	u (ft./sec.)	y/r_w	u/u_m	u^+	$y^+ \mu_m$ (cp.)
0.018	11.3	3.832	0.043	0.713	13.38	35.4
0.032	13.0	4.110	0.077	0.765	14.44	62.9
0.055	14.4	4.326	0.133	0.805	16.24	108.1
0.080	15.6	4.502	0.193	0.838	16.91	157.3
0.130	17.2	4.728	0.313	0.880	17.76	255.6
0.180	18.6	4.917	0.434	0.915	18.46	353.9
0.230	19.9	5.085	0.554	0.947	19.09	452.2
0.280	20.9	5.212	0.675	0.970	19.57	550.5
0.330	21.6	5.298	0.795	0.986	19.99	648.8
0.380	22.0	5.346	0.915	0.995	20.47	747.1
0.029	11.6	3.883	0.070	0.723	14.57	57.0
0.050	13.4	4.173	0.120	0.777	15.67	98.3
0.075	14.7	4.371	0.181	0.814	16.41	147.5
0.100	16.1	4.574	0.241	0.852	17.17	196.6
0.150	17.6	4.783	0.361	0.890	17.95	294.9
0.200	18.8	4.943	0.482	0.920	18.56	393.2
0.250	20.2	5.123	0.602	0.954	19.24	491.5
0.300	20.9	5.212	0.723	0.970	19.57	589.8
0.350	21.8	5.322	0.843	0.991	19.98	688.1
0.400	22.1	5.359	0.964	0.998	20.22	786.4

TABLE 8. (Continued)

Velocity Profile Data

Run No. 20-B

y (in.)	ΔH_v	u (ft./sec.)	y/r_w	u/u_m	u^+	$y^+ \mu_m$ (cp.)
0.018	13.8	7.322	0.043	0.673	15.11	64.3
0.030	16.8	8.078	0.072	0.742	16.08	107.2
0.055	18.7	8.523	0.133	0.783	17.59	196.6
0.080	20.1	8.837	0.193	0.812	18.24	286.0
0.30	22.8	9.411	0.313	0.865	19.42	464.9
0.180	24.8	9.816	0.434	0.902	20.36	643.5
0.230	26.6	10.17	0.554	0.934	20.98	822.3
0.280	28.1	10.45	0.675	0.960	21.56	1001
0.330	29.3	10.67	0.795	0.980	22.02	1179
0.380	30.1	10.81	0.916	0.993	22.32	1358
0.014	11.2	6.617	0.034	0.606	13.66	50.0
0.027	15.7	7.834	0.065	0.717	16.17	96.5
0.050	17.8	8.341	0.120	0.764	17.22	178.7
0.075	19.6	8.754	0.181	0.802	18.07	268.0
0.100	20.9	9.039	0.241	0.828	18.65	357.4
0.150	23.2	9.423	0.361	0.872	19.66	536.1
0.200	25.4	9.964	0.482	0.913	20.57	714.8
0.250	27.1	10.29	0.602	0.943	21.25	893.5
0.300	28.4	10.54	0.723	0.965	21.74	1072
0.350	30.1	10.85	0.843	0.993	22.39	1251
0.400	30.4	10.90	0.964	0.998	22.50	1430

TABLE 8. (Continued)

Velocity Profile Data

Run No. 20-C

y (in.)	ΔH_v	u (ft./sec.)	y/r_w	u/u_m	u^+	$y^+ \mu_m$ (cp.)
0.027	33.1	11.45	0.065	0.708	16.40	139.0
0.050	39.0	12.43	0.120	0.768	17.81	257.4
0.075	43.1	13.06	0.181	0.807	18.71	386.2
0.100	46.0	13.49	0.241	0.834	19.38	514.9
0.150	51.6	14.29	0.361	0.884	20.48	772.3
0.200	55.9	14.88	0.482	0.920	21.32	1030
0.250	59.7	15.24	0.602	0.942	21.84	1287
0.300	62.8	15.77	0.723	0.975	22.59	1545
0.350	64.1	15.93	0.843	0.985	22.82	1802
0.400	66.0	16.16	0.964	0.999	23.16	2060
0.018	29.5	10.76	0.043	0.668	15.42	92.7
0.030	36.3	11.94	0.072	0.741	17.10	154.5
0.055	40.7	12.64	0.133	0.785	18.12	283.2
0.080	44.0	13.14	0.193	0.816	18.83	411.9
0.130	49.6	13.95	0.313	0.866	20.00	669.4
0.180	54.2	14.61	0.434	0.907	20.93	926.8
0.230	58.2	15.32	0.554	0.951	21.95	1184
0.280	65.8	15.47	0.675	0.961	22.17	1442
0.330	64.5	15.91	0.795	0.988	22.81	1700
0.380	65.8	16.07	0.916	0.998	23.04	1957

TABLE 8. (Continued)

Velocity Profile Data

Run No. 35-A

y (in.)	ΔH_v	u (ft./sec.)	y/r_w	u/u_m	u^+	$y^+ \mu_m$ (cp.)
0.014	8.0	3.424	0.034	0.610	11.93	28.7
0.029	11.0	4.016	0.070	0.715	13.99	59.5
0.050	13.1	4.382	0.120	0.781	15.27	102.6
0.075	14.4	4.595	0.181	0.818	16.00	153.9
0.100	15.1	4.705	0.241	0.838	16.39	205.2
0.150	17.2	5.021	0.361	0.894	17.49	307.8
0.200	18.2	5.165	0.482	0.920	18.00	410.4
0.250	19.2	5.305	0.602	0.945	18.48	513.0
0.300	20.0	5.414	0.723	0.964	18.87	615.6
0.350	20.7	5.508	0.843	0.981	19.19	718.2
0.400	21.4	5.600	0.964	0.998	19.51	820.8
0.032	12.3	4.246	0.077	0.756	14.08	65.7
0.055	13.8	4.498	0.133	0.801	15.67	112.9
0.080	14.7	4.642	0.193	0.827	16.17	164.2
0.130	16.8	4.962	0.313	0.884	17.29	266.8
0.180	17.8	5.108	0.434	0.910	17.79	369.4
0.230	18.8	5.250	0.554	0.935	18.29	472.0
0.280	19.8	5.387	0.675	0.960	18.77	574.6
0.330	20.5	5.482	0.795	0.976	19.10	677.2
0.380	21.3	5.587	0.916	0.995	19.47	779.8

TABLE 8. (Continued)

Velocity Profile Data

Run No. 35-B

y (in.)	ΔH_v	u (ft./sec.)	y/r_w	u/u_m	u^+	$y^+ \mu_m$ (cp.)
0.014	11.9	6.998	0.034	0.613	13.15	53.2
0.027	15.7	8.038	0.065	0.704	15.10	102.6
0.050	18.8	8.795	0.120	0.770	16.53	190.1
0.075	20.8	9.251	0.181	0.810	17.39	285.1
0.100	22.2	9.559	0.241	0.837	17.96	380.2
0.150	24.7	10.08	0.361	0.883	18.94	570.3
0.200	26.6	10.46	0.482	0.916	19.66	760.4
0.250	28.5	10.83	0.602	0.948	20.35	950.5
0.300	30.0	11.11	0.723	0.973	20.88	1141
0.350	31.2	11.33	0.843	0.992	21.29	1331
0.400	31.6	11.40	0.964	0.998	21.43	1521
0.018	12.1	7.071	0.043	0.618	13.29	68.4
0.030	16.8	8.332	0.072	0.728	15.65	114.1
0.055	19.8	9.045	0.133	0.790	17.00	209.1
0.080	21.4	9.404	0.193	0.822	17.67	304.2
0.130	24.0	9.959	0.313	0.870	18.71	494.3
0.180	26.3	10.42	0.434	0.911	19.59	684.4
0.230	28.0	10.76	0.554	0.940	20.21	874.5
0.330	31.0	11.32	0.795	0.989	21.27	1255
0.380	31.6	11.43	0.916	0.998	21.47	1445

TABLE 8. (Continued)

Velocity Profile Data

Run No. 35-C

y (in.)	ΔH_v	u (ft./sec.)	y/r_w	u/u_m	u^+	$y^+ \mu_m$ (cp.)
0.014	24.6	10.15	0.034	0.607	13.56	74.9
0.027	33.6	11.86	0.065	0.709	15.84	144.4
0.050	39.5	12.86	0.120	0.769	17.17	267.4
0.075	43.5	13.49	0.181	0.807	18.02	401.2
0.100	46.4	13.93	0.241	0.833	18.61	534.9
0.150	51.9	14.74	0.361	0.881	19.68	802.3
0.200	56.5	15.38	0.482	0.920	20.54	1070
0.250	60.2	15.87	0.602	0.949	21.20	1337
0.300	63.6	16.31	0.723	0.976	21.79	1605
0.350	65.8	16.59	0.843	0.992	22.17	1872
0.400	66.7	16.71	0.964	0.999	22.31	2140
0.018	29.9	11.12	0.043	0.669	14.85	96.3
0.030	37.4	12.43	0.072	0.748	16.61	160.5
0.055	41.7	13.13	0.132	0.790	17.53	294.2
0.080	45.0	13.64	0.193	0.821	18.22	427.9
0.130	50.7	14.48	0.313	0.871	19.34	695.4
0.180	55.4	15.13	0.434	0.911	20.21	962.8
0.230	59.5	15.68	0.554	0.944	20.95	1230
0.280	62.7	16.10	0.675	0.969	21.51	1498
0.330	65.2	16.41	0.795	0.988	21.93	1765
0.380	66.5	16.58	0.916	0.998	22.15	2033

TABLE 8. (Continued)

Velocity Profile Data

Run No. 50-A

y (in.)	ΔH_v	u (ft./sec.)	y/r_w	u/u_m	u^+	$y^+ \mu_m$ (cp.)
0.014	7.8	3.661	0.033	0.600	11.19	32.0
0.029	10.9	4.328	0.070	0.709	13.23	64.7
0.050	13.3	4.781	0.120	0.783	14.61	111.5
0.075	14.5	4.992	0.181	0.817	15.26	167.3
0.100	15.0	5.077	0.241	0.831	15.52	223.1
0.150	17.3	5.453	0.361	0.893	16.67	334.6
0.200	18.3	5.608	0.482	0.918	17.14	446.2
0.250	19.4	5.774	0.602	0.946	17.65	557.8
0.300	20.2	5.892	0.723	0.965	18.01	669.3
0.350	20.9	5.993	0.843	0.981	18.32	780.8
0.400	21.6	6.093	0.964	0.998	18.63	892.4
0.018	8.4	3.800	0.043	0.622	11.62	40.2
0.055	14.0	4.905	0.133	0.803	15.00	122.7
0.080	14.8	5.044	0.193	0.826	15.42	178.5
0.130	17.0	5.405	0.313	0.885	16.52	290.0
0.180	18.0	5.562	0.434	0.911	17.00	401.6
0.230	19.1	5.730	0.554	0.938	17.52	513.1
0.280	20.0	5.863	0.675	0.960	17.92	624.7
0.330	20.7	5.965	0.795	0.977	18.23	736.2
0.380	21.4	6.065	0.916	0.993	18.54	847.8

TABLE 8. (Continued)

Velocity Profile Data

Run No. 50-B

y (in.)	ΔH_v	u (ft./sec.)	y/r_w	u/u_m	u^+	$y^+ \mu_m$ (cp.)
0.014	10.0	6.619	0.034	0.557	11.42	55.4
0.029	15.1	8.134	0.070	0.685	14.02	114.7
0.050	19.3	9.195	0.120	0.774	15.55	197.8
0.75	21.3	9.660	0.181	0.813	16.55	296.6
0.100	22.8	9.995	0.241	0.841	17.23	395.5
0.150	25.3	10.51	0.361	0.886	18.15	593.3
0.200	27.2	10.92	0.482	0.918	18.82	791.0
0.250	28.9	11.25	0.602	0.947	19.39	988.8
0.300	30.5	11.56	0.723	0.973	19.93	1187
0.350	31.5	11.75	0.843	0.989	20.26	1384
0.400	32.1	11.86	0.964	0.998	20.44	1582
0.018	13.2	7.605	0.043	0.640	13.11	71.2
0.055	20.3	9.431	0.133	0.794	16.26	217.5
0.080	22.2	9.862	0.193	0.830	17.01	316.4
0.130	24.8	10.42	0.313	0.878	17.97	514.1
0.180	27.0	10.87	0.434	0.916	18.75	711.9
0.230	28.8	11.23	0.554	0.946	19.36	909.6
0.280	30.3	11.52	0.675	0.970	19.86	1107
0.330	31.2	11.69	0.795	0.984	20.16	1305
0.380	31.9	11.82	0.916	0.995	20.38	1503

TABLE 8. (Continued)

Velocity Profile Data

Run No. 50-C

y (in.)	ΔH_v	u (ft./sec.)	y/r_w	u/u_m	u^+	$y^+ \rho_m$ (cp.)
0.014	23.6	10.23	0.034	0.585	12.61	77.5
0.029	34.7	12.41	0.070	0.709	15.29	160.5
0.050	41.4	13.55	0.120	0.774	16.70	276.8
0.075	45.7	14.24	0.181	0.814	17.54	415.1
0.100	48.3	14.64	0.241	0.837	18.04	553.5
0.150	53.8	15.45	0.361	0.883	19.03	830.3
0.200	58.4	16.09	0.482	0.920	19.83	1107
0.250	62.4	16.64	0.602	0.951	20.50	1383
0.300	65.6	17.06	0.723	0.975	21.01	1660
0.350	67.8	17.34	0.843	0.991	21.36	1937
0.400	68.9	17.48	0.964	0.999	21.53	2214
0.018	30.3	11.49	0.043	0.663	14.15	99.6
0.032	38.3	12.91	0.077	0.745	15.91	177.1
0.055	44.2	13.87	0.133	0.800	17.09	304.4
0.080	47.3	14.35	0.193	0.828	17.69	442.8
0.130	53.1	15.21	0.313	0.877	18.73	719.5
0.180	57.7	15.85	0.434	0.914	19.53	996.3
0.230	61.7	16.39	0.554	0.946	20.19	1273
0.280	65.4	16.88	0.674	0.974	20.79	1550
0.330	67.6	17.16	0.795	0.990	21.14	1827
0.380	68.8	17.31	0.916	0.999	21.33	2103

In Table (9) columns (2) and (5) give, respectively, the temperature and the reduced temperature obtained while moving the probe away from the wall. Columns (3) and (6) give the temperature obtained while moving towards the wall.

TABLE 9.

Temperature Profile Data

y (in.)	T (°F.)	T (°F.)	y/r_w	$\frac{T - T_w}{T_c - T_w}$	$\frac{T - T_w}{T_c - T_w}$
		Run No. W-G			
0.025	108.8	108.9	0.060	0.845	0.842
0.050	107.8	107.7	0.121	0.876	0.880
0.075	107.3	107.3	0.181	0.892	0.892
0.100	106.9	106.9	0.241	0.905	0.905
0.125	106.4	106.4	0.301	0.920	0.920
0.175	105.7	105.9	0.422	0.946	0.946
0.225	105.3	105.1	0.542	0.955	0.961
0.275	104.7	104.7	0.663	0.975	0.975
0.325	104.3	104.3	0.783	0.986	0.986
0.375	104.1	104.1	0.904	0.994	0.994
0.410	103.9	103.9	0.988	1.000	1.000
		Run No. W-H			
0.025	105.1	105.1	0.060	0.845	0.845
0.050	104.3	104.3	0.121	0.867	0.867
0.075	103.6	103.7	0.181	0.885	0.887
0.100	103.3	103.4	0.241	0.895	0.895
0.125	102.9	103.0	0.301	0.907	0.905
0.175	102.2	102.1	0.422	0.926	0.930
0.225	101.3	101.3	0.542	0.952	0.952
0.275	100.8	100.9	0.663	0.966	0.964
0.325	100.3	100.4	0.783	0.980	0.977
0.375	100.0	99.9	0.904	0.990	0.992
0.410	99.6	99.6	0.988	1.000	1.000

TABLE 9. (Continued)

Temperature Profile Data

y (in.)	T (°F.)	T (°F.)	y/r_w	$\frac{T - T_w}{T_c - T_w}$	$\frac{T - T_w}{T_c - T_w}$
		Run No. W-I			
0.025	105.8	105.9	0.060	0.844	0.840
0.040	105.1	105.1	0.096	0.865	0.865
0.075	104.3	104.4	0.181	0.889	0.889
0.100	103.6	103.6	0.241	0.907	0.907
0.125	103.0	103.1	0.301	0.926	0.926
0.175	102.2	102.2	0.422	0.950	0.950
0.225	102.0	101.8	0.542	0.955	0.961
0.275	101.6	101.5	0.663	0.967	0.970
0.325	101.2	101.1	0.783	0.980	0.981
0.375	100.8	100.8	0.904	0.991	0.991
0.410	100.5	100.5	0.988	1.000	1.000
		Run No. W-J			
0.025	102.6	102.7	0.060	0.855	0.852
0.040	102.0	101.8	0.096	0.870	0.876
0.075	101.3	101.4	0.181	0.890	0.887
0.100	100.8	100.8	0.241	0.904	0.904
0.125	100.3	100.2	0.301	0.917	0.920
0.175	99.6	99.6	0.422	0.936	0.936
0.225	99.0	99.2	0.542	0.954	0.948
0.275	98.6	98.6	0.663	0.964	0.964
0.325	97.9	98.0	0.783	0.984	0.980
0.375	97.4	97.5	0.904	0.997	0.995
0.410	97.3	97.3	0.988	1.000	1.000

TABLE 9. (Continued)

Temperature Profile Data

y (in.)	T (°F.)	T (°F.)	y/r_w	$\frac{T - T_w}{T_c - T_w}$	$\frac{T - T_w}{T_c - T_w}$
		Run No. W-K			
0.025	103.0	103.0	0.060	0.856	0.856
0.050	102.1	102.3	0.121	0.897	0.887
0.075	101.8	101.9	0.181	0.910	0.905
0.125	101.4	101.3	0.301	0.929	0.933
0.175	101.1	101.0	0.422	0.946	0.946
0.225	100.7	100.7	0.542	0.960	0.960
0.275	100.3	100.4	0.663	0.976	0.974
0.325	100.1	100.2	0.783	0.986	0.981
0.375	99.8	100.0	0.904	1.000	0.991
0.410	99.8	99.8	0.988	1.000	1.000
		Run No. 10-A			
0.025	105.3	105.3	0.060	0.841	0.841
0.050	104.6	104.5	0.121	0.874	0.879
0.075	104.1	103.9	0.181	0.896	0.906
0.125	103.7	103.6	0.301	0.916	0.920
0.175	103.3	103.1	0.422	0.935	0.944
0.225	102.9	102.9	0.542	0.954	0.954
0.275	102.6	102.4	0.663	0.967	0.976
0.325	102.3	102.3	0.783	0.981	0.981
0.375	102.1	102.1	0.904	0.991	0.991
0.410	101.9	101.9	0.988	1.000	1.000

TABLE 9. (Continued)

Temperature Profile Data

y (in.)	T (°F.)	T (°F.)	y/r_w	$\frac{T - T_w}{T_c - T_w}$	$\frac{T - T_w}{T_c - T_w}$
		Run No. 10-B			
0.025	105.0	105.2	0.060	0.885	0.875
0.050	104.6	104.8	0.121	0.903	0.895
0.075	104.3	104.5	0.181	0.916	0.908
0.125	104.0	104.1	0.301	0.930	0.925
0.175	103.6	103.8	0.422	0.947	0.939
0.225	103.2	103.4	0.542	0.965	0.956
0.275	102.9	103.0	0.663	0.980	0.975
0.325	102.6	102.7	0.783	0.992	0.987
0.375	102.5	102.5	0.904	0.996	0.996
0.410	102.4	102.4	0.988	1.000	1.000
		Run No. 10-C			
0.025	102.0	101.9	0.060	0.844	0.849
0.050	101.6	101.5	0.121	0.866	0.872
0.075	101.4	101.3	0.181	0.878	0.884
0.125	101.0	101.0	0.301	0.901	0.901
0.175	100.6	100.5	0.422	0.924	0.930
0.225	100.2	100.1	0.542	0.947	0.954
0.275	100.1	99.9	0.663	0.954	0.960
0.325	99.9	99.8	0.783	0.960	0.971
0.375	99.6	99.5	0.904	0.983	0.989
0.410	99.3	99.3	0.988	1.000	1.000

TABLE 9. (Continued)

Temperature Profile Data

y (in.)	T (°F.)	T (°F.)	y/r_w	$\frac{T - T_w}{T_c - T_w}$	$\frac{T - T_w}{T_c - T_w}$
		Run No. 20-A			
0.025	104.9	104.8	0.060	0.874	0.879
0.050	104.3	104.2	0.121	0.904	0.910
0.075	104.0	104.0	0.181	0.920	0.920
0.125	103.6	103.6	0.301	0.940	0.940
0.175	103.5	103.3	0.422	0.945	0.955
0.225	103.2	103.2	0.542	0.960	0.960
0.275	103.0	103.0	0.663	0.970	0.970
0.325	102.7	102.6	0.783	0.985	0.985
0.375	102.6	102.5	0.904	0.990	0.995
0.410	102.4	102.5	0.988	1.000	0.995
		Run No. 20-B			
0.025	105.5	105.6	0.060	0.867	0.862
0.050	105.0	105.0	0.121	0.893	0.893
0.075	104.6	104.8	0.181	0.914	0.904
0.125	104.2	104.4	0.301	0.934	0.924
0.175	104.1	104.0	0.422	0.939	0.944
0.225	103.8	103.8	0.542	0.954	0.954
0.275	103.4	103.5	0.663	0.975	0.970
0.325	103.3	103.2	0.783	0.980	0.985
0.375	103.1	103.0	0.904	0.990	0.995
0.410	102.9	102.9	0.988	1.000	1.000

TABLE 9. (Continued)

Temperature Profile Data

y (in.)	T (°F.)	T (°F.)	y/r_w	$\frac{T - T_w}{T_c - T_w}$	$\frac{T - T_w}{T_c - T_w}$
		Run No. 20-C			
0.025	102.0	102.0	0.060	0.890	0.890
0.050	101.6	101.7	0.121	0.910	0.905
0.075	101.4	101.3	0.181	0.920	0.925
0.125	101.1	101.0	0.301	0.936	0.941
0.175	100.8	100.8	0.422	0.952	0.952
0.225	100.6	100.5	0.542	0.962	0.968
0.275	100.4	100.2	0.663	0.974	0.984
0.325	100.2	100.1	0.783	0.984	0.990
0.375	100.0	100.0	0.904	0.995	0.995
0.410	99.9	100.0	0.988	1.000	0.995
		Run No. 35-A			
0.025	106.2	106.2	0.060	0.865	0.865
0.050	105.8	105.8	0.121	0.885	0.885
0.075	105.5	105.4	0.181	0.900	0.906
0.125	105.2	105.1	0.301	0.916	0.921
0.175	104.8	104.9	0.422	0.937	0.932
0.225	104.6	104.7	0.542	0.948	0.943
0.275	104.2	104.3	0.663	0.969	0.964
0.325	103.9	104.0	0.783	0.985	0.980
0.375	103.6	103.8	0.904	1.000	0.990
0.410	103.6	103.6	0.988	1.000	1.000

TABLE 9. (Continued)

Temperature Profile Data

y (in.)	T (°F.)	T (°F.)	y/r_w	$\frac{T - T_w}{T_c - T_w}$	$\frac{T - T_w}{T_c - T_w}$
		Run No. 35-B			
0.025	102.1	102.0	0.060	0.869	0.876
0.050	101.8	101.9	0.121	0.894	0.885
0.075	101.7	101.7	0.181	0.902	0.902
0.125	101.4	101.5	0.301	0.926	0.918
0.175	101.2	101.3	0.422	0.942	0.935
0.225	101.0	101.2	0.542	0.959	0.942
0.275	100.9	100.9	0.663	0.967	0.967
0.325	100.7	100.8	0.783	0.984	0.975
0.375	100.6	100.6	0.904	0.992	0.992
0.410	100.4	100.4	0.988	1.000	1.000
		Run No. 35-C			
0.025	100.5	100.6	0.060	0.875	0.869
0.050	100.1	100.2	0.121	0.902	0.895
0.075	100.0	100.0	0.181	0.909	0.909
0.125	99.8	99.8	0.301	0.921	0.921
0.175	99.6	99.5	0.422	0.935	0.941
0.225	99.3	99.3	0.542	0.955	0.955
0.275	99.0	99.1	0.663	0.974	0.967
0.325	98.9	98.9	0.784	0.980	0.980
0.375	98.7	98.7	0.904	0.994	0.994
0.410	98.6	98.6	0.998	1.000	1.000

TABLE 9. (Continued)

Temperature Profile Data

y (in.)	T (°F.)	T (°F.)	y/r_w	$\frac{T - T_w}{T_c - T_w}$	$\frac{T - T_w}{T_c - T_w}$
		Run No. 50-A			
0.025	108.6	108.6	0.060	0.871	0.871
0.050	108.1	108.0	0.121	0.894	0.902
0.075	107.7	107.8	0.181	0.911	0.907
0.125	107.0	107.1	0.301	0.942	0.938
0.175	106.7	106.8	0.422	0.956	0.951
0.225	106.5	106.5	0.542	0.965	0.965
0.275	106.2	106.3	0.663	0.979	0.974
0.325	106.0	106.1	0.783	0.986	0.982
0.375	105.8	105.8	0.904	0.996	0.996
0.410	105.7	105.7	0.988	1.000	1.000
		Run No. 50-B			
0.025	102.4	102.3	0.060	0.874	0.879
0.050	102.0	101.9	0.121	0.896	0.901
0.075	101.8	101.7	0.181	0.907	0.914
0.125	101.3	101.3	0.301	0.936	0.936
0.175	101.0	101.1	0.422	0.954	0.949
0.225	100.8	100.7	0.542	0.965	0.971
0.275	100.6	100.6	0.663	0.977	0.977
0.325	100.4	100.5	0.784	0.988	0.983
0.375	100.3	100.3	0.904	0.995	0.995
0.410	100.2	100.2	0.988	1.000	1.000

TABLE 9. (Continued)

Temperature Profile Data

y (in.)	T (°F.)	T (°F.)	y/r_w	$\frac{T - T_w}{T_c - T_w}$	$\frac{T - T_w}{T_c - T_w}$
		Run No. 50-C			
0.025	102.7	102.8	0.060	0.875	0.869
0.050	102.3	102.3	0.121	0.899	0.899
0.075	102.0	101.9	0.181	0.916	0.922
0.125	101.7	101.6	0.301	0.934	0.940
0.175	101.5	101.4	0.422	0.946	0.952
0.225	101.3	101.2	0.542	0.959	0.964
0.275	101.1	101.0	0.663	0.970	0.976
0.325	100.9	100.8	0.783	0.981	0.988
0.375	100.8	100.6	0.904	0.988	1.000
0.410	100.7	100.6	0.988	0.994	1.000

TABLE 10.

Observed Heat Transfer Data

Run No.	T_1 (°F.)	T_2 (°F.)	T_3 (°F.)	T_4 (°F.)	T_5 (°F.)	T_6 (°F.)	T_7 (°F.)	T_8 (°F.)	T_{b1} (°F.)	T_{b2} (°F.)
W-G	169.0	172.3	165.7	163.6	157.0	158.0	131.0	132.9	83.0	105.2
W-H	170.4	173.0	166.5	165.5	159.6	159.3	3.5.5	134.5	81.4	104.1
W-I	165.0	168.2	159.3	159.7	154.2	152.0	134.7	133.5	88.6	105.4
W-J	169.2	172.3	160.1	158.2	154.3	156.0	134.7	133.0	86.1	102.4
W-K	149.0	153.5	143.5	145.1	138.5	137.9	120.5	119.4	88.1	100.8
10-A	162.0	166.5	153.5	152.0	145.8	145.2	124.0	122.7	79.7	105.3
10-B	158.5	153.5	143.4	142.8	139.8	139.0	125.5	124.2	86.6	103.9
10-C	144.0	148.5	134.6	132.8	128.4	126.6	117.3	115.6	88.3	101.5
20-A	163.7	167.1	154.5	152.0	143.5	145.1	123.4	121.0	80.3	105.8
20-B	151.0	155.1	143.5	141.8	134.5	134.0	123.4	121.6	87.2	104.7
20-C	145.2	148.1	135.5		131.0	128.6	119.3	118.0	87.2	102.0
35-A	163.7	165.7	149.5	150.2	147.2	146.1	123.5	122.0	81.1	106.0
35-B	148.5	151.9	133.5	131.7	125.7	125.0	113.3	112.2	85.6	101.8
35-C	149.9	152.2	132.0	129.0	127.4	124.7	114.5	113.0	86.4	102.0
50-A	155.2	159.5	140.0	138.4	134.4	131.4	118.5	116.5	84.0	102.9
50-B	173.0	175.6	162.7	160.5	153.0	152.0	128.7	127.5	84.6	108.9
50-C	148.5	152.0	135.0	132.0	131.7	129.8	118.2	116.5	86.0	104.2

TABLE 11.

Calculated Heat Transfer Data

Run No.	$\dot{W}$ (lbs./sec.)	Re x 10^{-4}	h (BTU/hr. ^{o}F. sq. ft.)	St x 10^{3}	St $(Pr)_c^{2/3}$ x 10^{3}
W-G	1.026	5.083	1030	1.046	2.521
W-H	1.066	5.281	1095	1.075	2.591
W-I	2.174	10.77	1855	0.891	2.147
W-J	3.077	15.24	2380	0.811	1.958
W-K	3.015	14.94	2460	0.856	2.063
10-A	1.007	2.000	1312	1.401	3.376
10-B	1.961	3.897	2036	1.123	2.706
10-C	2.941	5.844	3016	1.108	2.670
20-A	0.997	1.618	1240	1.418	3.417
20-B	1.983	3.218	2140	1.230	2.964
20-C	2.948	4.783	2975	1.150	2.772
35-A	1.000	1.096	1130	1.391	3.352
35-B	2.020	2.215	2182	1.330	3.205
35-C	2.956	3.241	3024	1.259	3.034
50-A	1.049	0.814	983	1.262	3.041
50-B	2.000	1.553	1932	1.303	3.140
50-C	2.956	2.293	3127	1.427	3.439

APPENDIX IV

NOMENCLATURE

The fundamental dimensions are represented by the following letters:

F = force, L = length, m = mass

t = time and T = temperature.

Symbol	Meaning	Dimensions
A	Area	L^2
A_c	Area of tube cross-section	L^2
A_o	Area of orifice	L^2
A_r	Area across which heat transfer in a tube takes place	L^2
A_w	Area of tube wall	L^2
A_n, A_{ln}	Constants	
B	Constant	
C, C_n	Constants	
C_p	Heat capacity	FL/mt
c	Pitot tube calibration constant	
c_o	Orifice calibration constant	
D	Diameter of tube	L
D_o	Diameter of orifice	L
f	Friction factor	
g	Acceleration of gravity	L/t^2
g_c	Gravitational constant	$ml/F\ t^2$
G	Mass flow rate	m/L^2t

Symbol	Meaning	Dimensions
ΔH_o	Deflection on orifice manometer	L
ΔH_T	Deflection on friction pressure loss measuring manometer	L
ΔH_V	Deflection on velocity manometer	L
h	Average heat transfer coefficient	F/LtT
h_l	Local heat transfer coefficient	F/LtT
j_H	Colburn's j factor for heat transfer	
K	Parameter defining shear stress--rate of shear behavior of liquids	
$\underline{K}$	Conversion factor for obtaining feet	
k	Thermal conductivity	F/Lt
L	Length of test section	L
$\underline{l}$	Prandtl mixing length	L
m	Mass	m
n	Exponent defining shear stress--rate of shear behavior of liquids	
P	Pressure	F/L^2
P_f	Friction pressure	F/L^2
ΔP_o	Pressure difference across orifice	F/L^2
ΔP_s	Static pressure difference	F/L^2
ΔP_T	Pressure drop across test section	F/L^2
ΔP_f	Pressure difference due to friction losses	F/L^2
q	Amount of heat transferred	FL/t
q_{mo}	Heat transferred by molecular conduction	FL/t

Symbol	Meaning	Dimensions
r	Radial distance from tube center	L
r_w	Tube wall radius	L
s	Summation index	
T	Temperature of fluid	T
T_c	Temperature of fluid at center of tube	T
T_w	Tube wall temperature	T
t	Time	t
U	Average velocity	L/t
u	Point velocity	L/t
u_m	Maximum point velocity	L/t
u^*	Friction velocity	L/t
u^+	Dimensionless velocity	
V	Volume	L^3
w	Mass flow rate	m/t
x	Distance co-ordinate, along tube length	L
y	Distance co-ordinate measured normal to tube wall	L
y^+	Dimensionless distance	
Z'	Height	L
α	Thermal diffusivity, k/C_p	L^2/t
ε	Energy dissipated per unit mass	FL/m
ε_H	Eddy diffusivity of heat	L^2/t
ε_M	Eddy diffusivity of momentum	L^2/t

Symbol	Meaning	Dimensions
λ_s	Eigenvalues	
μ	Viscosity	m/Lt
μ_c	Viscosity of continuous phase	m/Lt
μ_m	Viscosity of dispersed phase	m/Lt
π	Constant, 3.142	
ρ	Density	m/L^3
ρ_e	Density of dispersion	m/L^3
ρ_m	Equivalent density of manometer fluids	m/L^3
τ	Shear stress in a flowing fluid	F/L^2
τ_w	Shear stress at the wall	F/L^2

Dimensionless Groups

Symbol	Definition
Nu	Nusselt number, hD/k
Pr	Prandtl number, $C_p\mu/k$
Pr_c	Prandtl number of the continuous phase
Pr_w	Prandtl number at the wall temperature
Re	Reynolds number, $DU\rho/\mu$
St	Stanton number h/GC_p